INTERFACE OPTIMISATION AND BONDING MECHANISM OF RUBBER-WOOD-PLASTIC COMPOSITES

By

Yonghui Zhou

A Thesis Submitted in Partial Fulfilment of the Requirements for the Degree of Doctor of Philosophy

Department of Civil and Environmental Engineering

College of Engineering, Design and Physical Sciences

Brunel University London

March 2018

DECLARATION

The work in this thesis is based upon the research carried out at the Department of Civil and Environmental Engineering, Brunel University London. Except where specific reference has been made to the work of others, this thesis is the result of my own work. No part of this thesis has been submitted elsewhere for any other degree or qualification.

Candidate: (Yonghui Zhou)

ACKNOWLEDGEMENTS

I would like to express my sincere gratitude and appreciation to my supervisor Professor Mizi Fan for his invaluable guidance, support, advice, encouragement and patience throughout the completion of this research.

The financial support from the European CIP-EIP-Eco-Innovation-2012 (Project Number: 333083) is gratefully acknowledged.

My grateful thanks are expressed to all the technicians, colleagues, and administrative staff in the Department of Civil and Environmental Engineering who kindly helped me in some form or other throughout four years.

ABSTRACT

The incorporation of waste tyre rubber into thermoplastics to develop a class of polymer composites with both elastomeric and thermoplastic behaviour has gained a lot of attention and is becoming one of the most straightforward and preferred options to achieve the valorisation of waste tyres. In view of the unique properties rubber possesses and the rapid expansion and versatile application of wood plastic composites (WPC) materials, the inclusion of tyre rubber as raw material into WPC to develop an entirely new generation of WPC, namely rubber-wood-plastic composites (RubWPC), was presumed to be another highly promising solution to turn waste tyres into value-added materials.

This research starts with the interfacial optimisation of Rubber-PE composites and WPC by the use of maleated and silane coupling agents, aiming at addressing their poor constituent compatibility and interfacial bonding, thus enabling the optimal design of RubWPC. Chemical, physical and mechanical bonding scenarios of both untreated and treated composites were revealed by conducting ATR-FTIR, NMR, SEM and FM analyses. The contribution of the optimised interface to the bulk mechanical property of the composites were assessed by carrying out DMA and tensile property analysis. The influence of the coupling agent treatments on the *in situ* mechanical property of WPC was first determined by nanoindentation analysis, which led to a thorough understanding of the interfacial characteristics and the correlation between *in situ* and bulk mechanical properties.

This research focuses on the novel formulation of RubWPC and the understanding of bonding mechanism. Chemical bonding and interface structure studies revealed that interdiffusion, molecular attractions, chemical reactions, and mechanical interlocking were mutually responsible for the enhancement of the interfacial adhesion and bonding of the coupling agent treated RubWPC. The improved interface gave rise to the increase of bulk mechanical properties, while the continuous addition of rubber particle exerted an opposite influence on the property of RubWPC. The composite with optimised interface possessed superior nanomechanical properties due to the resin penetration into cell lumens and vessels and the reaction between cell walls and coupling agents.

TABLE OF CONTENTS

LIST OF FIGURES

LIST OF TABLES

LIST OF ABBREVIATIONS

ANBR	Acrylonitrile butadiene rubber
APS	3-aminopropyl-triethoxy-silane
ATR-FTIR	Attenuated total reflectance-Fourier Transform Infrared spectroscopy
AVI	Absolute Virtual Instrument
BCF	Bamboo cellulose fibres
BP	Benzophenone
CB	Carbon black
CPMAS	Cross-polarisation/magic angle spinning
DMA	Dynamic mechanical analysis
DTG	Derivative Thermogravimetry
ED	Epoxy dispersions
ENR	Epoxidized NR
EVA	Ethylene-vinyl acetate
FM	Fluorescence Microscope
FTIR	Fourier Transform Infrared spectroscopy
GM	Glycidyl methacrylate
GTR	Ground tyre rubber
HDPE	High density polyethylene
KH560	Glycidoxypropyltrimethoxysilane
LDPE	Low density polyethylene
MA	Maleic anhydride
MAPE	Maleated polyethylene
MAPP	Maleated polypropylene

MAS	Magic angle spinning
MFI	Melt flow index
MPS	g-methacryloxypropyl trimethoxy silane
NBR	Nitrile butadiene rubber
NMR	Nuclear Magnetic Resonance spectroscopy
NR	Natural rubber
OPEFB	Oil palm empty fruit bunch
OPEFB-g-PMA	Poly(methyl acrylate) grafted OPEFB
PAPS	3-phenyl-aminopropyl-trimethoxy-silane
PE	Polyethylene
PHA	Polyhydroxyalkanoate
PHB	Poly(3-hydroxybutyrate)
PHBV	Poly(3-hydroxybutyrate-co-3-hydroxyvalerate)
PF	Phenol-formaldehyde
PLA	Polylactic acid
PLLA	Poly(L-lactic acid)
PP	Polypropylene
PS	Polystyrene
PU	Polyurethane
PVC	Polyvinyl chloride
RHP	Rice husk powder
RNP	Recycled newspaper
RubWPC	Rubber-wood-plastic composites
S	NaOH solution
SA	Silane agent

SBR	Styrene butadiene rubber
SCF	Sugarcane waste fibre
SEBS-g-MA	MA grafted styrene–ethylene/butylene–styrene
SEM	Scanning Electron Microscope
Si69	Bis(triethoxysilylpropyl)tetrasulfide
TCI	Trichloroisocyanuric acid
TGA	Thermogravimetric Analysis
TPE	Thermoplastic elastomers
TPS	Thermoplastic starch
UV	Ultraviolet
VTMS	Vinyltrimethoxysilane
WPC	Wood plastic composites
XPS	X-ray photoelectron spectroscopy
12-HSA	12-Hydroxyoctadecanoic acid

Chapter 1 Introduction

1.1 Background of Research

Used tyres are among the largest and most problematic sources of waste, due to the large volume produced and their durability. The environmental issues from the disposal of these tyres have led to increasing interests in economic recycling of tyre rubber (Torretta *et al.*, 2015; Zanetti *et al.*, 2015). The rubber in tyres is vulcanised and cannot be molten or dissolved, which makes the recycling challenging (Fuhrmann and Karger-Kocsis, 1999; De *et al.*, 2006; Sonnier *et al.*, 2006; Sienkiewicz *et al.*, 2012). As a result, a large number of used, worn out tyres are ground for the benefits of expanding their applications (Kumar *et al.*, 2002). The application related to the ground or powdered tyre rubber includes outdoor flooring and pavement, sports tracks, road construction, etc., which fall into the sectors with limited demand and added value. Concerning the economic recycling and valorisation of the discarded tyres, ground tyre rubber (GTR) has been used in thermoplastics to develop a class of polymer blends or compounds consisting of materials with both thermoplastic character and elastomeric behaviour. It is widely accepted that the successful incorporation of even small amount of GTR into thermoplastics would lead to a considerable increase of waste tyre consumption due to the massive market share of thermoplastic materials, which in the meantime transforms the waste tyre to value-added products (Kakroodi and Rodrigue, 2013).

Wood plastic composites (WPC) are composed of wood (virgin or waste) or other cellulose-based fibre fillers such as hemp fibre, flax fibre, oil palm fibre, pulp fibre, peanut hulls, bamboo and straw, and virgin or waste plastics including polyethylene (PE), polypropylene (PP), polyvinyl chloride (PVC), polystyrene (PS), acrylonitrile butadiene styrene (ABS), polylactic acid (PLA), etc. It has been considered as one of the most advanced materials, consistently growing in the last decade for uses in many industrial sectors, such as decking, automotive, siding, fencing and outdoor furniture, mainly because of the advantages that wood or fibre material possesses, namely ubiquitous availability at low cost and in a variety of forms, biorenewability and biodegradability, low density, nontoxicity, flexibility during processing, and acceptable specific strength

properties (Zhang, 2014; Xie *et al.*, 2010; Kuo *et al.*, 2009; Bengtsson *et al.*, 2007; Bengtsson and Oksman, 2006; Belgacem and Gandini, 2005; Bengtsson *et al.*, 2005). However, inherently highly polar and hydrophilic nature of wood or fibre makes it incompatible with hydrophobic and non-polar matrices, especially hydrocarbon matrices (e.g. PE and PP) (Cantero *et al.*, 2003; Bledzki *et al.*, 1998), this may cause problem in composite processing and material performance, such as uneven distribution of the filler in the matrix during the compounding process and insufficient wetting of wood flour or fibre by the matrix, which result in weak interfacial adhesion and strength (Xie *et al.*, 2010; Belgacem and Gandini, 2005; Azwa *et al.*, 2013; Dittenber and Gangarao, 2012; Araújo *et al.*, 2008; Dhakal *et al.*, 2007). In order to formulate a reasonable WPC with optimum interface bonding, various modifications including both physical (e.g. corona, plasma, gamma radiation) and chemical approaches (e.g. alkaline, acetylation, benzoylation, peroxide, silane and maleated coupling agent treatments) have been attempted to decrease the hydrophilicity of wood flour or fibre, enhance the wettability of wood flour or fibre by matrix polymer and eventually promote the interfacial adhesion of the constituents within the composite. With respect to the commercial production of WPC, incorporating coupling agents is probably the best available and feasible strategy for its interface optimisation (Pickering, 2008).

In view of the rapid expansion of WPC materials, the incorporation of GTR as raw material into WPC might be another highly promising approach for realising the valorisation of used tyres apart from GTR filled thermoplastic composites, which would generate a new generation of WPC, namely rubber-wood-plastic composites (RubWPC). This is a new concept and the resulted RubWPC will have many additional properties beyond WPC considering the unique vibration damping, slip resistance, wearing and acoustic performance rubber possesses. In the literature, there have been several investigations of cellulosic thermoplastic elastomers (TPE) with the inclusion of wood flour or fibre, aiming to reduce the consumption of petroleum product (thermoplastics), improve the biodegradability of the novel composite, and provide the existing TPE with multifunctional performance (Ismail and Nasir, 2001; Abdelmouleh *et al.*, 2007). The major difference between RubWPC and cellulosic TPE is the rubber phase:

virgin natural rubber (NR) or synthetic rubber such as nitrile butadiene rubber (NBR) and styrene butadiene rubber (SBR) are employed in the study of cellulosic TPE, both of which are unvulcanised and miscible with thermoplastics (Kumar *et al.*, 2002; Sonnier *et al.*, 2006; Ratnam *et al.*, 2001a), while the GTR in RubWPC is vulcanised with highly crosslinked structure and is not capable of entangling with the polymer molecules composing thermoplastic matrix, leading to insufficient adhesion between rubber and thermoplastic phases (Kakroodi and Rodrigue, 2013; Kumar *et al.*, 2002). Therefore, the compatibility and bonding of wood-plastic, rubber-plastic and wood-rubber are the indispensable issues to be dealt with and overcome in order to formulate a reasonable RubWPC bearing the advantageous features of both tyre rubber and WPC.

1.2 Aims and Objectives of Research

This research aims at: 1) the interface optimisation of Rubber-PE composites and WPC by the use of coupling agents and the thorough understanding of their bonding scenarios; 2) the incorporation of GTR as raw material to develop a new generation of WPC, namely RubWPC, with the focus on its interface optimisation and structure and performance characterisation.

The specific objectives of this research include:

1) To improve the compatibility, homogeneity and interfacial adhesion of Rubber-PE composites
2) To reveal the interface structure and bonding scenarios, and unveil the chemical, physical and mechanical bonding mechanisms of WPC
3) To determine the influence of the coupling agent treatments on the bulk and *in situ* mechanical properties of WPC
4) To examine the variation of the chemical functionalities and structure, interface microstructure, and bonding scenarios during coupling agent treatments of RubWPC
5) To explore the contribution of the additional use of GTR and the incorporation of coupling agents to the bulk and *in situ* mechanical properties of RubWPC
6) To establish the correlation between the structure and performance of RubWPC

1.3 Scope of Research

This research presents the formulation and characterisation of Rubber-PE composites, WPC and RubWPC materials. The effort is devoted to the interfacial optimisation of the materials by employing three different coupling agents, i.e. maleated polyethylene (MAPE), bis(triethoxysilylpropyl)tetrasulfide (Si69) and vinyltrimethoxysilane (VTMS). The first part of research investigates the influence of the compatibilisation treatments on the constituent compatibility, interfacial bonding, and mechanical properties of the formulated Rubber-PE composites. Attenuated total reflectance-Fourier Transform Infrared spectroscopy (ATR-FTIR) and solid state ^{13}C Nuclear Magnetic Resonance spectroscopy (NMR) analyses were carried out to study the generation and variation of the chemical functionalities and structure during compatibilisation treatments, microscopic technique was used to reveal the microstructure (e.g. rubber wettability, homogeneity, interfacial adhesion, etc.) of the composites, dynamic mechanical analysis (DMA) and tensile test were conducted to assess the mechanical properties.

The second part of research systematically studies the physical, chemical and mechanical bonding scenarios of both untreated and treated WPC by carrying out ATR-FTIR, NMR, Scanning Electron Microscope (SEM) and Fluorescence Microscope (FM) analyses. The influence of the coupling agents treatments on the bulk and *in situ* mechanical properties of the composites were determined by carrying out a set of assessments including DMA, tensile property analysis and nanoindentation analysis. First and second parts of research provide fundamental basis for the third part of research that focuses on the novel development of RubWPC with optimised interface by using single coupling agent along with the combinations. The surface chemical distribution and structure of RubWPC were scrutinised by applying spectroscopic techniques (ATR-FTIR and NMR), while microscopic tool was employed to investigate the morphological structure of the composites, which together gave rise to the understanding of the improvement of interfacial bonding. The effect of the coupling agent treatments and the compositional variation on the bulk mechanical properties was assessed

by DMA and tensile test, and the nanomechanical properties of the composites were determined by nanoindentation analysis.

1.4 Significance of Research

The application of maleated and silane coupling agents would improve the existing insufficient compatibility, homogeneity and interfacial adhesion between vulcanised rubber and PE in Rubber-PE composites. The scrupulous investigation of chemical functionalities, structure and bonding of the composites after compatibilisation treatments leads to a better understanding of microstructure formulation and bonding scenarios. The explored correlation between the structure and property of the composites should benefit the further design and commercialisation of Rubber-PE composites.

Although coupling agent treatments of WPC have been extensively studied, this research focuses on the correlation of the chemical reactions and bonding resulted from the coupling agent treatments with physical and mechanical bonding scenarios, which have rarely been approached. Hence, the physical, chemical and mechanical bonding mechanisms of WPC are systematically revealed. The determination of the *in situ* mechanical properties of the composites by nanoindentation leads to further in-depth understanding of interfacial characteristics, helps in evaluating the overall property and thus enables the optimal design of WPC.

WPC industry is using virgin as well as recycled wood and plastic as raw materials. Additional use of used tyre rubber as a constituent raw material will not only improve the environmental properties of new material (RubWPC), but also alleviate the raw material competition with energy and other industrial sectors, because the inclusion of rubber means a reduction of wood which has become a major resource for energy and bio-fuel. The chemical structure and microstructure analyses of the formulated RubWPC will reveal the chemical reactions between the coupling agents and the constituents, constituent compatibility, filler distribution and wettability, composite homogeneity, interfacial adhesion, and hence bonding mechanisms. The mechanical property analysis will assess and verify the contribution of the optimised interface and enhanced bonding after coupling agent treatments to the performance of

RubWPC. This research provides a highly promising approach for the valorisation of used tyres, and it shall serve as a fundamental basis for the further research and industrialisation of RubWPC.

Chapter 2 Literature Review

2.1 GTR filled thermoplastic composites

The development of ground tyre rubber (GTR) filled thermoplastic composites has been perturbed by the poor interfacial adhesion between GTR particles and polymer matrix, mainly because the molecules of highly crosslinked GTR were not capable of entangling with those of thermoplastics. To overcome this problem, various modification or treatment methods such as devulcanisation or reclaiming, reactive and nonreactive compatibilisation, have been explored in GTR filled thermoplastic composites (Kakroodi and Rodrigue, 2013; Kaynak *et al.*, 2001; Karger-Kocsis *et al.*, 2013).

2.1.1 Devulcanisation and reclaiming of GTR in thermoplastic composites

Vulcanisation is a chemical process for converting natural rubber or related polymers into more durable materials by the addition of sulfur or other equivalent curatives or accelerators. Devulcanisation is the process of cleaving the monosulfidic (C-S), disulfidic (S-S), and polysulfidic crosslinks (C-S_x-C) of vulcanised rubber (Diao *et al.*, 1999). Ideally, devulcanisation would yield a product that could serve as a substitute to virgin rubber, albeit the devulcanisation processes might cause the diminution of some properties over those of the parent rubber. Reclaiming is a procedure that vulcanised rubber is converted by using mechanical and thermal energy, and chemicals into a state in which it can be mixed, processed and vulcanised again. Although the principle of reclaiming process is devulcanisation, it is usually accompanied with considerable polymeric chain scission leading to lower molecular mass fractions, while devulcanisation is generally limited to chemical interactions involving sulfur atoms. Irrespective to the above distinctions, the processes adopted could hardly be categorised into devulcanisation or reclaiming.

Rubber devulcanisation by using ultrasonic energy has been widely employed in GTR filled thermoplastic composites. It was a batch process in which the vulcanised rubber was devulcanised under powerful ultrasonic waves (20 kHz to 500 MHz) by efficiently breaking down C-S and S-S bonds but not C-C bonds. The rate of devulcanisation depended on the levels of pressure and temperature. The

properties of the revulcanised rubber were found to be close to those of original vulcanisates (Karger-Kocsis *et al.*, 2013). Hong (Hong and Isayev, 2001) prepared GTR/high density polyethylene (HDPE) and ultrasonically devulcanised GTR/HDPE blends in a Brabender internal mixer and a twin screw extruder. It was found that the dynamic devulcanisation led to increase of mechanical properties of the blends. Among all the blends, HDPE/GTR blends mixed in the twin screw extruder prior to devulcanisation and dynamically devulcanised in the presence of HDPE matrix suggested better tensile properties and impact strength.

Microwave technology had also been used to devulcanise the GTR in thermoplastic composites. This process applied volumetric heat uniformly on GTR, the application of a controlled amount of microwave energy devulcanised the sulfur-vulcanised rubber to a state in which it could be compounded and revulcanised into useful products. However, the rubber being treated by this technique must be polar enough to accept energy at a rate sufficient to generate the necessary heat (>250^{o}C) for devulcanisation (Karger-Kocsis *et al.*, 2013). A study on the influence of microwave devulcanisation process on dynamically revulcanised GTR/PE blends indicated that the viscoelastic behaviour of the blends was significantly influenced by the exposure time to microwave (Sousa *et al.*, 2016), the lack of adhesion between the phases impaired the rheological properties, which thus resulted in poor mechanical properties of the blends, especially the blends exposed to microwave for longer time.

The other devulcanisation or reclaiming processes of GTR were thermomechanical and thermochemical processes. In thermomechanical process, vulcanised rubber was subjected to shear and/or elongational stresses at either ambient or high temperatures on suitable equipment such as internal mixers and twin screw extruders, giving rise to a prominent decrease in molecular mass since considerable heat was generated even in ambient process. This technique was used in conjunction with the above ultrasonic and microwave processes. Thermochemical process was referred to the performing of thermomechanical process with the addition of chemical reclaiming agents (e.g. organic solvents, oils, and inorganic compounds) (Diao *et al.*, 1999; Maridass and Gupta, 2008; Jana

et al., 2006). This processing method might be not economical and environmentally friendly due to the additional use of chemicals, and has been rarely used in the devulcanisation or reclaiming of the GTR in thermoplastic composites.

2.1.2 Surface activation of GTR in thermoplastic composites

The objective of the surface activation of GTR was to increase the bonding between GTR and thermoplastic matrix in the composites. Various nonreactive and reactive strategies have been attempted to trigger the molecular entanglement and/or chemical coupling of GTR with the matrix or additionally incorporated compatibilisers. The effect of surface activation on mechanical property of GTR filled composites were summarised in Table 2.1.

Gamma irradiation was used for the *in situ* compatibilisation of recycled HDPE/GTR blends by Sonnier (Sonnier *et al.*, 2006). The compatibilisation mechanisms consisted of the formation of free radicals which led to the chain scission of GTR particles, crosslinking of PE matrix, and co-crosslinking between GTR and PE at the interface. The mechanical properties of the blends, such as elongation at break and Charpy impact strength, were significantly enhanced due to the generation of an adhesion between GTR and surrounding PE matrix under the irradiation doses of 25-50 kGy. Nevertheless, further increase of irradiation (e.g. 100 kGy) impaired the compatibilisation of the composite which was confirmed by its relatively inferior mechanical performance.

High energy (electron beam) irradiation treatment has been proven to be an effective compatibilising technology for GTR filled PE and PE/ethylene-vinyl acetate (EVA) composites (Mészáros *et al.*, 2012a; Mészáros *et al.*, 2012b). This treatment first produced free radicals on the surface of GTR, which attracted PE molecules, leading to the formation of covalent bonds between two phases. On the other hand, the irradiation induced the crosslinking of PE, which was responsible for the increase of mechanical properties and shape memory behaviour of the material. Specifically, the 200 kGy electron beam absorbed dose (in air) resulted in enhanced tensile strength and elongation at break with no effect on tensile modulus, indicating more rubber-like properties of the treated composite. The addition of EVA into the composite improved the compatibility

between the components by showing higher relaxation temperatures, and the modest increase of hardness of the irradiated composites confirmed the crosslinking effect of the electron beam irradiation.

Surface activation of GTR by photografting technique was carried out by Lee (Lee *et al.*, 2009) with allylamine monomer in the presence of ultraviolet (UV) radiation and benzophenone (BP) photoinitiator. Thus, the treated GTR was incorporated into PP matrix to prepare thermoplastic composites. The presence of allylamine on the surface of GTR was first confirmed by chemical structure analysis. Compared to the untreated counterpart, the treated GTR suggested much higher surface energy and activity, which were attributed to the grafting of allylamine on GTR surface. Moreover, the allylamine grafting and UV radiation promoted the dispersion of GTR in PP matrix by showing smaller size of aggregates, giving rise to enhanced mechanical properties. Aiming at overcoming the poor miscibility and compatibility of GTR/PP blends, compatibilisers including maleic anhydride grafted styrene–ethylene/butylene–styrene (SEBS-g-MA) and maleated polypropylene (MAPP) were also employed by Lee (Lee *et al.*, 2007b). It was found that the blend of GTR and PP was simply a physical mixture of two incompatible polymers in which the continuous thermoplastic matrix phase was principally responsible for its mechanical performance. Improved mechanical properties were obtained with the addition of SEBS-g-MA and MAPP into the blends, due to the increased constituent compatibility through the chemical reactions between the functional groups (maleic anhydride, MA) of the compatibilisers and matrix polymers.

Pretreatments including sulfuric acid (H_2SO_4) etching, silane coupling agent, and chlorination with trichloroisocyanuric acid (TCI) were also performed on GTR in order to improve its compatibility with HDPE (Colom *et al.*, 2006). H_2SO_4 pretreatment equipped the GTR with a rough surface which benefitted its mechanical adhesion (i.e. interlocking) with the matrix, silane coupling agent chemically interacted with both GTR and HDPE of the composites owing to its intrinsic multifunction, whilst TCI did not appear to be an effective pretreatment due to the subtle distinction of the structure and property of the treated composite from those of the untreated.

Table 2.1 Mechanical properties of GTR filled plastic composites

Composite	**Modification method**	**Tensile strength (MPa)**	**Stain at break**	**Elastic modulus (MPa)**	**Reference**
Coarse recycled rubber-Epoxy composite	Untreated	52.8±2.1	0.27±0.01	286±2	(Kaynak *et al.*, 2003)
	3-aminopropyltriethoxysilane (2 wt%)	60.9±2.5	0.28±0.01	331±5	
GTR-PE	Untreated	Approx. 7.0	Approx. 0.65	Approx. 341	(Mészáros *et al.*, 2012a)
	EVA (20 wt%)	Approx. 5.8	Approx. 1.55	Approx. 242	
	EVA (20 wt%) and electron beam radiation (100 kGy)	Approx. 6.9	Approx. 1.82	Approx. 228	
GTR-PP	Untreated	9.7	0.62	-	(Lee *et al.*, 2009)
	SEBS-g-MA	10.3	1.65	-	
	MAPP	8.6	1.9	-	
	SEBS-g-MA and MAPP	10.2	4.4	-	
GTR-HDPE	Untreated	Approx. 12.2	Approx. 0.17	Approx. 364	(Sonnier *et al.*, 2006)
	Γ irradiation (50 kGy)	Approx. 15.6	Approx. 0.09	Approx. 393	

2.2 Lignocellulosic polymer composites

Lignocellulosic polymer composite has experienced a rapid expansion over the last decade, mainly due to the advantageous features that lignocellulosic biomass provides over inorganic fillers and/or reinforcements, i.e. abundance, environmental friendliness, biodegradability, nontoxicity, low cost and density, flexibility during processing, and high tensile and flexural modulus (Ja *et al.*, 2016; Fernandes *et al.*, 2013; Mukhopadhyay *et al.*, 2003; George *et al.*, 2001; Khalil and Ismail, 2001; Lu *et al.*, 2000; Bledzki and Gassan, 1999; Zadorecki and Michell, 1989). Compared to wood materials, lignocellulosic polymer composite possesses better flexural and impact strength, higher moisture resistance, less shrinkage and improved weatherability. However, regardless these benchmarking characteristics, optimisation of the interfacial bonding between cellulosic filler and polymer matrix is one of the most indispensable procedures with respect to the optimal formulation of lignocellulosic polymer composite (Zhou *et al.*, 2016; George *et al.*, 2001).

The filler-matrix interface is a reaction or diffusion zone in which two phases or components are physically, mechanically and/or chemically combined. Interfacial adhesion between wood flour or fibre and matrix plays a fundamental role regarding the factors governing the mechanical characteristics of lignocellulosic polymer composites (Kabir *et al.*, 2012). The factors affecting the interfacial bonding between wood flour or fibre and matrix are mechanical interlocking, molecular attractive forces and chemical bonds. However, the naturally hydrophilic wood flour or fibre is not inherently compatible with hydrophobic polymers. In addition to the pectin and waxy substances in wood flour or fibre acting as a barrier to interlock with nonpolar polymer matrix, the presence of plenty hydroxyl groups hinders its operative reaction with the matrix (Cantero *et al.*, 2003; Kazayawoko *et al.*, 1999; Bledzki *et al.*, 1998; Raj *et al.*, 1989). Therefore, the modification of surface characteristics of wood flour or fibre and hydrophobic polymer matrix is in particular essential in order to formulate a reasonable composite with superior interfacial bonding and effective inherent stress transfer throughout the interface. Numerous approaches, including physical treatments (e.g. solvent extraction, heat treatment, corona and

plasma treatments), physic-chemical treatments (e.g. laser, γ-ray and UV bombardment) (John and Anandjiwala, 2008) and chemical modifications, have been attempted for improving the compatibility and bonding between the lignocellulosic molecules and hydrocarbon-based polymers (El-Abbassi *et al.*, 2015; Glasser *et al.*, 1999; Saheb and Jog, 1999).

2.2.1 Compatibility between constituents of lignocellulosic polymer composites

2.2.1.1 Compatibility between wood flour or fibre and synthetic polymer

The main components of wood flour or fibre include cellulose, hemicellulose, lignin, pectin, waxes and other low-molecule substances. Cellulose is the fundamental structural component found in the form of slender rod like crystalline microfibril, aligned along the length of fibre. It is a semicrystalline polysaccharide consisting of a linear chain of hundreds to thousands of β-(1-4)-glycosidic bonds linked D-glucopyranose with the presence of large amount of hydroxyl groups. Hemicellulose is a lower molecular weight polysaccharide that functions as a cementing matrix between cellulose microfibrils, presented along with cellulose in almost all plant cell walls. While cellulose is crystalline, strong, and resistant to hydrolysis, hemicellulose has a random, amorphous structure with little strength. Furthermore, it is hydrophilic and can be easily hydrolysed by dilute acids and bases. Lignin is a class of complex hydrocarbon polymers (crosslinked phenol polymers) that gives rigidity to plant. It is relatively hydrophobic and aromatic in nature. Pectin is a structural heteropolysaccharide contained in the primary cell walls of plants giving the plants flexibility. Wax and water soluble substances are used to protect fibre on fibre surface (Azwa *et al.*, 2013; Summerscales *et al.*, 2010; Wong *et al.*, 2010; John and Thomas, 2008). The unique chemical structure makes the wood flour or fibre hydrophilic in nature.

Although there are many advantages associated with the use of wood flour or fibre as reinforcement in polymer composites, the incorporation of wood flour or fibre in hydrophobic and non-polar polymers leads to indecent systems due to the lack of moderate compatibility and adhesion between the filler and matrix. These would also cause some problems in the composite processing and material performance, including poor moisture resistance, inferior fire resistance, limited

processing temperatures, the formation of hydrogen bonds within fibre itself, agglomeration of fibre bundles, uneven fibre distribution in matrix during compound processing, and insufficient wetting of fibre by the matrix which results in weak interfacial adhesion (Azwa *et al.*, 2013; Dittenber and Gangarao, 2012; Araújo *et al.*, 2008; Dhakal *et al.*, 2007).

By this token, various physical and chemical modifications have been attempted to decrease the hydrophilicity of wood flour or fibre, enhance the wettability of wood flour or fibre by polymers and also promote the interfacial adhesion. These modification approaches are of different efficiency and mechanism in regard to optimising interfacial characteristics of the composite. Physical treatments, such as electric discharge, in general alter the structural and surface properties of wood flour or fibre by introducing surface crosslinking, modifying the surface energy and/or generating reactive free radicals and groups, and thereby influence the mechanical bonding to the matrix. Chemical modification provides the means of permanently altering the nature of wood flour or fibre cell walls by grafting polymers onto the fibres, crosslinking of the fibre cell walls, or by using coupling agents (Xie *et al.*, 2010). Such modification strategies tackling with the compatibility and interfacial bonding of lignocellulosic polymer composites will be discussed in detail in the next section.

2.2.1.2 Compatibility between wood flour or fibre and bioplastic polymer

The research of polymers obtained from different biorenewable resources generally referred as biobased polymers and designed to be biodegradable has substantially increased recently. It is well known that renewable resources such as bioproducts (e.g. cellulose or chitin, vegetable fats and oils, corn starch, etc.), bacteria as well as non-renewable petroleum (e.g. aliphatic/aliphatic-aromatic copolymer) are sources of a variety of polymeric materials (Satyanarayana *et al.*, 2009; Gáspár *et al.*, 2005; Heredia, 2003; Kurita, 2001; Wollerdorfer and Bader, 1998). Accordingly, the biodegradable polymers can be classified as naturally occurring or synthetic based on their origins. Natural polymers are available in large quantities from renewable sources, i.e. cellulose, pectin, lignin, collagens, chitin/chitosan, starch, proteins, lipids, etc. Microbially synthesised polymers include polyhydroxyalkanoate (PHA) and bacterial cellulose, while chemically

synthesised polymers are produced from conventionally petroleum-based resource monomers including polyacids, poly(vinyl alcohols), polyesters, etc. (Satyanarayana *et al.*, 2009; Matas *et al.*, 2004; Deshmukh *et al.*, 2003; Xu *et al.*, 2003). Biodegradable bioplastics can break down in either anaerobic or aerobic environments, depending on how they are manufactured, and thus are being envisaged as prospective alternatives to their counterparts in olefin plastics. The incorporation of wood flour or fibre into bioplastics to fabricate fully biodegradable composite materials has attracted significant attention for various purposes (Table 2.2), in particular for multifunctional applications, since many of these polymers, in addition to being biodegradable, also possess antimicrobial and antioxidant properties (Thakur and Thakur, 2015). At this stage, the main impediment to the rampant use of bioplastic polymers is the high initial cost, currently cost three to five times of the extensively used resins such as PP, PVC, HDPE and low density polyethylene (LDPE) (Yan *et al.*, 2014).

Table 2.2 Wood flour or fibre reinforced biodegradable polymer composites

Biopolymer matrix	**Reinforcement**	**References**
Pregelatinised cassava starch	Luffa fibre	(Kaewtatip and Thongmee, 2012)
Thermoplastic corn starch	Bleached *E. urograndis* pulp	(Curvelo *et al.*, 2001)
Cellulose derivatives/starch blends	Sisal fibre	(Alvarez and Vazquez, 2004)
Thermoplastic rice starch	Cotton fibre	(Prachayawarakorn *et al.*, 2010)
Thermoplastic corn starch	Sugarcane and banana fibres	(Guimarães *et al.*, 2010)
Thermoplastic cassava starch	Cassava bagasse cellulose nanofibrils	(Teixeira *et al.*, 2009)
Thermoplastic maize starch	Wheat straw cellulose nanofibrils	(Kaushik *et al.*, 2010)
Thermoplastic cassava starch	Jute and kapok fibres	(Prachayawarakorn *et al.*, 2013)
PLA	Wood fibre	(Ding *et al.*, 2016; Faludi *et al.*, 2014)
PLA	Bamboo fibre and flour	(Wang *et al.*, 2014; Okubo *et al.*, 2009; Nuthong *et al.*, 2013)
PLA	Kenaf fibre	(Ochi, 2008)
PLA	Flax fibre	(Bocz *et al.*, 2014)
PLA	Jute fibre	(Rajesh and Prasad, 2014)

PLA	Banana fibre	(Jandas *et al.*, 2011)
PLA	Grewia optiva and nettle fibres	(Bajpai *et al.*, 2013)
PLA	Nanocellulose fibre	(Song *et al.*, 2014)
PHB	Jute and lyocell fibres	(Gunning *et al.*, 2013)
PHB	Bamboo micro fibril	(Krishnaprasad *et al.*, 2009)
PHA	Eucalyptus pulp fibre	(Loureiro *et al.*, 2014)
PHA	Tea plant fibre	(Wu, 2013)
PHA	Beer spent grain fibre	(Cunha *et al.*, 2015)
PHA	Wood flour	(Coats *et al.*, 2008)
PHBV	Wood fibre	(Bhardwaj *et al.*, 2006; Bhardwaj *et al.*, 2006)
PHBV	Recycled cellulose fibre	(Bhardwaj *et al.*, 2006)
PHBV	Cellulose nanowhisker	(Jiang *et al.*, 2008)

2.2.2 Modification of constituents of lignocellulosic polymer composites

2.2.2.1 Physical treatments

Physical treatments of wood flour or fibre alter the structure and surface properties of the fillers without using chemical agents, and thereby influence the mechanical bonding with the matrix in the composite. Radiation and discharge treatments such as UV radiation, gamma radiation, corona and plasma treatments are the most commonly used physical techniques in lignocellulosic polymer composite with regards to the improvement of the functional properties of wood flour or fibre (Table 2.3 and Table 2.4), which in general lead to significant physical and chemical changes as well as changes in the surface structure and surface energy of wood flour or fibre (Khan *et al.*, 2009; 2008; Li *et al.*, 2015; Zaman *et al.*, 2010; Gassan and Gutowski, 2000).

A typical treatment of gamma radiation is known to deposit energy on the wood flour or fibre in the composite and radicals are then produced on the cellulose chain by hydrogen and hydroxyl abstraction, ruptures of some carbon-carbon bonds and chain scission. Simultaneously, peroxide radicals are generated when matrix polymers are irradiated in the presence of oxygen. These active sites in both fibre and matrix produced by the gamma radiation result in better bonding between the filler and polymer matrix, which consequently improves the mechanical strength of the composite (Khan *et al.*, 2009; 2008; Li *et al.*, 2015; Haydaruzzaman *et al.*, 2009).

Corona treatment is a surface modification technique that uses a low temperature corona discharge plasma to impart changes on the properties of a surface (e.g. surface energy). The corona plasma is generated by the application of high voltage to an electrode that has a sharp tip. A linear array of electrodes is often used to create a curtain of corona plasma. The corona treatment of wood flour or fibre causes the formation of high-energy electromagnetic fields close to the charged points, with consequent ionisation in their proximity. In the ionised region, the excited species (i.e. ions, radicals, etc.) are present and the latter are active in surface modification, typically by the introduction of oxygen-containing groups in the molecular chain of wood flour or fibre (Kim and Mai, 1998). Plastic

is a man-made synthetic material, which contains long homogeneous molecular chains that form a strong and uniform product. The molecular chains are normally joined end to end to form even longer chains, leaving only a few open chain ends, thus providing a small amount of bonding points at the surface. The small amount of bonding points cause the low adhesion and wettability, which is a problem in converting processes. A high frequency charge would provide a more efficient and controllable method of increasing the adhesion and wettability of a plastic surface. During corona discharge treatment, electrons are accelerated into the surface of the plastic resulting in the long chains to rupture, producing a multiplicity of open ends and forming free valences. The ozone from the electrical discharge creates an oxygenation, which in turn forms new carbonyl groups with a higher surface energy. The result is an improvement of the chemical connection between the molecules in the plastic and the applied media/liquid. This surface treatment will not reduce or change the strength, neither will it change the appearance of the material. Corona treatment has been expansively applied in lignocellulosic composites especially in composites involving polyolefins as the matrix (Ragoubi *et al.*, 2012; Ragoubi *et al.*, 2010; Gassan and Gutowski, 2000).

Plasma treatment is another useful physical technique to improve the surface properties of wood flour or fibre and polymeric materials by utilising the ingredients such as high-energy photons, electrons, ions, radicals and excited species. Generally, the modification of wood flour or fibre by the treatment in cold oxygen plasma under optimal operating conditions turns the substrate into a semi-active filler for the lignocellulosic compounds (Vladkova *et al.*, 2006; Vladkova *et al.*, 2004a; Vladkova *et al.*, 2004b). Thus, the adhesion at the fibre/matrix interface increases with the plasma treatment. The resulted impact is the improvement of the mechanical properties (i.e. flexural strength and modulus, tensile strength and modulus) of the composites. Nevertheless, the fibre may degrade under longer time of exposure due to the constant impact of particles on the surface, which inevitably weakens the interfacial adhesion (Sarikanat *et al.*, 2014; Oporto *et al.*, 2009; Morales *et al.*, 2006).

UV radiation has also been employed to modify the surface characteristics of lignocellulosic polymer composites (Zaman *et al.*, 2009; Seldén *et al.*, 2004; Gassan and Gutowski, 2000). The UV treatment of single jute fibre and jute yarn resulted in higher gains in polarity in comparison with those in relation to corona-treated counterparts. The polarity and yarn tenacity could be adjusted by increasing treatment time at a constant bulb-sample distance or alternatively decreasing the distance. For the benefits of improving the overall mechanical properties of the composites, an appropriate balance between increased polarity of fibre surface and the decrease of fibre strength due to excessive surface oxidation by UV radiation or corona discharge should be accomplished (Gassan and Gutowski, 2000).

Table 2.3 Recent work on physical treatment of lignocellulosic polymer composites

Composite	**Treatment**	**Effect and outcome of the treatment**	**References**
Jute fibre/PE/PP composite	UV radiation	The tensile strength and bending strength of the composite increased with the strengthening of UV radiation up to 50 radiation dose; compared to the untreated composite, the treated composite showed an increase of 18% tensile strength and 20% bending strength respectively.	(Zaman *et al.*, 2009)
Miscanthus fibre/PP and miscanthus fibre/PLA composites	Corona treatment	The corona treatment of fibres resulted in a surface oxidation and an etching effect, leading to an improvement of the interfacial compatibility between fibre and matrices; hence, the mechanical and thermal properties (Young's modulus, stress at yield, T_g, and decomposition temperature) of the treated composites were greatly enhanced due to the better interaction between the constituents.	(Ragoubi *et al.*, 2012)
Flax fibre/polyester composite	Plasma treatment	After the air plasma treatment of flax fibre at a plasma power of 300 W, the tensile strength, flexural strength, flexural modulus and interlamilar shear strength of flax fibre-reinforced polyester composites increased by 34%, 31%, 66% and 39% respectively, primarily due to the improved adhesion between the treated fibre and polyester matrix.	(Sarikanat *et al.*, 2014)

Table 2.4 Mechanical properties of physically and chemically treated lignocellulosic polymer composites

Composite	**Modification method**	**Tensile strength (MPa)**	**Elongation at break (%)**	**Elastic modulus (MPa)**	**Reference**
Hemp fibre-PP	Untreated	28.6	5.4	1079	(Ragoubi *et*
	Corona treatment (15 kV)	37.8	5.2	1215	*al.*, 2010)
Flax fibre-polyester	Untreated	78.7	-	17650	(Sarikanat *et*
	Air plasma (100 W)	88.0	-	22150	*al.*, 2014)
	Argon plasma (100 W)	82.5	-	19415	
Flax fibre-MAPP	Untreated	Approx. 32.1	-	Approx. 4120	(Bledzki *et*
	Acetylation (18%)	Approx. 37.5	-	Approx. 4950	*al.*, 2008)
	Acetylation (18%) and MA	Approx. 47.2	-	Approx. 4565	
Wood flour-HDPE	Untreated	23.8	2.2	4000	(Ou *et al.*,
	MAPE (2 wt%)	40.1	6.1	4190	2014)
Wood flour-HDPE	Untreated	18.8±0.7	6.3±0.8	1116.7±60.4	(Bengtsson
	Vinyltrimethoxysilane	21.5±0.4	17.0±2.0	912.7±48.0	*et al.*, 2005)

2.2.2.2 Chemical treatments

Alkaline treatment or mercerisation

The chemical treatments of lignocellulosic composites have been reported (Table 2.4 and Table 2.5). Alkali treatment is one of the most used chemical methods of modifying the cellulosic molecular structure of wood flour or fibre when it is used to reinforce thermoplastics and thermosets. This treatment, usually performed in aqueous NaOH solution, disrupts fibre clusters and forms amorphous at the expense of highly packed crystalline cellulose. The important modification occurred is the disruption of hydrogen bonding in the network structure. During the treatment, the sensitive hydroxyl groups (OH) are broken down, and thus react with water (H-OH) leaving the ionised reactive molecules to form alkoxide with NaOH (Scheme 1).

$$Fibre - OH + NaOH \rightarrow Fibre - O - Na + H_2O + impurity \qquad \text{(Scheme 1)}$$

As a result, the hydrophilic OH groups are reduced and the surface roughness of the fibre is increased. It also removes a certain portion of hemicellulose, lignin, waxes, and oils covering the external surface of the fibre cell walls, depolymerises cellulose and exposes the short-length crystallites (Ahmed *et al.*, 2014; Li *et al.*, 2007; Mohanty *et al.*, 2000). Therefore, when the alkaline treated wood flour or fibre is used to reinforce polar polymer composites, in comparison with the composite filled with untreated wood flour or fibre, the enhanced surface roughness and increased reactive sites exposed on the surface would lead to a better mechanical interlocking and adhesion with the matrix, both of which are in charge of the interfacial strength of the composite (Ouajai and Shanks, 2005; Ray *et al.*, 2001). However, it should be pointed out that a superfluous alkali concentration would result in excess delignification of fibre, thus weaken or damage the fibre being treated (Li *et al.*, 2007; Wang *et al.*, 2007).

The alkali treatment of wood flour or fibre can also be carried out in combination with other treatments. Figure 2.1 shows the surface structures of untreated jute fibre, alkali treated jute fibre and alkali/organosilane/aqueous epoxy dispersions (ED) treated jute fibre (Doan *et al.*, 2012). The untreated jute fibre has rather smooth surface due to the cementing made up of fats, waxes, lignin,

pectin, and hemicellulose forming on the fibre surface (Mwaikambo and Ansell, 2002). The alkali treatment provided the fibre with a flaky or grooved surface by partially removing the cementing. The NaOH/(APS+ED) treated fibre was covered by a sizing of varying thickness, forming a film on the fibre surface. In contrast, the NaOH/PAPS treated fibre showed a much rougher surface since the sizing was less uniform in thickness or rather varying on a much higher scale, and appeared more flaky and less attached (Doan *et al.*, 2012).

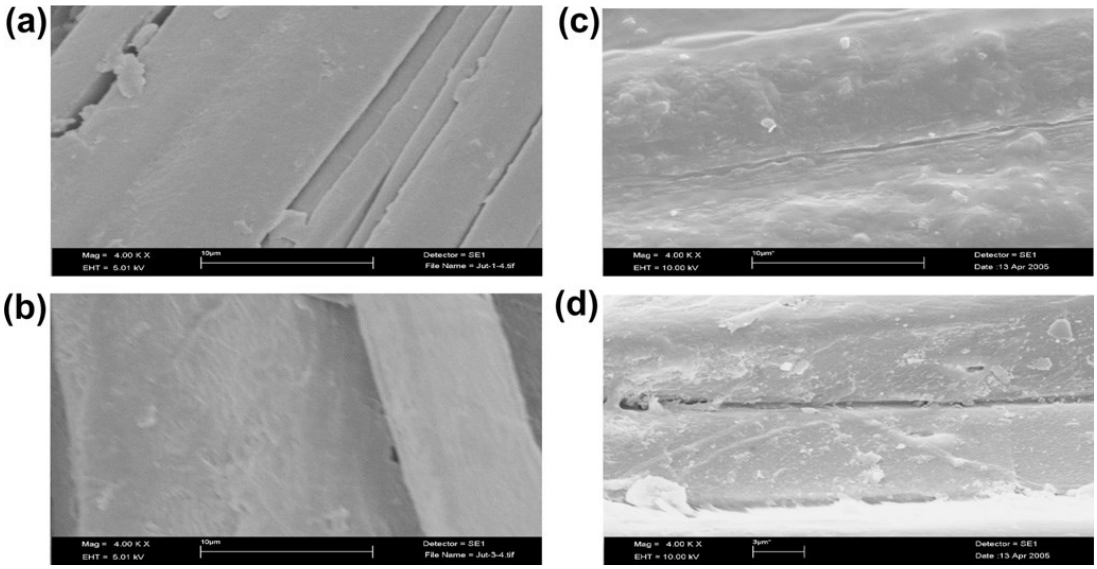

Figure 2.1 SEM images of (a) untreated, (b) NaOH treated, (c) NaOH/(APS+ED), and (d) NaOH/PAPS treated fibres (APS: 3-aminopropyl-triethoxy-silane, PAPS: 3-phenyl-aminopropyl-trimethoxy-silane) (Doan *et al.*, 2012)

Acetylation treatment

Acetylation of wood flour or fibre is known as an esterification method causing plasticisation of the substrate by introducing the acetyl functional group CH_3COO^-. The main principle of the reaction is to substitute hydrophilic hydroxyl groups (OH) of the cell wall with acetyl group CH_3COO^- from acetic anhydride (CH_3COO-C=O-CH_3), therefore rendering the substrate surface more hydrophobic (Scheme 2).

$$Fibre - OH + CH_3 - C(=O) - O - C(=O) - CH_3 \rightarrow Fibre - O - COCH_3 + CH_3COOH \quad \text{(Scheme 2)}$$

The reactive hydroxyl groups are those from the minor constituents of the fibre, i.e. hemicelluloses, lignin and amorphous cellulose. This is because the hydroxyl groups in crystalline regions of the fibre are closely packed with strong interlock

bonding, and are fairly inaccessible to chemical reagents (Bledzki *et al.*, 2008). In order to accelerate the reaction and maximise the degree of acetylation, acid catalysts such as sulfuric acid and acetic acid are commonly used in the treatment (Kabir *et al.*, 2012; Bledzki *et al.*, 2008). The esterification reaction not only stabilises the cell walls, with particular regards to moisture uptake and consequent dimensional variation of lignocellulosic fibre, but also provides the fibre rough surface tomography with less void contents, thereby the adhesion of the fibre to the matrix can be improved (Haseena *et al.,* 2007; Zurina *et al.*, 2004; Sreekala *et al.*, 2002). It has been reported that the acetylation treatment of wood flour or fibre resists up to 65% moisture absorption depending on the degree of acetylation (Bledzki *et al.*, 2008; Bledzki and Gassan, 1999). More importantly, in comparison to the composite reinforced with untreated fibre, this esterification of fibre results in the improvement of the stress transfer efficiency at the interface and the mechanical properties (tensile, flexural and impact properties) of its composites (Joseph *et al.*, 2005). In addition, the enhanced hydrophobicity of the treated fibres was able to provide the composite with higher volume resistivity than the untreated counterpart by reducing the dielectric constant of the composite (Haseena *et al.*, 2007).

Benzoylation treatment

Benzoylation treatment, an important transformation in organic synthesis, is another treatment aiming at decreasing the hydrophilicity of wood flour or fibre. Prior to carrying out the reaction with benzoyl groups ($C_6H_5C{=}O$), wood flour or fibre should be initially pretreated with NaOH aqueous solution in order to activate and expose the hydroxyl groups on the surface. Thus, wood flour or fibre can be treated with benzoyl chloride, the reaction is given in Scheme 3 (Wang *et al.*, 2007; Joseph *et al.*, 2003; Joseph *et al.*, 1996). This creates more hydrophobic nature of the fibre and improves fibre matrix adhesion, thereby considerably increases the strength and thermal stability of the composite (Kalaprasad *et al.*, 2004).

$$Fibre - O - Na + C_6H_5 - COCl \rightarrow Fibre - O - CO - C_6H_5 + NaCl \quad \text{(Scheme 3)}$$

Peroxide treatment

Interface property of lignocellulosic polymer composite can also be improved by peroxide treatment. Peroxide is a chemical compound with the specific functional group ROOR containing the divalent ion bond O-O. In contrast to oxide ions, the oxygen atoms in the peroxide ion have an oxidation state of -1. Benzoyl peroxide and dicumyl peroxide are the most used chemicals for wood flour or fibre surface modification in organic peroxides family. Both these chemicals are highly reactive and are inclined to decompose to free radicals (RO·), and then the RO· can be grafted onto cellulose macromolecules and polymer chains by reacting with the hydrogen groups of wood flour or fibre and polymer matrix (Scheme 4) (Wang *et al.*, 2007; Kalaprasad *et al.*, 2004; Joseph *et al.*, 1996). As a result, good fibre matrix adhesion occurs along the interface of the composite (Sreekala *et al.*, 2002; Sreekala *et al.*, 2000).

$$RO - OR \rightarrow 2RO^{\cdot}, RO^{\cdot} + Polymer \rightarrow ROH + Polymer^{\cdot}$$

$$RO^{\cdot} + Cellulose \rightarrow ROH + Cellulose^{\cdot}$$

$$Polymer^{\cdot} + Cellulose^{\cdot} \rightarrow Polymer - Cellulose \qquad \text{(Scheme 4)}$$

Silane treatment

Silane is an inorganic chemical compound with chemical formula SiH_4. Silanes are used as coupling agents to modify wood flour or fibre surface. A typical silane coupling agent bears two reactive groups, one end of silane agent with alkoxysilane groups is capable of reacting with hydroxyl-rich surface, namely wood flour or fibre, whereas the other end is left to interact with the polymer matrix. Specifically, in the presence of moisture, the silane (hydrolysable alkoxy group) could react with water to form silanol, which would further react with the hydroxyl groups attached to the cellulose, hemicellulose and lignin molecules in the filler through an ether linkage with the removal of water (Zhou *et al.*, 2015). The uptake of silane is very much dependent on a number of factors including temperature, pH, hydrolysis time and organofunctionality of silane (John and Anandjiwala, 2008). The reaction scheme is given in Scheme 5. On the other hand, the hydrophobic bonds in silane molecules are able to react with polymer matrix. Therefore, the hydrocarbon chains provided by the application of silane restrain

the swelling of the fibre by creating an entangled/crosslinked network due to the covalent bonding between the fibre and matrix (Kalia *et al.*, 2009; Li *et al.*, 2007). In addition, the introduced hydrocarbon chains were assumed to affect the wettability of the fibres and improve the chemical affinity of polymer matrix, thus the interfacial adhesion between fibre and matrix was enhanced (Kalaprasad *et al.*, 2004; Mohanty *et al.*, 2004).

$$Fibre - OH + R - Si(OH)_3 \rightarrow Fibre - O - Si(OH)_2 - R \qquad \text{(Scheme 5)}$$

Maleated coupling agents

The use of maleated coupling agents has proven to be an extremely efficient means of improving interfacial interactions between wood flour or fibre and polymer matrices. The MA groups react with the hydroxyl groups and remove them from the fibre cells reducing hydrophilic tendency. The reaction scheme is given in Scheme 6. Moreover, the maleated coupler forms C-C bond with the polymer chains of the matrix (George *et al.*, 2001). The strongest adhesion can be achieved when the covalent bonds are formed at the interface between fibres and coupling agent along with molecular entanglement between coupling agent and the polymer matrix (Huda *et al.*, 2006). The reaction mechanism of coupling agent with wood flour or fibre and matrix can be explained as the activation of the copolymer by heating before the fibre treatment and then the esterification of the cellulosic fibre. This treatment increases the surface energy of wood flour or fibre to a level much closer to that of the matrix, and thus results in better wettability and enhances the interfacial adhesion between the filler and matrix (Li *et al.*, 2007).

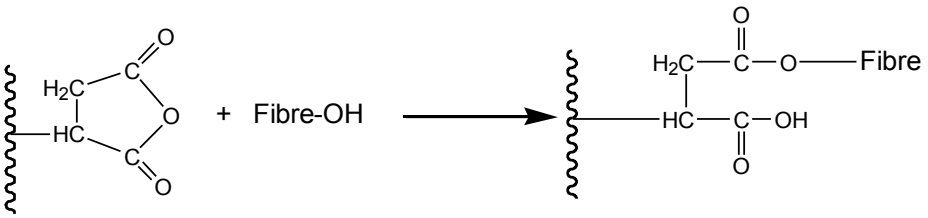

(Scheme 6)

Table 2.5 Recent work on chemical treatment of lignocellulosic polymer composites

Composite	**Treatment**	**Effect and outcome of the treatment**	**References**
Jute fibre/epoxy composite	Mercerisation	The alkali treatment removed the cementing layer consisting of low molecular fats, lignin, pectin and hemicellulose in cellulose fibrils, leading to a cleaner and rougher fibre surface; thus, the resin wetting, and the interaction and mechanical interlocking between fibre and matrix were significantly improved, i.e. the interfacial shear strength of the composite was increased up to 40% after the treatment.	(Doan *et al.*, 2012)
Flax fibre/PP composite	Acetylation	The tensile and flexural strength of the treated composites increased with the increasing of acetylation up to 18% and then decreased; the increase was due to the removal of lignin and extractives, the increase in cellulose content, effective surface area and thus interfacial adhesion; the decrease was because of the degradation of cellulose and generation of internal crack and damage in the fibres.	(Bledzki *et al.*, 2008)
Flax fibre/PE composite	Benzoylation Peroxide treatment	It was observed more uniform dispersion of the treated fibres within the polymer matrix, and also less agglomerated fibres with the presence of dissociated fibres in the matrix, which contributed to more	(Wang *et al.*, 2007)

		efficient stress transfer from the matrix to the fibres upon stress solicitation, resulting in superior physical and mechanical properties.	
Jute/polyester and jute/epoxy composites	Siloxane treatment	The bifunctional siloxane molecules created molecular continuity across the interface through covalently bonding with both cellulose surface and polymer resin of the composite; as a result, the tensile strength, flexural strength, and interlaminar shear strength of the composites were increased.	(Seki, 2009)
Jute fibre/HDPE composite	Maleated coupling agent treatment	With respect to the untreated composite, the composites fabricated at 1% MAPE concentration suggested considerable enhancement in tensile, flexural and impact strength (38%, 45% and 67% respectively); the γ and α relaxation peaks shifted to higher temperature regions after the treatment due to the segmental immobilisation of the matrix chains at the fibre surface, indicating the enhanced interfacial adhesion.	(Mohanty and Nayak, 2006; Mohanty *et al*., 2006)

2.2.3 Bonding mechanisms of lignocellulosic polymer composites

In lignocellulosic polymer composites, the main constituents are the reinforcing fibres and polymer matrix. The properties and performance of the composites rely on three main parameters: matrix, reinforcement and interface. The interface region between the fibre and the matrix has been recognised to play a predominant role in governing the global material behaviour. The interface in composites, often considered as an intermediate region formed due to the bonding of the fibre and matrix, is in fact a zone of compositional, structural, and property gradients, typically varying in width from a single atom layer to micrometers. There is a close relationship between the processes occur on the atomic, microscopic and macroscopic levels at the interface. In fact, the knowledge of the sequences of the events occurring on different levels is extremely important in understanding the nature of interfacial phenomena. The interface region controls the stress transfer between the fibre and matrix, which is primarily dependent on the level of interfacial adhesion (George *et al.*, 2001). A reasonable interfacial strength ensures the maximum stress level and can be maintained across the interface and from fibre to matrix without disruption. The efficiency of the load transfer is determined by the molecular interaction at the interface along with the thickness and strength of the interfacial region formed (Ngah, 2013; Drzal and Madhukar, 1993). The fibre-matrix interfacial bonding mechanisms in general include interdiffusion, electrostatic adhesion, chemical reactions and mechanical interlocking, which together are responsible for adhesion and usually one of them plays a dominant role.

Interdiffusion occurs on the basis of intimate intermolecular interactions between the molecules of the fibre substrate and the resin resulting from Van der Waals forces or hydrogen bonding (Liu *et al.*, 2012). In fact, there are two stages involved in this adhesion mechanism, i.e. adsorption and diffusion. In the first stage, two constituents, fibre and matrix should have intimate contact which is in turn governed by two actions including spreading and penetration. Once good wetting occurs, permanent adhesion is developed through molecular attractions, e.g. covalent, electrostatic, and Van der Waals. On the other hand, good wetting between the substrates leads to the interdiffusion of both fibre and matrix

molecules. The extent and degree of diffusion depends primarily on the chemical compatibility of the constituents and penetrability of the substrate (Kim and Pal, 2011). Electrostatic adhesion is attributed to the creation of opposite charges (anionic and cationic) on the interacting surfaces of fibre and polymer matrix; thus, an interface consisting of two layers of opposites charges is formed, which accounts for the adhesion of two constituents of the composite. Chemisorption occurs when chemical bonds including atomic and ionic bonds are created between the substances as a result of chemical reactions (Liu *et al.*, 2012). Available physical and chemical bonds depend on the surface chemistry of the substrate and are sometimes collectively described as thermodynamic adhesion.

The mechanical interlocking phenomenon explains the adhesion when a matrix penetrates into the peaks, holes, valleys and crevices or other irregularities of the substrate, and mechanically locks to it (Liu *et al.*, 2012). It happens on a millimetre or micron length scale, while diffusion entanglement within the cell wall pores of the fibre occurs on a nanoscale. The adhesion theories relying on mechanical interlocking can occur over larger length scale on the contact area. Adhesion, capillary forces, and other interaction factors can be ignored in most microscopic devices but they often dominate the behaviour of bonding quality at nanometre scales. Flow of polymer resin proceeds into the interconnected network of lumens and open pores of the natural fibre, with flow moving primarily in the path of least resistance. The adhesive occupies the free volume within the cell wall and therefore inhibits shrinking and swelling. The adhesive penetration of fibre occurs on two or more scales. There is micro-penetration, which occurs through the cell lumens and pits. Additionally, there is nano-penetration that occurs in the cell wall. Macro penetration of adhesive through process-induced cracks is also worth considering. Penetration of adhesive on any scale will impact bonding quality. The permeability is also a fibre related factor controlling the resin penetration. Permeability varies by surface characteristics and by direction e.g. tangential, radial and longitudinal. The mechanical interlocking mechanism is often used in polymer composites by etching the polymer surface to increase the surface roughness thereby increasing the contact area for adhesive penetration and mechanical interlocking of the substrate (Kim

and Pal, 2011). On the other hand, an increase in mechanical interlocking gives rise to the enhancement of other bonding systems/mechanisms.

2.2.4 Interface structure of lignocellulosic polymer composite

2.2.4.1 Morphology

SEM is the mostly used technique for investigating fibre-matrix interactions at fracture surfaces and polymer distributions in lignocellulosic polymer composites. It allows the observation of monomer impregnated samples directly and after cure to polymer composites to yield information on fibre-polymer interactions (George *et al.*, 2001). Migneault (Migneault *et al.*, 2015) investigated the variations of the wetting of the fibres employed in HDPE composites, including aspen wood, spruce bark and spruce wood fibres by SEM (Figure 2.2). It was found that aspen fibres were completely wetted (noted A) whereas spruce and bark fibres are not in close contact with HDPE (noted C). The SEM micrographs also showed variation in interfacial adhesion and mechanical interlocking at the fibre-matrix interface. Aspen fibres presented macro-fibrils at the surface interlocking with the polymer matrix, thus increasing fibre reinforcement (noted B). The wetting and interlocking phenomena suggested a superior stress transfer in the case of aspen wood fibres, which explained the better performance of the aspen fibre reinforced composite than other fibres reinforced composites.

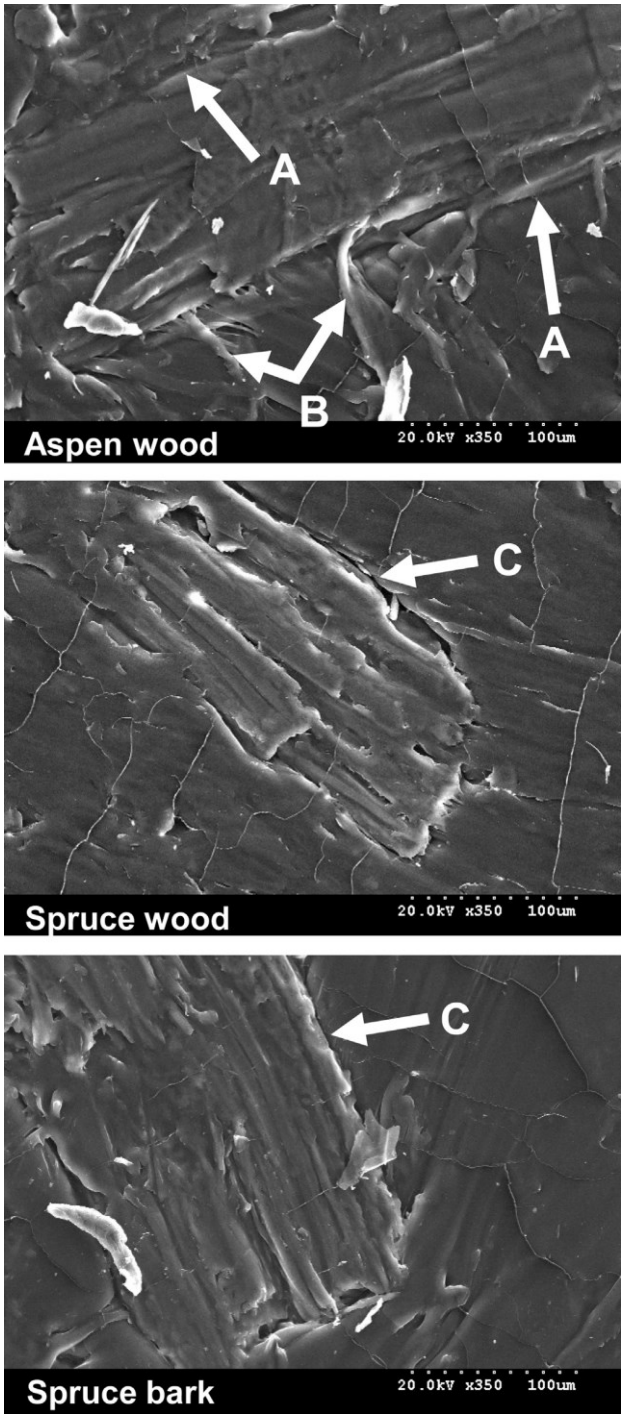

Figure 2.2 Morphology of WPC made with selected fibres (legend: A = close contact/good wetting, B = macro-fibrils, C = no close contact) (Migneault *et al.*, 2015)

Pinto (Pinto *et al.*, 2013) examined the effect of silane treatment and Z-axis reinforcement on the morphological structure of jute-epoxy laminated composites by the use of SEM, the results were shown in Figure 2.3. The fibres in the untreated plain weave sample (Figure 2.3a) appeared largely intact and

undisturbed from their aligned position, denoting that the fibre/matrix interface failed before enough stress could be transferred to the fibres to break or pull them out. The untreated unidirectional sample (Figure 2.3c) showed similar fracture with the features (A) fracutred matrix and (B) intact and aligned fibres to the untreated plain weave sample. The difference in this case was the dominance of clean matrix fracture without any visible fibres suggesting the delamination resistance of this sample was primarily governed by matrix failure. Figure 2.3b showed the significant changes of the fracture surface of silane treated sample over that of untreated counterpart, i.e. (A) pulled-out and fractured fibres and (B) matrix fragments clinging to the surface. Although the matrix fracture was still present, the fibre pull-out and breakage were seen to contribute to the sample's fracture resistance, implying the interface between fibre and matrix was strong enough to support the stress transfer to fibre to avoid the failure of the interface. The improved stress transfer from matrix to the fibre, which led the fibre to be pulled out prior to debonding, can also be seen on the surface of silane treated unidirectional composite with the presence of the more removed fibres from the epoxy matrix (A, Figure 2.3d) and the great deal of matrix fragments attached to the surface (B, Figure 2.3d).

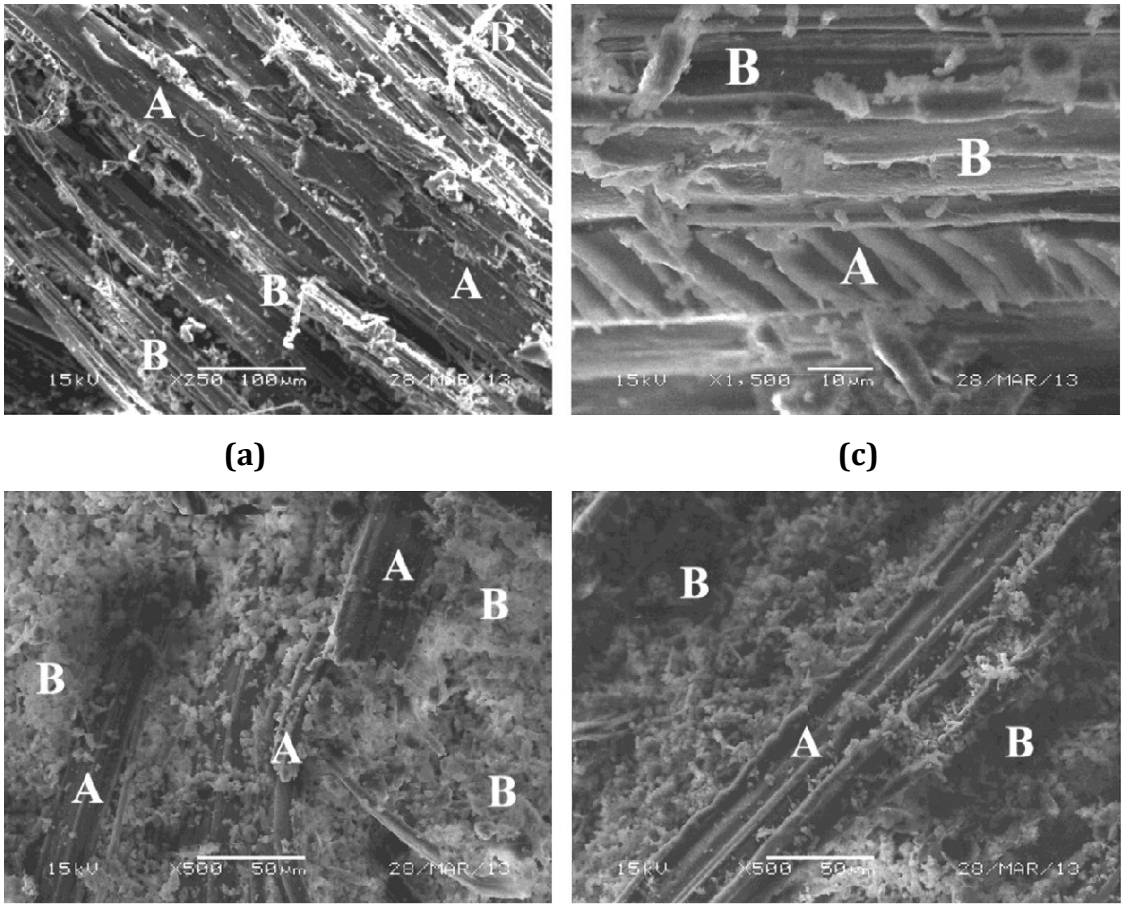

Figure 2.3 Morphology of the failure surfaces of (a) untreated and (b) silane treated plain weave jute-epoxy composites; and (c) untreated and (d) silane treated unidirectional jute-epoxy composites (Pinto *et al.*, 2013)

2.2.4.2 Interfacial bonding capacity

2.2.4.2.1 Micromechanical measurements of interface shear capacity

The interpretation of fibre/matrix adhesion is of special significance for the successful design and proper utilisation of lignocellulosic polymer composites. There are several micromechanical testing methods for measuring the fibre/matrix interfacial adhesion, examples are single fibre fragmentation test, single fibre pull-out test, microbond test, etc. The detailed summarisation of these tests can be found in the book of Kim & Mai (Kim and Mai, 1998).

The single fibre fragmentation test is originally developed from the early work of Kelly & Tyson (Kelly and Tyson, 1965), who investigated the brittle tungsten fibre that broke into multiple segments in a metal matrix composite. In the

fragmentation test (Figure 2.4), a single fibre is totally encapsulated in a chosen polymer matrix, which in turn is loaded in tension. This experiment is conducted under a light microscope in order to *in situ* observe the fragmentation process. The fibre inside the resin breaks into increasingly smaller fragments at locations where the fibre's axial stress reaches its tensile strength. This requires the resin system to be of a sufficiently higher strain-to-failure than the fibre. When the fibre breaks, the tensile stress at the fracture location reduces to zero. Due to the constant shear in the matrix, the tensile stress in the fibre increases roughly linearly from its ends to a plateau in longer fragments. The higher the axial strain, the more fractures will be caused in the fibre, but at some level the number of fragments will become constant as the fragment length is too short to transfer enough stresses into the fibre to cause further breakage. The shortest fibre length that can break on application of stress is defined as the critical fibre length, l_c. The average interfacial shear strength τ, with regards to the fibre strength σ, and the fibre diameter d, can be estimated from a simple force balance expression for a constant interfacial shear stress: $\tau = \sigma_f d/2l_c$ (Feih et al., 2004).

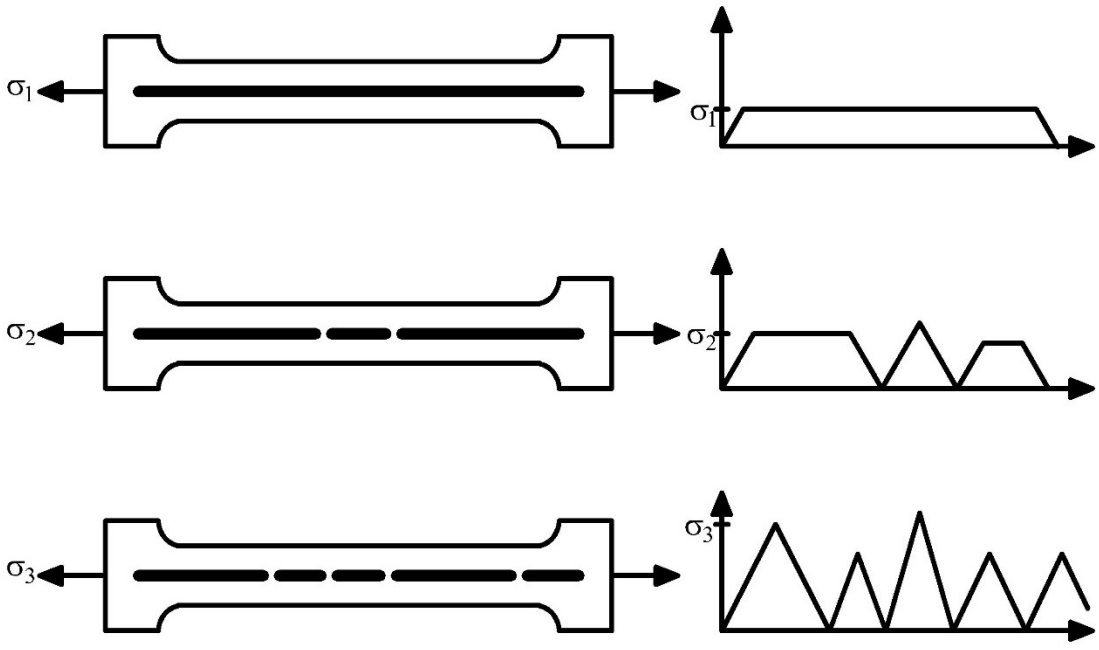

Figure 2.4 Schematic of single fibre fragmentation test (Feih *et al.*, 2004)

In the single fibre pull-out test (Figure 2.5), the fibre is embedded in a block of matrix. The free end is gripped and an increasing load is applied as the fibre is pulled out of the matrix while the load and displacement are measured (Pickering, 2008). At the first stage of pull-out loading, the induced shear stresses along the fibre do not exceed the bond strength between the fibre and matrix. Once the force required to pull the fibre out of the block is determined, the corresponding interfacial shear strength can be calculated. The maximum load, F, measured before the detachment of the fibre from the matrix is related to the average value of the fibre-matrix shear strength, τ, through the equation $F = \tau\pi dl$, where πd is the fibre circumstance and l is the embedded fibre length (Pickering, 2008).

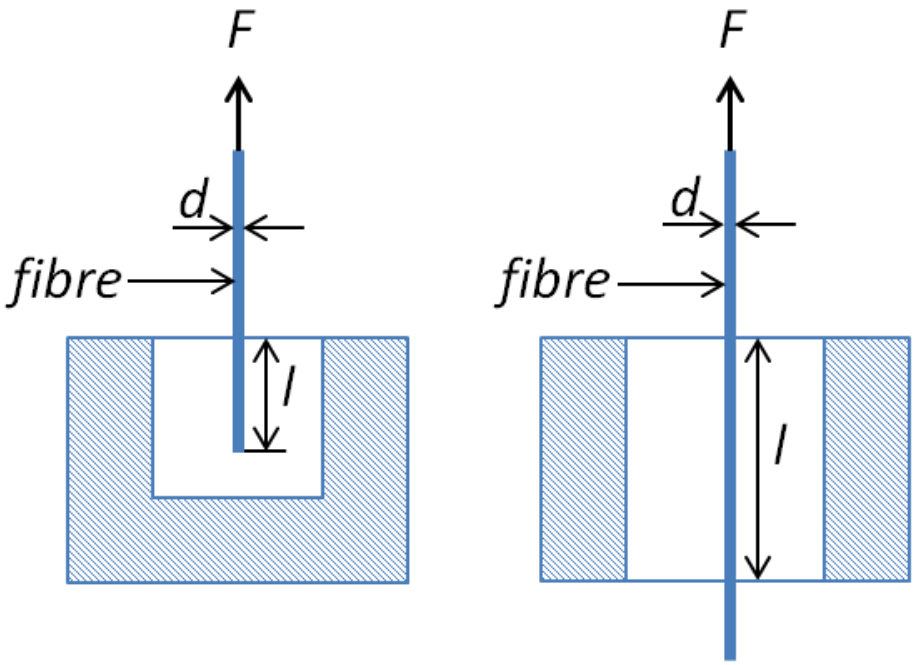

Figure 2.5 Schematic of single fibre pull-out test

The other test method of interfacial shear strength, microbond test, is considered as a modified single fibre pull-out test. It consists of first applying small amount of resin onto the fibre surface in the form of a droplet that forms concentrically around the fibre in the shape of an ellipsoid, and then applying a shearing force to pull the fibre out of the droplet or vice-versa, thus the bead is restrained by opposing knife edges (Figure 2.6) and stripped off, the applied load and the blade displacement are recorded. Assuming that the interface is in a uniform state of shear stress, the average of shear stress can be calculated by dividing the

maximum measured force of debonding by the embedded area of fibre, i.e. $\tau = F/\pi dl$. The bond strength value can be used for investigating the dependence of composite performance on the energy absorbing characterisation of the interface and to establish the extent to which the fibre surface treatment can alter bonding (George *et al.*, 2001).

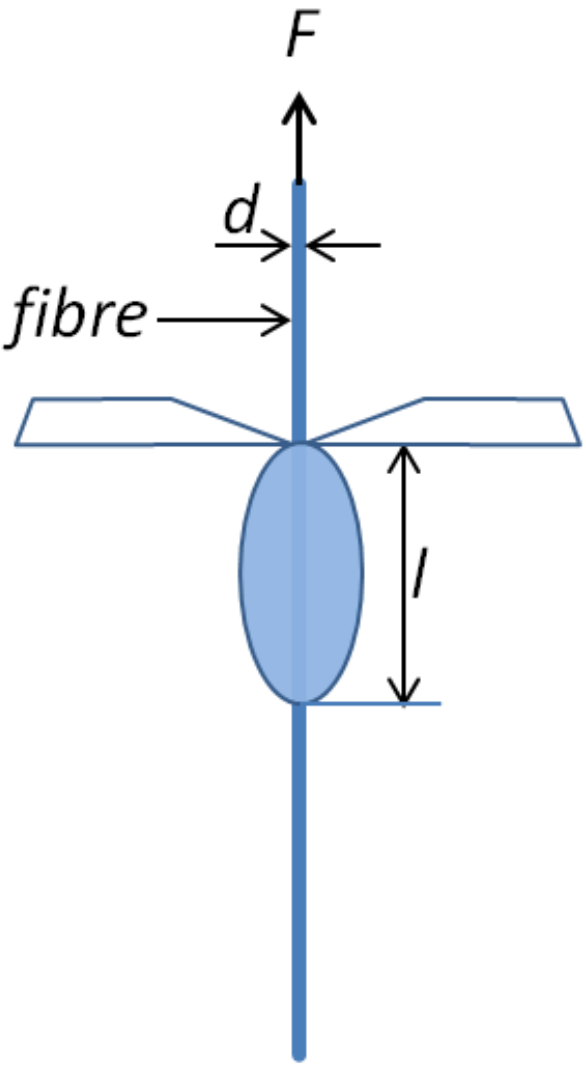

Figure 2.6 Schematic of microbond test

2.2.4.2.2 Nanomechanical measurements of interface bonding capacity

Nanoindentation technique is an effective method in determining material surface properties at nanoscale, and has recently found its application feasible to plastics and natural fibres (Ghomsheh *et al.*, 2015; Lee and Deng, 2013; Zhang *et al.*, 2012; Wu *et al.*, 2010; Xing *et al.*, 2009; Lee *et al.*, 2007a; Tze *et al.*, 2007; Gindl *et al.*, 2006; Hobbs *et al.*, 2001; Oliver and Pharr, 1992).This method is achieved

by monitoring a probe penetrating into the specimen surface and synchronously recording the penetration load and penetration depth (Zhang *et al.*, 2012). A schematic representation of a typical loading-displacement curve obtained during a full cycle of loading and unloading is presented in Figure 2.7.

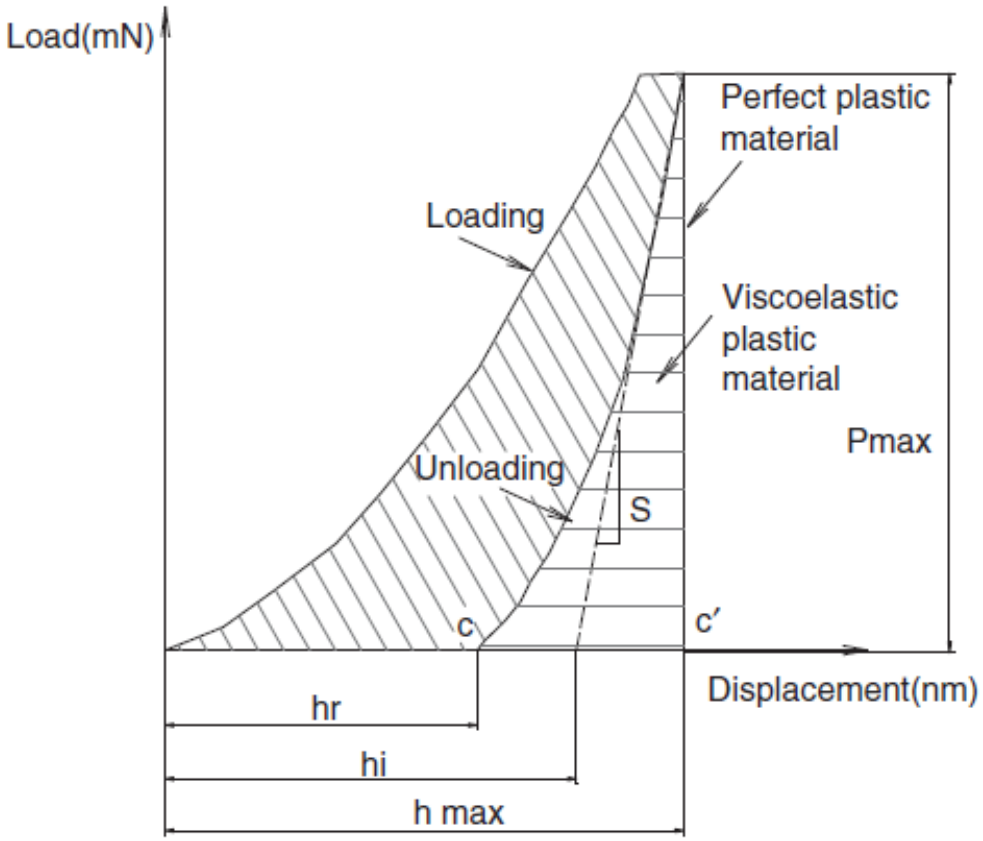

Figure 2.7 Typical loading-unloading curve of nanoindentation test (Dhakal *et al.*, 2014)

In a typical test, a load in the range of 10 μN to 500 mN is applied to an indenter in contact with the specimen surface, an indent/impression is made (typically 10-500 nm) that consists of plastic and elastic deformation (Dhakal *et al.*, 2014). The maximum load P_{max}, the maximum depth h_{max}, the final depth after unloading h_r, and the slope of the upper portion of the unloading curve S are monitored in the loading-unloading cycle. The material properties, such as elastic modulus and hardness, can be extracted by analysing the data with the method developed by Oliver & Pharr (Oliver and Pharr, 1992). The nanoindentation technique is being established as the primary tool for investigating the mechanical properties of wood or fibre cell walls and polymers at nanoscale. However, extremely few

studies have been performed the interfacial properties of lignocellulosic polymer composite by using this technique.

Lee (Lee *et al.*, 2007a) investigated the hardness and elastic modulus of cellulose fibre and PP in a cellulose fibre-reinforced PP composite by the use of nanoindentation with a continuous stiff measurement technique. The hardness and elastic modulus in the interface region were measured with different indentation depth and spacing. It was assumed that the width of interface region (property transition zone) was less than 1 μm. However, 3D Finite Element Analysis-based results showed that even a perfect interface without property transition had almost same interface width as that measured by nanoindentation. Therefore, it would be difficult to calculate the exact mechanical properties using existing nanoindentation techniques without considering the effect of neighbouring material property in at least 8 times smaller region than indent size. Dhakal (Dhakal *et al.*, 2014) studied the effect of water absorption on the nanohardness of woven fabric flax and jute fibre-reinforced bioresin-based epoxy biocomposites with the application of nanoindentation following the immersion at room temperature. The nanohardness decreased from 0.207 GPa for the flax dry sample to 0.135 GPa for the flax wet sample owing to the weaker fibre interface resulted from the water immersion, whereas it seemed like the water absorption did not have adverse effect on the harness values of jute samples, which were 0.107 GPa and 0.112 GPa for dry and wet specimens respectively.

2.2.4.2.3 Spectroscopic measurements of interface bonding capacity

Fourier transform infrared spectroscopy (FTIR)

FTIR offers quantitative and qualitative analysis for organic and inorganic materials. It identifies chemical bonds in a molecule by producing an infrared absorption spectrum. The resulting spectra produce a profile of the sample, a distinctive molecular fingerprint that can be used to screen and scan samples for many different components. This effective analytical instrument for detecting functional groups and characterising chemical bonding information has been extensively used in composite materials.

Lu (Lu *et al.*, 2014) investigated the effects of alkali soaking and silane (i.e. glycidoxypropyltrimethoxysilane, KH560) coupling modification of bamboo cellulose fibres (BCF) and MA grafting of poly(L-lactic acid) (PLLA) on the improved interfacial property of cellulose/PLLA composites. The FTIR was applied to study the chemical structure of virgin cellulose and the changes after the pretreatments, and also the chemical structure of PLLA and cellulose/PLLA composites, with the results showing in Figure 2.8. The OH stretching vibration peak of virgin cellulose at 3421 cm^{-1} was shifted to 3415 cm^{-1} after the alkali treatment, which was ascribed to the disturbing of hydrogen bond interaction that linked the cellulose and the impurities. The KH560 treated fibre demonstrated that new chemical bonds had been formed after the treatment by showing the peak at 1117 cm^{-1} corresponded to Si-O-C stretching vibration and the peak at 802 cm^{-1} related to Si-C stretching in its FTIR spectrum. This was because the OH groups on silanol hydrolysed from KH560 condensed with the OH groups on cellulose, thus the $CH_2CH(O)CH_2O(CH_2)_3SiO$- group was grafted onto the lignocellulosic molecules. The improved interfacial adhesion between the lignocellulosic fibre and the matrix after the modifications can also be confirmed by the FTIR analysis of the composites, i.e. the filling of untreated BCF in the composite did not lead to the changes of absorption peaks owing to the poor interaction between the fibre and matrix, while after the modifications, the OH stretching vibration at 3657 cm^{-1} had shifted to about 3650 cm^{-1}, indicating the superior interactions between the BCF and PLLA.

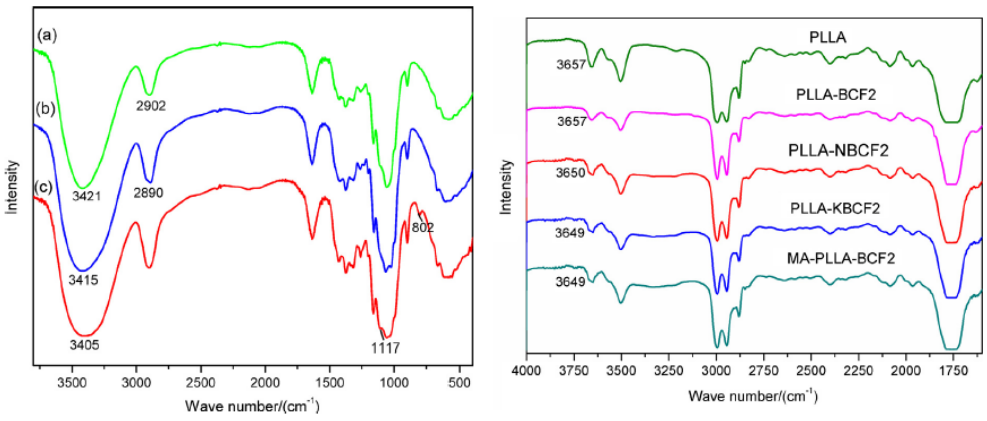

Figure 2.8 FTIR spectra of a) BCF, b) NaOH treated BCF, c) KH560 treated BCF, PLLA and cellulose/PLLA composites (Lu *et al.*, 2014)

Nuclear magnetic resonance spectroscopy (NMR)

NMR is an analytical chemistry technique used in quality control and research for determining the composition and purity of a sample as well as its molecular structure. The principle behind NMR is that many nuclei have spin and all nuclei are electrically charged. An energy transfer from the base energy to a higher energy level (generally a single energy gap) happens when an external magnetic field is applied. The energy transfer takes place at a wavelength that corresponds to radio frequencies and when the spin returns to its base level, and energy is emitted at the same frequency. The signal that matches this transfer is measured in many ways and processed in order to yield an NMR spectrum for the nucleus concerned.

NMR has become one of the significative techniques for surface characterisation of lignocellulosic polymer composites. Tavares (Tavares *et al.*, 2002) characterised the polyurethane (PU)/natural fibres (sisal fibre and sugarcane waste fibre (SCF)) composites focusing on interaction, homogeneity and compatibility between composite components by the use of solid-state NMR with the employed magic angle spinning (MAS) and cross-polarisation/magic angle spinning (CPMAS) techniques. Figure 2.9 presented the comparison of CPMAS and MAS ^{13}C NMR spectra for PU/sisal and PU/SCF composites. In comparison to fibres, the PU/SCF and PU/sisal composites changed the chemical shifts of C anomeric to low frequency, and their proton values $T_1^H\rho$ were higher than those of fibres. In addition, the values determined for CH-OH and CH_2-OH were increased for PU/SCF compared with SCF and decreased for PU/sisal compared with sisal. These behaviour suggested that the PU/SCF had a better interaction between the matrix and the filler. Furthermore, since the relaxation parameter values increased, the modifications in the molecular packing and fibre chains ordination would lead the PU to be acting as a plasticiser as well.

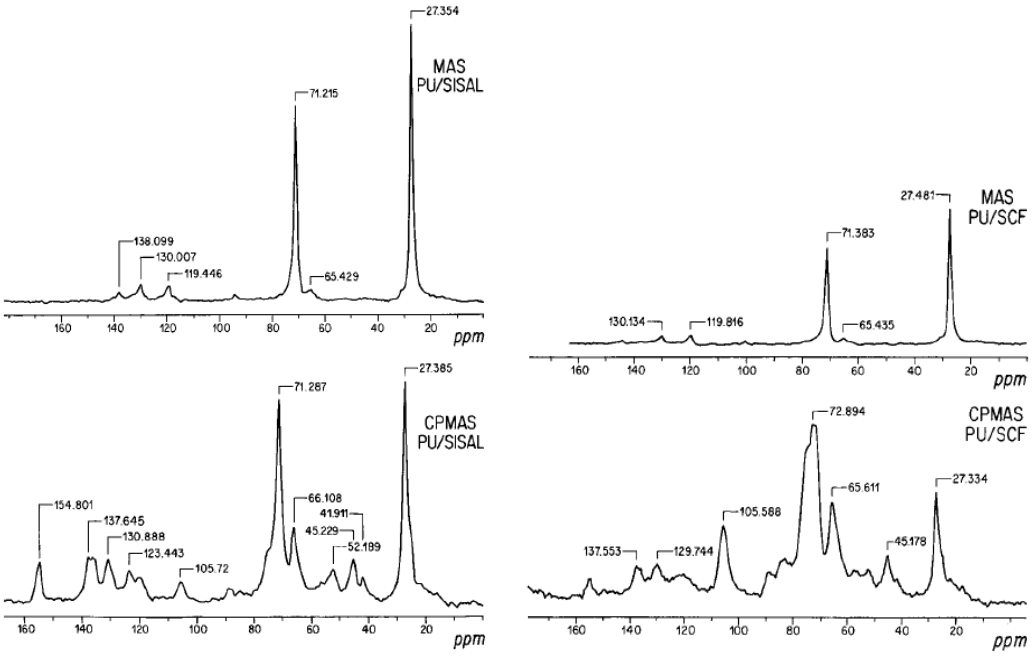

Figure 2.9 Comparison of CPMAS and MAS ^{13}C NMR spectra for PU/sisal and PU/SCF composites (Tavares *et al.*, 2002)

X-ray photoelectron spectroscopy (XPS)

XPS is a well-established technique for analysing the surface chemistry of a material, which provides valuable quantitative and chemical state information from the surface of the material being studied. XPS spectra are obtained by irradiating a solid surface with a beam of X-rays while simultaneously measuring the kinetic energy and electrons that are emitted from the top 1-10 nm of the material being analysed. A photoelectron spectrum is recorded by counting ejected electrons over a range of electron kinetic energies. Peaks appear in the spectrum from atoms which emit electrons of a particular characteristic energy. The energies and intensities of the photoelectron peaks enable the identification and quantification of all surface elements (except hydrogen). XPS has been used by researchers to qualitatively and quantitatively scrutinise the surface chemistry of treated and untreated wood flour or fibres and their composites (Kodal *et al.*, 2015; Tran *et al.*, 2013; Gironès *et al.*, 2007). Apart from the information about the effect of surface treatments it offers, this technique might also indirectly help in establishing mechanisms of interfacial behaviour such as identifying boundary layers (Pickering, 2008).

2.3 Lignocellulosic thermoplastic elastomers

2.3.1 Formulation of lignocellulosic thermoplastic elastomers

2.3.1.1 Modification of lignocellulosic filler and rubber-plastic matrix

Previous studies on TPE revealed that the plastic and rubber are miscible (Kumar *et al.*, 2002; Sonnier *et al.*, 2006; Ratnam *et al.*, 2001a). This has generated increasing interest in further study of incorporation of biomass into the existing TPE to achieve superior and multifunctional performance. The reported studies on wood flour or fibre filled rubber-plastic composite are shown in Table 2.6. Similar to wood flour or fibre filled polymer composites, surface modification is an indispensable issue to be dealt with during the formulation of natural fibre filled rubber-plastic composite.

In the literatures, surface modification using MAPP and silane coupling agents has gained great attention (Kakroodi *et al.*, 2012; Zurina *et al.*, 2004; Osman *et al.*, 2010a). MAPP was an active substance that on one hand formed covalent bonding and ester linkages with hydroxyl groups in cellulose, on the other hand reacted with the polymer radicals in plastic and rubber matrices, thus increased the crosslinking between the filler and matrices. Silane has been reported to be able to act like MAPP to improve the interactions at the rice husk powder (RHP)-acrylonitrile butadiene rubber (ANBR)-PP interface (Santiagoo *et al.*, 2011). Moreover, silane was able to help the composite to form a protective layer at the interfacial zone, which consequently prevented the diffusion of oil and water molecules into the silane-treated ANBR-PP composite.

Mansour (Mansour *et al.*, 2006) reported the modification of 1mm particle sized wood flour with NaOH solution (S, mercerisation), MA (esterification), glycidyl methacrylate (GM, oligoesterification), silane agent (SA) and also combinations of these treatments. The chemically treated wood flour was incorporated into SBR-PS composites. Both the mechanical and rheological properties of the composites followed the sequence: untreated wood flour<SA-treated flour<S-treated flour <S-MA-treated flour<S-MA-GM treated flour. This result could be ascribed to the consequent decreasing of hydroxyl groups of wood flour. Esterification was also adopted by Ratnam (Ratnam *et al.*, 2008) for the

modification of oil palm empty fruit bunch (OPEFB) fibre using methyl acrylate. The treated fibre filled ENR-PVC composites showed better interfacial adhesion between the fibre and polymer matrices than untreated fibre filled composites, which led to an increase of mechanical properties. However, no evidence suggested there was formation of any new covalent bonds between the treated fibre and rubber and plastic matrices.

Table 2.6 Wood flour and other natural fibres filled thermoplastic elastomers.

Wood/Fibre	**Rubber**	**Plastic**	**References**
Wood flour/powder	NR	PVC	(Salmah and Ismail, 2008; Kakroodi *et al.*, 2012; Raju *et al.*, 2008; Vladkova *et al.*, 2004a; Vladkova *et al.*, 2006; Vladkova *et al.*, 2004b; Ismail *et al.*, 2003; Mansour *et al.*, 2006; Vladkova *et al.*, 2003; Ismail and Nasir, 2001)
	SBR	PP	
	NBR	PS	
Rice husk powder	NR	PS	(Ahmed *et al.*, 2014; Wahab *et al.*, 2012a; Zurina *et al.*, 2004; Ratnam *et al.*, 2008)
	SBR	PP	
	ANBR	PE	
Oil palm empty fruit bunch fibre	NR	PVC	(Raju *et al.*, 2008; Ratnam *et al.*, 2008)
	Epoxidized NR (ENR)		
Kenaf fibre	NR	PP	(Anuar *et al.*, 2006; Anuar and Zuraida, 2011; Anuar *et al.*, 2007)
Microcrystalline fibre	NR	PE	(Abdelmouleh *et al.*, 2007)
Recycled newspaper	NR	PP	(Osman *et al.*, 2010a; Osman *et al.*, 2010b)

2.3.1.2 Processing of lignocellulosic thermoplastic elastomers

The most important manufacturing methods of TPE are extrusion, compression and injection moulding. The methods and equipment used for the formulation of conventional thermoplastics are generally suitable for wood flour or fibre filled thermoplastic rubbers. The treatments of wood flour or fibre using silane coupling agent, NaOH solution and MA solution were carried out before they were mixed with the previously mixed plastic and rubber matrices in the mixer. However, maleated coupling agents should be added during the mixing process of the filler and matrices. A preheating of the uniformly mixed filler-matrix compounds generated an easier and better formulation of the final product when compression moulding was employed as the fabrication method. It should also be noticed that the cooling process after compression was operated under pressure in order to prevent the deformation of the composites from the sudden change of pressure.

2.3.2 Properties of lignocellulosic thermoplastic elastomers

2.3.2.1 Curing characteristics

The curing characteristics of wood flour or fibre filled rubber-plastic composite were influenced by the treatment of filler, filling level, curing agent and the nature of polymer matrices. Increasing filler loading enhanced the interfacial interactions between the filler and rubber-plastic matrix, thus reduced the mobility of the polymer chains. The exhibition was the increase of both minimum torque and maximum torque (Wahab *et al.*, 2012a; Vladkova *et al.*, 2006; Zurina *et al.*, 2004; Santiagoo *et al.*, 2011; Vladkova *et al.*, 2003). The addition of curing agents was able to facilitate the crosslinking formulation, which increased the viscosity of the system and promoted the formulation of stable network structure. As a result, a higher resistance was exerted to the rotation of mixing rotor and the stabilisation torque increased (Salmah and Ismail, 2008; Ismail and Nasir, 2001). The thermoplastic rubber blend filled with MAPP or silane treated wood flour or fibre showed a higher stabilisation torque compared to the untreated and/or unfilled composites. This was because the enhanced interactions between the filler and matrices caused further increase of the viscosity of the mixing system (Zurina *et al.*, 2004; Ratnam *et al.*, 2008). However, the

stabilisation torque of RHP filled PS-SBR composite decreased when MA was employed as the modifier of RHP. This could be ascribed to the lubricant action from MA component in the composite (Zurina *et al.*, 2004). In addition, the comparison of curing characteristics of NBR compounds to that of NBR/PVC compounds suggested that the vulcanisation process was accelerated in the presence of PVC. Furthermore, minimum and maximum torques increased with the increase of wood flour loading when NBR was predominant or equal to PVC, but both parameters decreased when PVC turned to be predominant in the rubber-plastic matrix (Vladkova *et al.*, 2003).

2.3.2.2 Mechanical properties

TPE show the typical advantages of both rubbery materials and plastic materials. The incorporation of wood flour or fibre into the polymer matrices decreased the elasticity and flexibility of the polymer chains which resulted in more rigid composites (Raju *et al.*, 2008; Vladkova *et al.*, 2004b). Therefore, the hardness of the composites increased when more filler particles were incorporated. Due to the same reason, the tensile or Young's modulus of the composites also increased with the increase of filler loading (Kakroodi *et al.*, 2012; Raju *et al.*, 2008; Vladkova *et al.*, 2004b; Zurina *et al.*, 2004; Ismail *et al.*, 2003; Sameni *et al.*, 2004; Santiagoo *et al.*, 2011). However, the increase of the filler loading had a deleterious effect on the tensile strength and elongation at break of the composites (Raju *et al.*, 2008; Zurina *et al.*, 2004; Ismail *et al.*, 2003; Santiagoo *et al.*, 2011; Osman *et al.*, 2010b). This was associated with a number of reasons including 1) irregular shape of filler present; 2) poor wetting of the filler by the matrix; and 3) low interfacial adhesion and compatibility between the filler and matrix. For the first reason, the irregular filler shape without uniform structure of cross section and high aspect ratio was not able to uphold the stress transferred from rubber and plastic (Santiagoo *et al.*, 2011; Osman *et al.*, 2010b). In the other two cases, due to the hydrophilicity of wood flour or fibre, the abundant hydrogen bonding allowed them to cling together and resisted them from being wet by the hydrophobic matrix, which further results in the poor dispersion of the filler and stress transferring, weak interfacial adhesion and bonding (Raju *et al.*, 2008; Osman *et al.*, 2010b). This is also the reason of carrying

out pretreament of wood flour or fibre which has been discussed above. Without the modification of the raw materials, the only adhesion mechanism between the filler and matrix is interdiffusion. The pretreatment strengthened the filler-matrix bonding and interaction through chemical reactions. As a result, the composites showed an improved tensile strength compared with unmodified and unfilled composites (Kakroodi *et al.*, 2012; Raju *et al.*, 2008; Osman *et al.*, 2010b).

2.3.2.3 Thermal properties

The thermal behaviour of natural fibre rubber composites is closely related to its constituents. The examination of the thermal property of recycled newspaper (RNP)/carbon black (CB) and RNP/silica hybrids filled PP/NR composites at different filler concentrations by using Thermogravimetric Analysis (TGA) and Derivative Thermogravimetry (DTG) showed that the dehydration as well as the degradation of the fibre significantly contributed to the severe weight loss of the composites appeared in the range of 200°C to 400°C due to the major decomposition of cellulose, hemicellulose and other organic components rather than the weight loss occurred in the temperature range from 50°C to 200°C (Osman *et al.*, 2010a). DTG study suggested that there existed two main degradation stages in every sample with the presence of two maximum peaks, i.e. the major degradation of inorganic components in RNP at a temperature above 390°C and the decomposition of saturated and unsaturated carbon atoms in PP at a temperature above 480°C. It should be noted that fibre filled composites were more thermally stable than the fibre alone. The thermal stability of the composites could be improved further by increasing the CB and silica contents in RNP/CB and RNP/silica hybrid fillers. However, the thermal analysis of OPEFB fibre and poly(methyl acrylate) grafted OPEFB (OPEFB-g-PMA) fibre reinforced PVC/ENR blend composites revealed that the addition of OPEFB fibre and OPEFB-g-PMA fibre did not affect the original thermal stability of PVC/ENR blend composite, due to the similar onset degradation temperatures and peak values among all three composites (Ratnam *et al.*, 2008). Furthermore, there was no apparent difference in the thermal stability of ungrafted and grafted fibres filled PVC/ENR composites.

2.3.3 Microstructure of lignocellulosic thermoplastic elastomers

SEM is an effective technique for the investigation of filler distribution, interfacial adhesion and compatibility between the filler and matrix of composite materials. Examination of the fracture surfaces of wood flour or fibre filled rubber-plastic composites suggested that untreated composite displayed immiscible surface with the presence of noticeable holes or voids and gaps between the filler and matrix, and some fillers were even pulled out from the matrix, which resulted in the detachment of the wood flour or fibre from the matrix indicating the poor interfacial adhesion and wettability of the filler by the matrix (Vladkova *et al.*, 2004a; Ismail *et al.*, 2003; Sameni *et al.*, 2004; Santiagoo *et al.*, 2011; Osman *et al.*, 2010b). The RHP filled acrylonitrile butadiene rubber-polypropylene (NBR-PP) composite reported by Santiagoo (Santiagoo *et al.*, 2011) was exemplarily adopted here to gain a better capturing of the morphological examination of the composites (Figure 2.10). When more filler was incorporated into the composites, the surface exhibited the agglomeration of the filler which was unevenly distributed in the matrix, and then worsened the interfacial adhesion and bonding of the composites. This was in agreement with the gradual decrease of tensile strength and elongation at break resulted from the increasing filler loading. With the chemical treatment of the raw materials, the microstructure tended to be more miscible with less gaps and filler pulling out and better attachment compared to that of untreated composite, which was clearly shown in Figure 2.10. These phenomena indicated the better interaction and adhesion between the filler and matrix, positively influencing the tensile properties of the composites (Sameni *et al.*, 2004; Ismail *et al.*, 2003; Osman *et al.*, 2010b). In addition, the coupling agent used in the composites might also act as a dispersing agent between the polar filler and the nonpolar polymer to form hydrogen bonding, promoting the dispersion of the filler in the matrix (Osman *et al.*, 2010b).

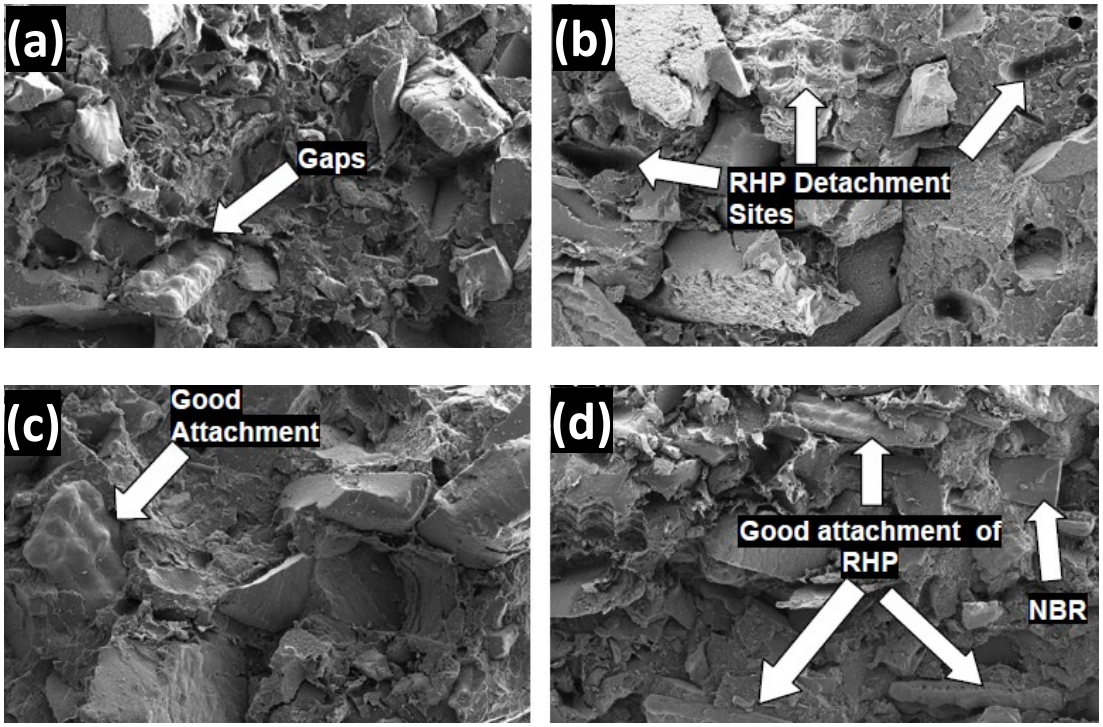

Figure 2.10 SEM images of 10 phr (a and c) and 30 phr (b and d) RHP filled ANBR-PP composites without silane coupling and with silane coupling (Santiagoo *et al.*, 2011).

2.4 Interim Conclusions

Thermoplastic composite materials have increasingly found their engineering applications in recent years especially in North America, Europe, China and Japan. The optimised interface governing the overall property has contributed to the successful formulation and thus commercialisation of the composites. Understanding the interface and bonding mechanisms is the key issue that requires significant research efforts in order to maximise the uptake and application of the composites. The development and/or selection of efficient and cost effective surface modifiers or dispersion aids or coupling agents for both filler and matrix are the first critical area to be considered for the development of the composites. The tendency is in favour of treatment that not only provides superb tailoring but also has minimal impact on economics and environment. Novel and advanced technologies for the formulation and characterisation of thermoplastic composites are, and continue to be of great significance to the sustainable development of waste biomass, worn tyres and recycled plastics, and many other end user industrial sectors.

Chapter 3 Materials and Methodologies

3.1 Introduction

This chapter describes the specifications of materials used in preparing Rubber-PE, WPC and RubWPC samples and sample preparation procedures. The analytical techniques employed in this work are described along with detailed explanation of testing procedures.

3.2 Materials

Recycled tyre rubber used in this research was supplied by J. Allcock & Sons Ltd (UK), with the particle size between 0.25 mm and 0.5 mm and bulk density of 0.36 kg/m^3; recycled wood flour was supplied by Rettenmeier Holding AG (Germany), with a bulk density of 0.285 kg/m^3; recycled polyethylene pellet with the melt flow index (MFI) of 0.6 g/10 min at 190^{o}C and bulk density of 0.96 kg/m^3 was obtained from JFC Plastics Ltd (UK).

Lubricants 12-Hydroxyoctadecanoic acid (12-HSA) and Struktol TPW 709 (A unique proprietary blend of processing aids made by Struktol company) were purchased from Safic Alcan UK Ltd (Warrington, UK); coupling agents, MAPE (MFI of 1.9 g/10 min at 190^{o}C, 0.5 wt% of maleic anhydride), Si69 (> 95% purity, 538.95 g/mol, 250^{o}C boiling point) and VTMS (> 98% purity, 148.23 g/mol, 123^{o}C boiling point), were purchased from Sigma-Aldrich (Dorset, UK), and their chemical formulae were presented in Figure 3.1. All the raw materials and additives were stored in a cool and dry place before uses.

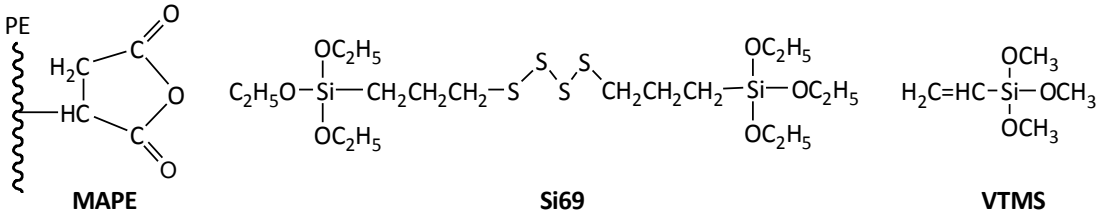

Figure 3.1 Chemical formulae of the coupling agents

3.3 Formulation of composites

The formulation of untreated and coupling agent treated Rubber-PE composites, WPC, and RubWPC with specific ratio (presented with percentage by weight) were summarised in Table 3.1, Table 3.2 and Table 3.3. All the composites were

carefully prepared under the same processing condition as follows: the required amount of PE for each batch was first placed in a Brabender Plastograph twin-screw mixer (Fig. 3.2) and allowed to melt at 100 rpm and 190°C for 2 min, and subsequently mixed with rubber powder and/or wood flour for 3 min. The lubricants and/or coupling agents were thus added into system and mixed for another 10 min. It should be mentioned that 3% of coupling agents was used constantly based on the results in the relevant literatures (Clemons *et al.*, 2011; Salimi *et al.*, 2009; Ismail *et al.*, 2002). The resulted mixture was thus ground to pellets by using a Retsch cutting mill (SM 100, Germany). The ground blends were compression moulded on an electrically heated hydraulic press. Hot-press procedures involved 20 min preheating at 190°C with no load applied followed by 10 min compressing at the same temperature under the pressure of 9.81 MPa, and subsequently air cooling under load until the mould reached 40°C.

Table 3.1 Formulation of Rubber-PE composites

Sample	Rubber (%)	PE (%)	TPW 709 (%)	12HSA (%)	MAPE (%)	Si69 (%)	VTMS (%)
Untreated	50	43	3.5	3.5	0	0	0
MAPE treated	50	40	3.5	3.5	3	0	0
Si69 treated	50	40	3.5	3.5	0	3	0
VTMS treated	50	40	3.5	3.5	0	0	3

Table 3.2 Formulation of WPC

Sample	Wood (%)	PE (%)	TPW 709 (%)	12HSA (%)	MAPE (%)	Si69 (%)	VTMS (%)
Untreated	50	43	3.5	3.5	0	0	0
MAPE treated	50	40	3.5	3.5	3	0	0
Si69 treated	50	40	3.5	3.5	0	3	0
VTMS treated	50	40	3.5	3.5	0	0	3

Table 3.3 Formulation of RubWPC

Sample	Rubber (%)	Wood (%)	PE (%)	TPW 709 (%)	12HSA (%)	MAPE (%)	Si69 (%)	VTMS (%)
Untreated	20	30	43	3.5	3.5	0	0	0
MAPE treated	20	30	40	3.5	3.5	3	0	0
Si69 treated	20	30	40	3.5	3.5	0	3	0
VTMS treated	20	30	40	3.5	3.5	0	0	3
MAPE&Si69	20	30	40	3.5	3.5	1.5	1.5	0
MAPE&VTMS	20	30	40	3.5	3.5	1.5	0	1.5
MAPE&Si69-10	10	40	40	3.5	3.5	1.5	1.5	0
MAPE&Si69-30	30	30	30	3.5	3.5	1.5	1.5	0

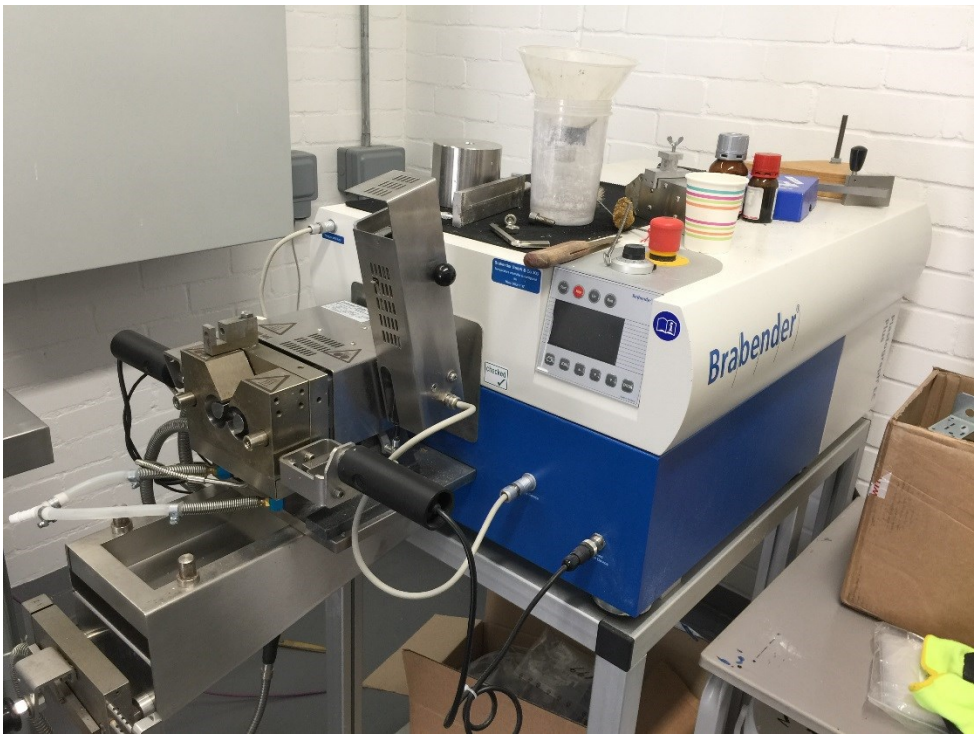

Figure 3.2 Brabender Plastograph twin-screw mixer

3. 4 Chemical structure and microstructure analyses

3.4.1 Solid state ^{13}C NMR analysis

Solid state ^{13}C NMR analysis was conducted on a Bruker spectrometer with a CPMAS probe operating at 100 MHz. The measurements were performed at ambient probe temperature with high power decoupling. Samples were packed in zirconium oxide rotors of 7 mm diameter fitted with Kel-F caps. Spectra were acquired at the spinning rate of 6 kHz, with 4096 scans per spectrum collecting in the region between -130 ppm and 270 ppm.

3.4.2 ATR-FTIR analysis

The FTIR spectra of the composites were recorded on a PerkinElmer Spectrum one Spectrometer equipped with diamond crystal and an incident angle of 45^{o} was used. The atmospheric compensation function minimises the effect of atmospheric water and CO_2 on the sample spectra without the need of reference or calibration spectra. The Absolute Virtual Instrument (AVI) in PerkinElmer actively standarises instrument response to improve repeatability and protect data integrity. The instrument was operated under the following conditions: 4000 – 650 cm^{-1} wave number range, 4 cm^{-1} resolution and 16 scans. The specimen dimension was 2 mm × 2 mm × 1 mm for both untreated and coupling agent treated composites, and the average of three measurements was reported.

3.4.3 SEM and FM analyses

All the composites were transversely cut by using a sliding microtome with the nominal thickness of around 25 microns for the morphological investigation of the cross sections. The SEM observation was conducted on a Leo 1430VP SEM operating at 10 kV, all the samples were conductively plated with gold by sputtering for 45 s before imaging. FM examination was conducted on a Carl Zeiss Axio imager microscope with a 100 W mercury burner, also, a green exciter-barrier filter set with 480/40 nm excitation wavelength and 510 nm emission wavelength was applied to observe the cross sections.

3.5 Physical and mechanical property analyses

3.5.1 Tensile property analysis

Tensile properties of the composites were determined at a crosshead speed of 1 mm/min according to the standard BS EN ISO 527-2:2012 on an Instron 5900 testing machine with 30 kN load capacity. Tensile strain is calculated by

measuring the length of stretch or elongation the specimen undergoes during tensile testing, is expressed as a percentage (%). For each sample, the tensile property reported is the average of six measurements. The tensile properties of recycled PE were also measured and given for reference: tensile stress at maximum load 23.05±0.17 MPa, tensile strain at maximum load 10.35±0.32%, tensile modulus 2385.41±133.25 MPa.

3.5.2 Dynamic mechanical analysis (DMA)

Dynamic mechanical properties of the composites were measured by using a dynamic mechanical analyser (Q800, TA Instruments, New Castle, USA) under single cantilever strain-controlled mode. The temperature ranges from -100^{o}C to 120^{o}C with a heating rate of 3 ^{o}C/min. The oscillation amplitude was 20 μm, the frequency was 1 Hz, and the specimen dimension was 17.5 mm × 10.8 mm × 1.4 mm.

3.5.3 Nanoindentation analysis

The samples for nanoindentation determination were prepared as follows: a sloping apex (around 45^{o}) was created on the cross section of the sample by using a sliding microtome, thus the sample was mounted onto a PowerTome ultramicrotome (Boeckeler Instruments, Figure 3.3) and transversely cut with a glass knife and a diamond knife to obtain an exceptionally smooth and flat surface. The cross section of the samples was firstly observed under an optical microscope to select the regions to be indented (Figure 3.4a). The tests were performed on a Nano Indenter (Hysitron TI 950 TriboIndenter, USA) equipped with a three-side pyramid diamond indenter tip (Berkovich) as shown in Figure 3.5. In each test region, the space between two adjacent testing positions was more than 30 times of the maximum indentation depth (Figure 3.4b and Figure 3.4c). The indentations were conducted under load-controlled mode consisting of three segments, i.e. loading with 150 μN in 5 seconds, holding for 2 seconds, and unloading in 5 seconds. A typical loading-displacement curve was presented in Figure 3.6. The maximum load P_{max}, the maximum depth h_{max}, the final depth after unloading h_r, and the slope of the upper portion of the unloading curve S were monitored in a full loading-unloading cycle. The material properties, such

as reduced elastic modulus and hardness, could be extracted by analysing the data with the method developed by Oliver and Pharr (Oliver and Pharr, 1992).

The hardness (*H*) was calculated as follows:

$$H = \frac{P_{max}}{A} \qquad \text{(Eq. 3.1)}$$

Where, *A* is the projected contact area at maximum load. *Er*, the reduced elastic modulus accounting for the compliance of the indenter tip, was determined as:

$$E_r = \frac{\sqrt{\pi}}{2}\frac{dP}{dh}\frac{1}{\sqrt{A}} \qquad \text{(Eq. 3.2)}$$

Where, *dP/dh = S*. The results reported in the work were from the indentations placed in the valid positions, namely clearly on the cells with intimate and firm resin contact, excluding the results from cracks and other positions.

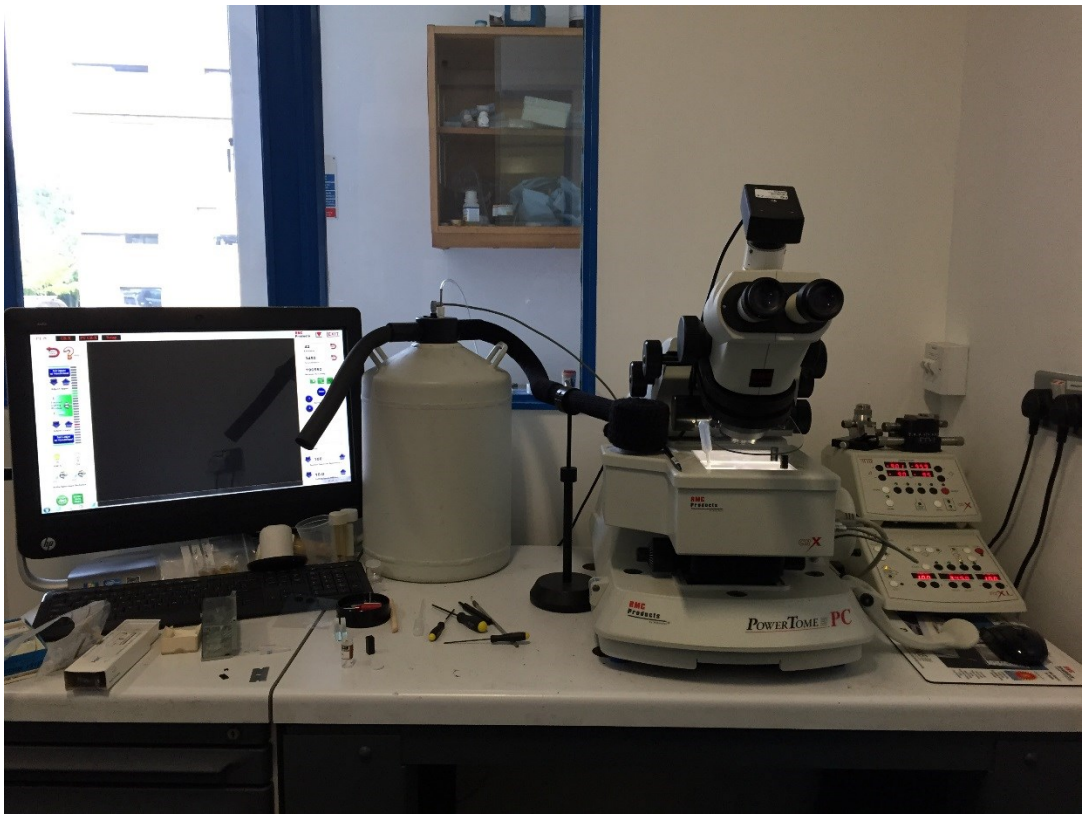

Figure 3.3 Boeckeler PowerTome ultramicrotome

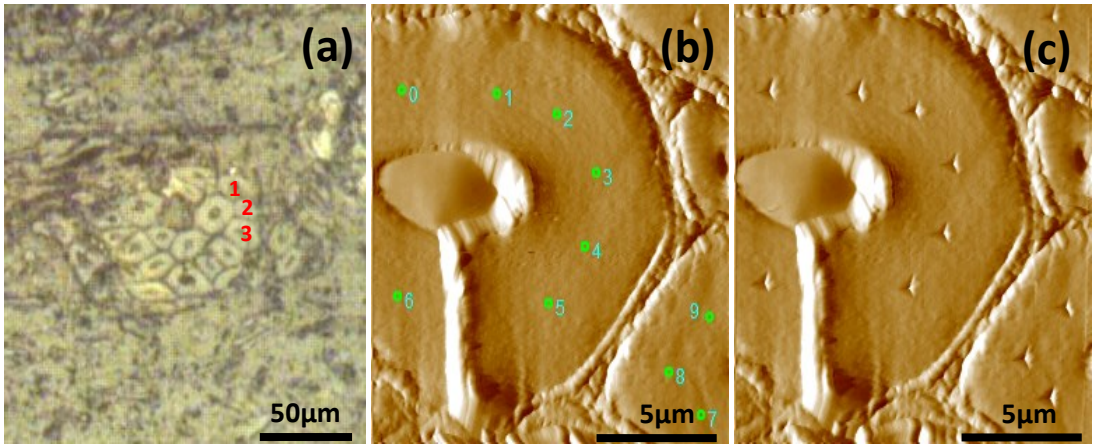

Figure 3.4 Typical *in situ* imaging nanoindentation test: (a) microscope image of testing cells in transverse section; (b) image of cell walls in region 1 of Figure 3.4a before indenting; (c) image of cell walls in region 1 of Figure 3.4a after indenting.

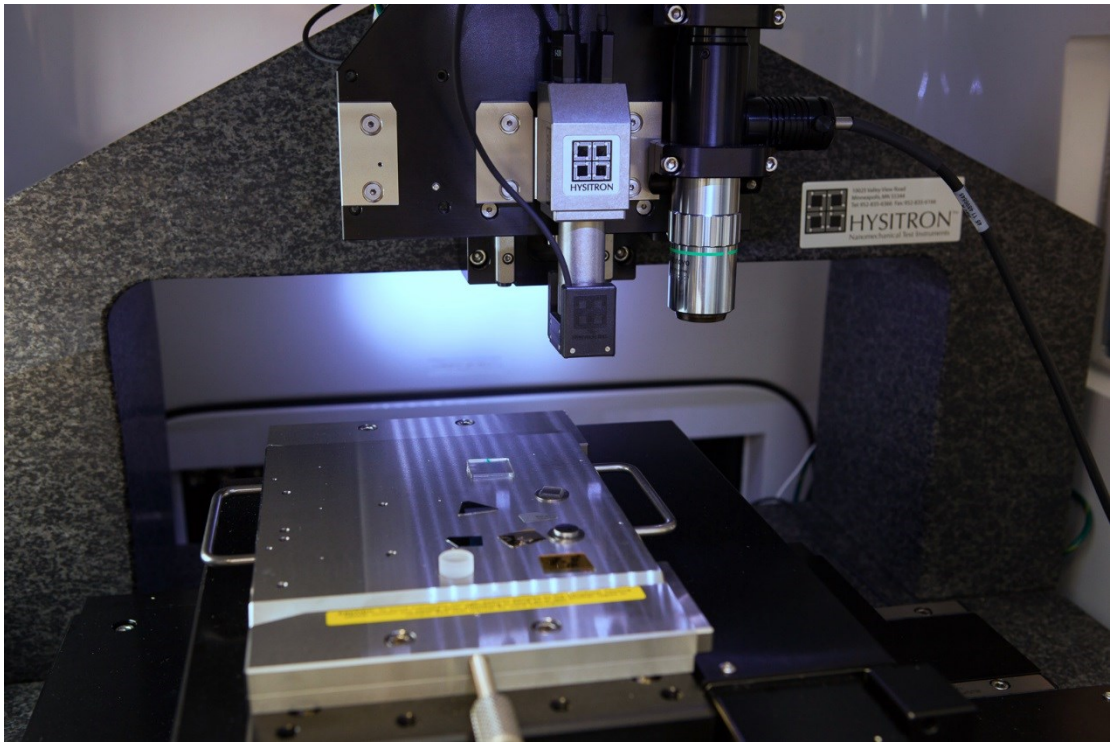

Figure 3.5 Hysitron TI 950 TriboIndenter for nanoindentation analysis

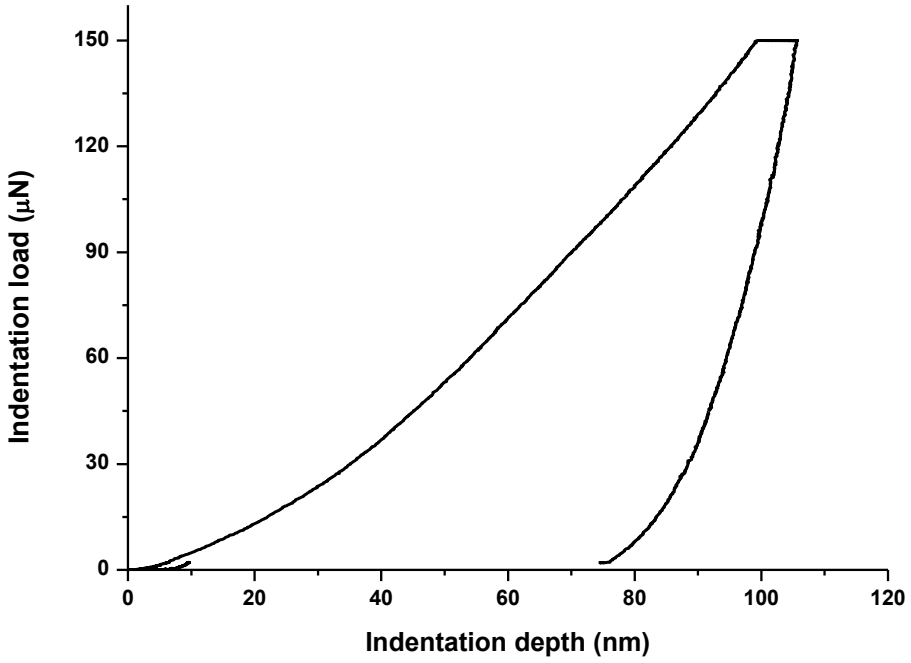

Figure 3.6 Typical loading-unloading curve of nanoindentation test.

3.6 Interim Conclusions

The details of the materials used in preparing Rubber-PE, WPC and RubWPC materials and the methods employed in formulating and analysing these composites have been presented in this chapter. The described methodologies were used to gather experimental results in Chapter 4, 5, 6, 7 and 8, except where specific experimental procedures were made in the following chapters, such that with thorough and detailed interpretation leads to achieving the goals of the project.

Chapter 4 Interfacial Optimisation and Characterisation of Rubber-PE Composites

4.1 Introduction

Coupling agents have been extensively employed in the development of ground tyre rubber (GTR) filled thermoplastic composites aiming at refining the disfavoured constituent compatibility and insufficient interfacial adhesion. Maleated olefins, such as MAPP or MAPE, had been proven to improve the adhesion between tyre rubber and polyolefins due to the presence of the MA functional group, resulting in smoother surface and better particle dispersion in a continuous matrix (Lee *et al.*, 2007b). Silane coupling agents were also found to be of the capability of enhancing the compatibility between recycled rubber and thermoplastics or thermosets by promoting rubber to interact with polymer matrix, which provided the compatibilised composites with more desirable mechanical properties than the uncompatibilised counterpart (Colom *et al.*, 2006; Kaynak *et al.*, 2003; Kaynak *et al.*, 2001). The effectiveness of these treatments was in general evaluated by the improvement in the physical and mechanical properties of the formulated composites. Nevertheless, the generation and variation of the chemical functionalities and structure during compatibilisation treatments, which undoubtedly concern the bonding scenario, microstructure and thus performance of the composites, unfortunately have not yet been thoroughly investigated.

In the present work, Rubber-PE composites were developed by the use of recycled tyre rubber and PE aiming at improving the sustainability of the recycling process of ground tyre rubber and thermoplastics and reducing the environmental impact from waste disposal. In order to formulate a reasonable composite, three different coupling agents, i.e. MAPE, Si69 and VTMS, were attempted to improve the compatibility, homogeneity and interfacial adhesion. The focus of this chapter was to reveal the chemical functionalities, structure and bonding of the formulated composites by carrying out ATR-FTIR and NMR analyses, thus, to explore their correlation with the microstructure and bonding scenarios, and eventually the contribution to the mechanical properties of the composites.

4.2 Results and Discussion

4.2.1 Chemical functionality and structure

4.2.1.1 NMR analysis

Figure 4.1 shows the ^{13}C NMR spectra of untreated and coupling agent treated Rubber-PE composites. The spectra were dominated by the resonances of PE at 43.71 ppm, 32.48 ppm, 26.17ppm and 21.57 ppm, which were assigned to methylene, methylene in the main chain, methine and methyl, respectively (Sombatsompop *et al.*, 2004b; Renneckar *et al.*, 2005). Resonances originated from rubber component were observed at 130.10 ppm and 14.67 ppm referring to aromatic C2 and C4 of SBR and -CH_3 at the branch chain of SBR (Figure 4.2) respectively (Arantes *et al.*, 2009; Sombatsompop *et al.*, 2004b). The diagnostic characteristics of isoprene units of NR (Figure 4.2) in tyre rubber were expected to be detected at around 33 ppm (C1), 28 ppm (C4) and 24 ppm (C5), which should have shifted and overlapped with the resonances of PE (Sakdapipanich *et al.*, 2006; Ricardo *et al.*, 2002; Buzaré *et al.*, 2001).

It was noticed that apart from the chemical shifts of rubber and PE, there was an additional peak presented at 74.50 ppm in the spectra of VTMS treated composite, which might be resulted from the oxidation of C-C bonds in rubber molecules under high temperature and pressure with the incorporation of VTMS. The general region of carbons with a single bond to oxygen ranged from 73 ppm to 83 ppm (Aganov and Antonovskii, 1982; Kehlet *et al.*, 2014). Epoxides were often anticipated to be the products of rubber oxidation, while the chemical shifts of which were rather around 55 ppm. Chemical shifts of secondary alcohols and in particular ethers could reach 73 ppm depending on the processing environment (Kehlet *et al.*, 2014). Peroxides and hydroperoxides might be the most downfield signals in the region between 72-75 ppm (Somers *et al.*, 2000; Aganov and Antonovskii, 1982).

It can be seen that the peaks at 92.08 ppm and 43.73 ppm in the spectra of treated composites were slightly broader than those in the spectrum of the untreated counterpart. This was primarily due to the fact that the width of resonance line was correlated to the segmental polymer motion. If the polymer molecules were

free to move in any direction, then the spectral line would be narrow, and vice versa (Somers *et al.*, 2000). In terms of the treatment processing, this might indicate that the addition of coupling agents into the composites resulted in more solid-like polymers with restricted molecular mobility. With respect to the potential crosslinking reactions between the coupling agents and raw materials owing to the treatments, NMR determination results did not unambiguously suggest the formulation of relevant chemical bonds. Specifically, C-S bonds and C-O-Si bonds were expected to be observed in the region of 45-55 ppm and 55-65 ppm respectively (Fyfe and Niu, 1995; Salon *et al.*, 2005; Zaper and Koenig, 1988; Silverstein *et al.*, 2014). In this regard, the lack of these bands in the corresponding NMR spectra might be explained by a number of reasons, including: 1) insufficient concentration of these bonds to be detected; 2) T_1 relaxation times of these units being much longer in comparison to the relaxation times of other molecular units in the polymers; and 3) T_2 relaxation times of these units being short enough to cause the signals to be broadened beyond detection (Sitarz *et al.*, 2013). Further scrutinising of the potential crosslinking between the coupling agents and constituents of the composites by other analytical technique would be of great significance for better understanding the compatibilisation impact of the treatments on the variations of chemical functionalities and structure of the composites, which was carried out in the next section.

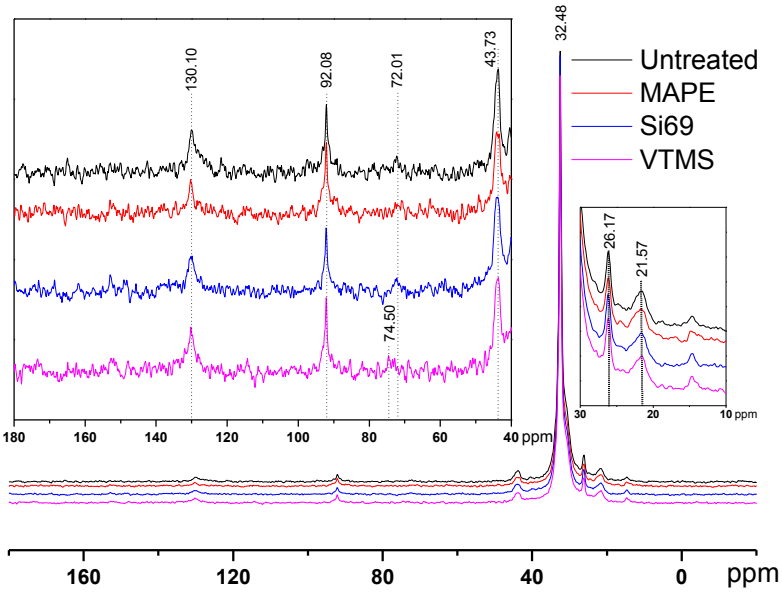

Figure 4.1 ^{13}C NMR spectra of untreated, MAPE, Si69 and VTMS treated Rubber-PE composites

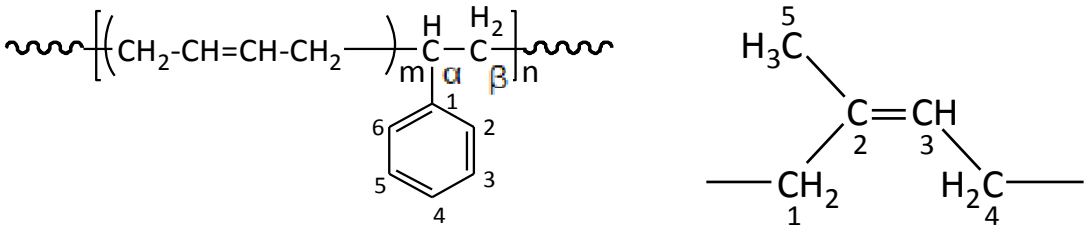

SBR **NR**

Figure 4.2 Chemical structure of SBR unit and NR unit

4.2.1.2 FTIR analysis

FTIR was employed to further explore the influence of the incorporation of the coupling agents on the chemical structure and bonding of the composites. Figure 4.3 demonstrates the comparison of the FTIR spectra of untreated and treated Rubber-PE composites. The spectral characteristics of the incorporated MAPE coupling agent were observed at 1713 cm^{-1} and 1637 cm^{-1} referring to C=O and C=C stretching vibrations of maleic anhydride moiety (Martínez-Barrera *et al.*, 2004; Lu *et al.*, 2005; Liu *et al.*, 2015). With respect to the spectral variation of rubber constituent, the band at 1062 cm^{-1} referring to the C-S-C stretching in the C-S bonds was shifted to 1095 cm^{-1} and became sharper after the treatment (Rai

et al., 2006; Akiba and Hashim, 1997). This might be an indication of the macromolecular entanglements between the rubber polymer chain and the grafted polyethylene in MAPE.

Si69 has been proven to be an effective coupling agent for improving the interfacial and overall property of rubber based composites, such as lignocellulosic fibre-rubber, geopolymer-rubber and carbon black-rubber composites (Noriman and Ismail, 2012; Salimi *et al.*, 2009; Thongsang and Sombatsompop, 2006; Choi, 2002; Ismail *et al.*, 2002; Ismail *et al.*, 1999). The effect of the silane treatment on the chemical structure of the composite could be clearly seen from the FTIR result. The Si69 treated composite demonstrated a much more intense band at 1053 cm^{-1} attributing to C-S-C stretching vibration, while the counterpart from the untreated was observed at 1062 cm^{-1} (Gunasekaran *et al.*, 2007; Rai *et al.*, 2006; Akiba and Hashim, 1997). The shift of wave number and increase of intensity may be attributed to the introduced Si-O-C bonds in Si69 and the C-S linkages formed between the silane and rubber polymers which may be proposed in Figure 4.4, namely the coupling agent Si69 with a sulfidic linkage between triethoxysilylpropyl groups was dissociated to form radicals under high temperature and pressure, thus the sulfide groups crosslinked with both SBR and NR macromolecules in rubber (Choi, 2002). The crosslinking with silane of rubber may trigger its further entanglement and/or chemical coupling with PE matrix owing to the activated surface (Karger-Kocsis *et al.*, 2013), which automatically reduced the chance to form sulfur-crosslinking within the sulfur-rich rubber molecules and simultaneously prevented the accumulation of rubber particles in the matrix to some extent (Choi, 2002; Thongsang and Sombatsompop, 2006). Thongsang (Thongsang and Sombatsompop, 2006) examined the effect of Si69 treatment on the properties of fly ash/NR composite, it was pointed out that with high loading of Si69 (4-8 wt%), the bulky triethoxysilylpropyl groups in Si69 might cause the steric hindrance to the linkage formation between the rubber molecules and the fly ash particles. In addition, a self-condensation of Si69 could occur at high Si69 contents, resulting in the formation of mono- and poly- layers of polysiloxane molecules on the surface of fly ash.

It was worth noting that the diagnostic characteristic of Si69, i.e. Si-O-C stretching at approximately 1100 cm^{-1} and 1072 cm^{-1}, was not found in the spectrum, which should have overlapped with the band of C-S-C stretching after being incorporated into the composite (Abdelmouleh *et al.*, 2007; Bengtsson and Oksman, 2006). These spectral characteristics unveiling the chemical interaction between the coupling agent and raw materials were unfortunately not detected in the above NMR analysis (Section 4.2.1.1) probably due to insufficient concentration or inappropriate relaxation time of the corresponding bonds (C-O and C-O-Si).

VTMS was another coupling agent applied for refining the interface of the composite. The FTIR spectra of the untreated and VTMS treated composites did not show considerable difference in terms of the band appearance and intensities, especially the bands corresponding to C-O-Si and C-S-C bonds (1020 cm^{-1} - 1100 cm^{-1}), which might be an indication of fairly limited crosslinking or entangling occurred between the coupling agent and raw materials. This result was consistent with the NMR analysis of this treatment.

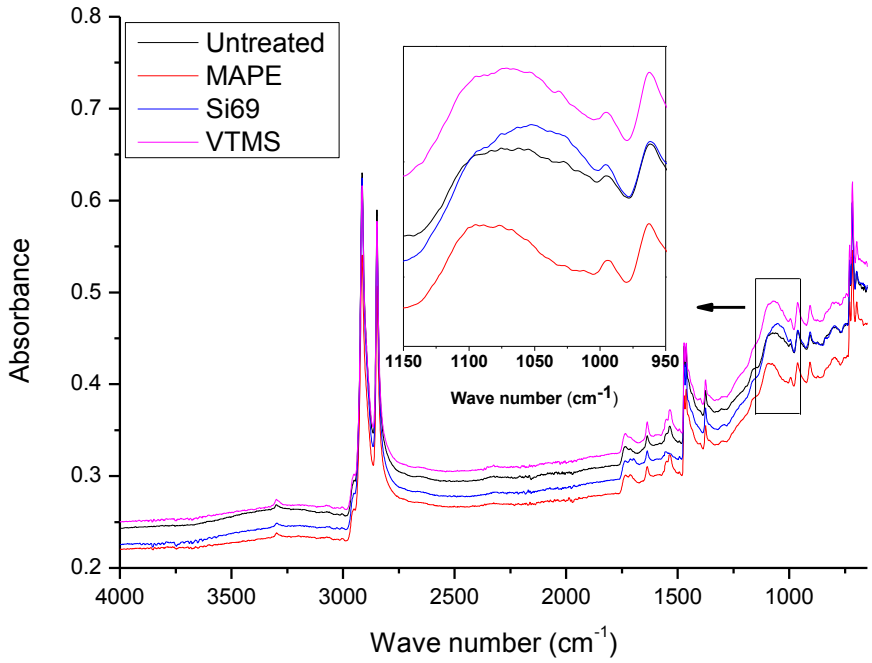

Figure 4.3 FTIR spectra of untreated, MAPE, Si69 and VTMS treated Rubber-PE composites

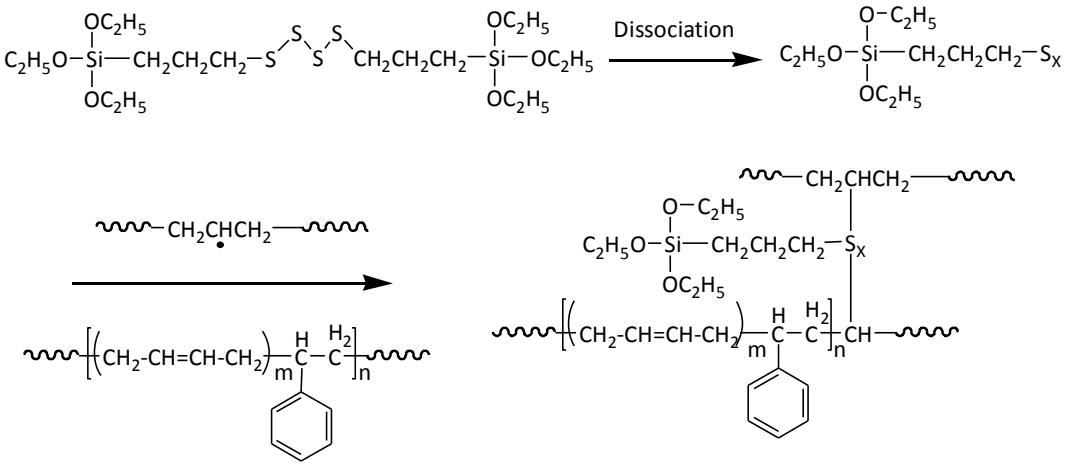

Figure 4.4 Proposed chemical reaction between Si69 and the polymers of Rubber-PE composite

4.2.2 Interface structure and bonding

The effect of the incorporation of the coupling agents on the interface structure and bonding scenario of Rubber-PE composites was scrutinised by SEM, with results presenting in Figure 4.5. Clear cracks and boundaries can be observed between the components of the untreated composite (Figure 4.5a), suggesting the poor compatibility between the untreated raw materials. The incompatibility seemed not only to prevent the close interaction between rubber and PE, but also to impede the hydrodynamic flow of the polymer resin, which gave rise to the formation of a number of voids within the matrix as shown in Figure 4.5a. These phenomena evidently indicated the inappropriate interfacial contact and adhesion of the untreated composite. The SEM image of MAPE treated composite (Figure 4.5b) demonstrated an improvement of constituent compatibility and wettability of the rubber by the resin after the treatment, by showing a greater embedment of the rubber particles in the matrix with subtle cracks and voids. The scenario in the Si69 treated composite is completely different from the others, displaying well embedded rubber particles in the matrix along with firmly bonded interface (Figure 4.5c). Moreover, the phase structure of the matrix was likely of interpenetrating network, being smoother and more compact than that of the other composites. These observations should be related to the enhanced chemical compatibility and interdiffusion through the intermolecular interactions between the MAPE and Si69 coupling agents and rubber and PE molecules, i.e. the macromolecular entanglements between the grafted PE moiety

in MAPE and the polymer chains of both rubber and PE in the composite, and the chemical crosslinking between dissociated Si69 and rubber molecules followed by the entangling with PE polymer (Section 4.2.1). These chemical interactions gave rise to the creation of entangled and/or crosslinked rubber-PE network accompanied by the increase of rubber wettability by matrix, constituent compatibility and interfacial adhesion of the corresponding composites.

It was presumed that the enhancement in the adhesion and bonding at the MAPE and Si69 treated Rubber-PE interfaces would benefit the performance of the composites given the interface was recognised to play a predominant role in governing the global composite behaviour by controlling the stress transfer between the constituents of a composite. In comparison to the untreated, the VTMS treated composite did not demonstrate significantly distinct interface structure and bonding scenario (Figure 4.5d), suggesting the inferior compatibilisation and interface refinery by VTMS treatment. This was in a good agreement with the previously discerned comparatively limited chemical interactions between this coupling agent and the constituents of the composite (Section 4.2.1).

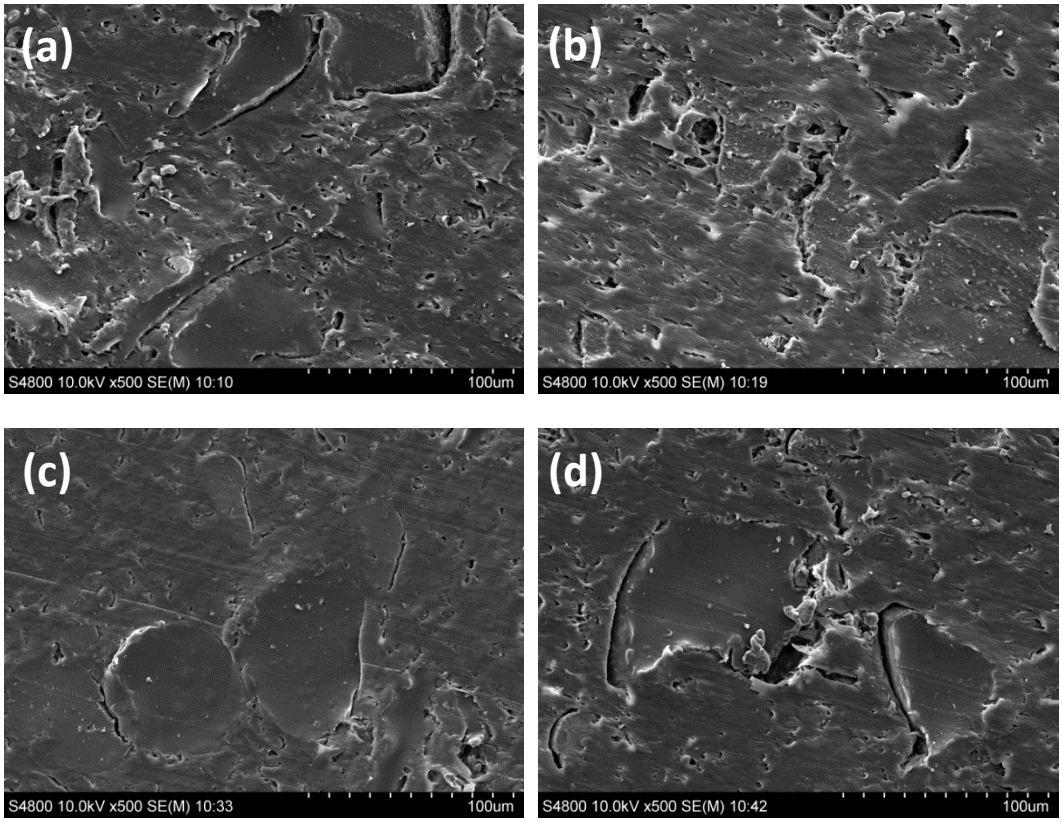

Figure 4.5 Microstructures of cross section of untreated (a), MAPE treated (b), Si69 treated (c) and VTMS treated (d) composites

4.2.3 Mechanical properties

4.2.3.1 Dynamic Mechanical Analysis (DMA)

Storage modulus is closely related to the load bearing capacity of a material (Mohanty and Nayak, 2006; Mohanty *et al.*, 2006). The temperature dependence of storage modulus of Rubber-PE composites was graphically enumerated in Figure 4.6. It was observed that the coupling agent treated composites had higher storage moduli than the untreated one, primarily due to the enhanced compatibility and interfacial adhesion between rubber and PE after the compatibilisation treatments as discussed in Section 4.2.2. The storage moduli in all composites decreased with the increase of temperature with a notable descent in the region from -75^{o}C to -25^{o}C, thus gradually reached a plateau region (50 – 120^{o}C) in which the modulus differentiation between the treated and untreated composite diminished.

The variation of loss modulus as a function of temperature was also presented in Figure 4.6 for the purpose of exploring the transition behaviour of the composites.

Both the untreated and treated composites demonstrated two relaxation peaks in their curves, i.e. the peaks at around 45°C were associated with the α transition of PE matrix, concerning the chain segment mobility in the crystalline phase due to the reorientation of defect area in the crystals (Bengtsson *et al.*, 2005; Mohanty and Nayak, 2006; Mohanty *et al.*, 2006), while the peaks at -45°C to -35°C were resulted from the molecular motion of rubber phase corresponding to its glass transition (Wahab *et al.*, 2012b). It was observed that the treated composites especially the MAPE and Si69 treated possessed higher loss moduli than the untreated one, and their glass transition peaks had shifted towards higher temperature regions (Table 4.1). These behaviours were associated with the generation of constraints on the segmental mobility of macromolecules at the relaxation temperatures due to the strengthened interfacial interaction and adhesion of the composites after the MAPE and Si69 treatments, which on the other hand accounted for the comparatively broader NMR resonance peaks as observed in section 4.2.1.1 (Ou *et al.*, 2014; López-Manchado *et al.*, 2002). The larger the interface area and the stronger the interfacial interaction, the greater the molecular motion were restricted (Azlinaa *et al.*, 2011).

The ratio of loss modulus to storage modulus tanδ was measured to further understand the damping behaviour and interface property of the composites (Figure 4.6). In the glassy plateau, the MAPE and Si69 treated composites showed inferior tanδ amplitude than the untreated composite, and their glass transition temperatures (T_g) were determined to be 3.1°C and 10.2°C higher than that of the untreated (-36.0 °C) respectively (Table 4.1). These findings substantiated the aforementioned enhanced interface bonding and immobility of molecular chains of the treated composites. When the composites were subjected to external stress, the external energy was dissipated by the friction between particle-particle and particle-matrix interaction through the interface (Azlinaa *et al.*, 2011). Therefore, the composites with comparatively poorer interface bonding (untreated and VTMS treated) were inclined to dissipate more energy due to the existence of particle-particle friction in weak agglomerates where particles touched each other and the particle-polymer friction at the interface where there was essentially no adhesion, leading to higher magnitude of the corresponding damping peaks (Ou *et al.*, 2014; Felix and Gatenholm, 1991; Ashida *et al.*, 1984).

In addition, it was noted that the melting points of MAPE and Si69 treated composites were shifted to higher temperatures, namely 107.6°C and 114.7°C respectively, which should be ascribed to the crosslinking occurred between the coupling agents and the polymer molecules.

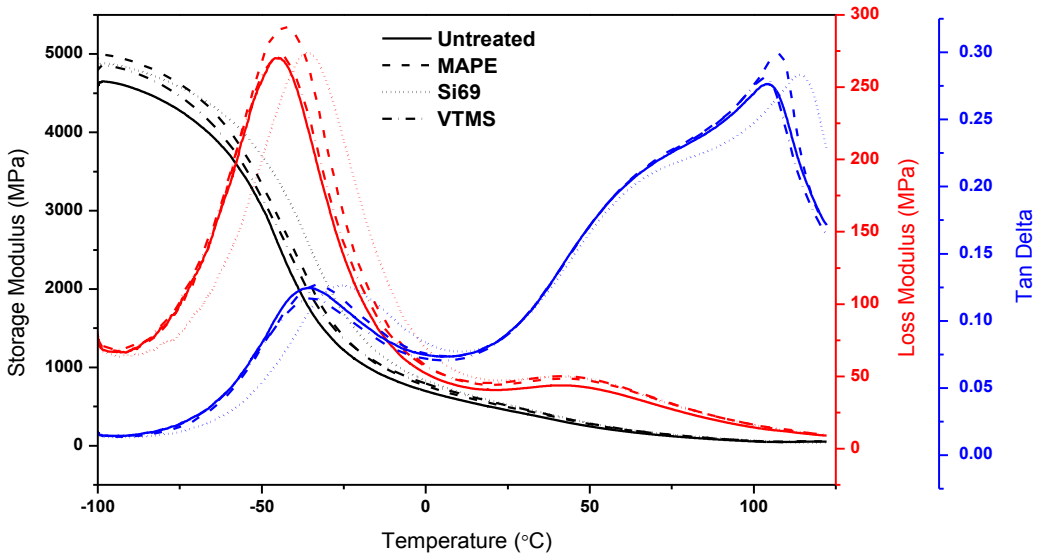

Figure 4.6 Storage modulus, loss modulus and tan δ of untreated and treated composites as a function of temperature

Table 4.1 Crucial parameters extracted from DMA curves of Rubber-PE composites

Sample	Temperature of rubber relaxation peak (T_r, °C)	Loss modulus at T_r (MPa)	Glass transition temperature (T_g, °C)	Tanδ at T_g
Untreated	-45.6	270.1	-36.0	0.124
MAPE treated	-42.7	291.6	-32.9	0.127
Si69 treated	-36.3	273.7	-25.8	0.126
VTMS treated	-43.5	271.4	-35.0	0.117

4.2.3.2 Tensile properties

Table 4.2 summarises the tensile properties of the untreated and treated Rubber-PE composites. The untreated composite showed a tensile strength of 4.66 MPa, while with the incorporation of MAPE and Si69 coupling agents into the composite, the corresponding tensile strength increased by 5.79% and 34.12% respectively. This result denoted that MAPE and Si69 treatments did not only result in the increase of interfacial adhesion and bonding of the composites, but also facilitated the stress transfer from the uniform matrix to the irregularly shaped rubber particles. In addition, the tensile strain of MAPE and Si69 treated composites was found to be notably higher (46.68% and 69.44% respectively) than that of the untreated, which could be explained by the enhanced resistance to crack propagation as a result of a set of better interfacial interactions (Mészáros *et al.*, 2012b). Due to the comparatively poorer compatibilisation and interface refinery of the VTMS treatment, the resulted composite demonstrated a subtle reduction of tensile strength to 4.50 MPa and increase of tensile strain to 8.28%. Furthermore, all the treated composites exhibited slightly lower tensile modulus values as compared to untreated composite, indicating the marginal decrease in stiffness after the coupling agent treatments.

Table 4.2 Tensile property of Rubber-PE composites

Sample	**Tensile stress (MPa)**	**Tensile strain (%)**	**Tensile modulus (MPa)**
Untreated	4.66±0.11	7.69±0.44	422.34±17.41
MAPE treated	4.93±0.25	11.28±0.53	411.82±20.36
Si69 treated	6.25±0.22	13.03±0.68	422.15±22.04
VTMS treated	4.50±0.23	8.28±0.61	403.45±18.57

4.3 Interim Conclusions

The compatibilisation influence of the application of MAPE, Si69 and VTMS coupling agents on the chemical structure, microstructure and mechanical property of Rubber-PE composites has been comprehensively investigated. FTIR results revealed that the crosslinking reactions occurred between the functional

groups of MAPE (MA groups) and Si69 (sulfide groups) and the constituents of the composites, which gave rise to the enhancement of chemical compatibility and interdiffusion, rubber wettability by the matrix, and thus the interfacial adhesion of the composites. The spectral characteristics unveiling the chemical interactions between the coupling agents and raw materials were unfortunately not detected in NMR analysis probably due to insufficient concentration or inappropriate relaxation time of the corresponding bonds (e.g. C-O and C-O-Si).

SEM observations substantiated the improvement of the constituent compatibility, rubber wettability and embedment, and interfacial bonding after MAPE and Si69 treatments. VTMS treatment was not as effective as MAPE and Si69 treatments by showing comparatively limited crosslinking with the constituents and poorer interface within the composite. NMR analysis suggested the constraints on the segmental mobility of the polymers resulting from the treatments, which contributed to the shift of glass transition peaks and inferior tanδ amplitude as explored in DMA study. The mechanical properties including storage modulus, tensile strength and tensile strain of the composites were increased due to the better interfacial compatibility and adhesion as well as more efficient stress transfer from the matrix to rubber particles after the treatments.

Chapter 5 Interface Structure and Bonding Mechanism of WPC

5.1 Introduction

The formulation of wood plastic composites (WPC) was perturbed by the inherently polar and hydrophilic nature of wood flour or fibre, which makes it least compatible with hydrophobic polymeric matrices. The poor combination of wood and polymer is not able to generate the designated performance (Belgacem and Gandini, 2005; Spear *et al.*, 2015). Although numerous physical and chemical modification strategies have been attempted to overcome these drawbacks (Spear *et al.*, 2015; Malkapuram *et al.*, 2009), concerning the industrial or commercial production of WPC, incorporating coupling agents seemed to be the most available and feasible approach for its interface optimisation (Pickering, 2008).

Silane crosslinking of WPC could improve the adhesion between the wood filler and PE matrix by forming a set of chemical links including Si-O-C bridges, hydrogen bonds and C-C crosslinks (Bengtsson *et al.*, 2007; Bengtsson and Oksman, 2006; Bengtsson *et al.*, 2005). As a result, the strength, toughness and creep resistance of the crosslinked composite were significantly increased. Maleated olefins, such as MAPP and MAPE, had been commonly reported to enhance the compatibility and interfacial adhesion of WPC by reacting with the surface hydroxyl groups of wood through their anhydride groups, and in the meantime entangling with the polymer matrix through the other end of the copolymers owing to their similar polarities (Mohanty and Nayak, 2006; Mohanty *et al.*, 2006; Gao *et al.*, 2012; Lai *et al.*, 2003). However, very few studies had paid specific attention to investigate the correlation of the chemical functionalities and reactions resulted from the coupling agent treatments with other bonding scenarios (i.e. physical and mechanical bonding), and their contribution to the bonding mechanism of the composites.

In this chapter, WPC materials were fabricated by the use of recycled wood flour and PE aiming at reducing the consumption of virgin raw materials and the environmental impact. The focus of this chapter was to optimise the interface of WPC by incorporating three different coupling agents, i.e. MAPE, Si69 and VTMS; hence to comprehensively reveal the interface structure and bonding scenarios,

and unveil the chemical, physical and mechanical bonding mechanisms of the formulated WPC by carrying out a set of assessments including ATR-FTIR, NMR, SEM and FM analyses.

5.2 Results and Discussion

5.2.1 Chemical structure and bonding

5.2.1.1 FTIR analysis

Figure 5.1 shows the FTIR spectra of the untreated and coupling agent treated WPC. It was found that in the spectrum of MAPE treated WPC, the bands at 3297 cm^{-1}, corresponding to OH stretching vibration, interestingly became sharper and stronger in comparison to the counterpart of untreated WPC, which was supposed to decrease to some extent due to the esterification reaction between the hydroxyl groups in wood flour and the polar groups in MAPE. The probable explanation was attributed to the strengthened intermolecular and intramolecular hydrogen bonding existing in the compatibilised composite. The diagnostic feature in the spectrum of MAPE treated WPC was the occurrence of more intense bands at 1637 cm^{-1} and 1734 cm^{-1} corresponding to C=C and C=O stretching vibrations (Osman *et al.*, 2010b; Ihemouchen *et al.*, 2013), which confirmed the introduction of C=C groups and formation of ester linkages (covalent bonding) between wood particle and MA moiety, as the reaction shown in Figure 5.2a. Carlborn (Carlborn and Matuana, 2006) reported that the regions of interest in the FTIR spectra of maleated polyolefins modified wood particles were the absorbance bands near 2900 cm^{-1} (CH stretching) and 1740 cm^{-1} (C=O stretching), suggesting the formation of ester linkages. A grafting index (GI) could be calculated by using the integrated areas under these peaks with the following equation:

$$GI_x = \frac{A_{x(treated)}}{A_{x(untreated)}} \quad \text{(Eq. 5.1)}$$

Where, x represents the absorbance band at either 2900 cm^{-1} or 1740 cm^{-1}, A_x represents the integrated peak area. Accordingly, the bands of interest in the spectra of untreated and MAPE treated WPC were observed at 2915 cm^{-1} and 1734 cm^{-1}, and the calculated *GIs* were shown as follows: GI_{2915} = 1.14 and GI_{1734} = 1.09. With regards to the reported MAPE modified wood particles, the

corresponding GI_{2900} and GI_{1740} at 5% MAPE were around 1.10 and 1.25, respectively (Carlborn and Matuana, 2006). The slightly higher GI_{1740} than GI_{1734} was resulted from the higher concentration of MAPE in the wood particles (5%) than that in WPC (3%). It was also noticed that the GI_{2900} and GI_{1740} increased with the MAPE content up to 15%, and appeared to be some levelling off between 15% and 20%, indicating a maximum level of grafting had been reached. The spectral bands at 1031 cm^{-1} in the spectra of both untreated and MAPE treated WPC were assigned to C-O deformation and C-O-C stretching vibrations of the ethers (Kotilainen *et al.*, 2000). The significant increase of the band intensity after the MAPE treatment should be resulted from the introduction of MA groups and the C-O-C covalent bonds formed between MA and wood particles.

The spectra of untreated and Si69 treated WPC did not show evident difference in terms of the band appearances and intensities, especially the bands corresponding to C-O-Si and Si-O-Si bonds (1020 cm^{-1} - 1100 cm^{-1}), which might be an indication of very limited crosslinking reaction occurred between the coupling agent and raw materials. The disappearance of the feeble peak at 1715 cm^{-1} and the slight reduction of intensity for the band at 3299 cm^{-1} in the spectrum of treated WPC might be resulted from the hydrogen bonding formation between wood and hydrolysed silane (silanol). Further scrutinising of the crosslinking between Si69 and the raw materials by another analytical technique (i.e. NMR) should be of great significance for confirming the above assumptions and was carried out in the next section.

VTMS was another coupling agent applied for refining the interface of WPC. The most distinguishing characteristic presented in the spectrum of VTMS treated WPC was the strengthened intensity of the band at 1031 cm^{-1}, which was resulted from the introduced Si-O-C groups in VTMS and the Si-O-C linkages formed between wood flour and VTMS. More importantly, it might also be attributed to the formation of Si-O-Si bonds within VTMS through the hydrolysis of the methyl ether linkages and consequent condensation with adjacent silanol groups (Ihamouchen *et al.*, 2012; Clemons *et al.*, 2011). Compared to that of untreated WPC, the slight reduction of intensity for the band at 1101 cm^{-1} of VTMS treated WPC might be attributed to the multiple linkages of Si-O_n-Si (Clemons *et al.*, 2011).

The chemical reactions occurred between VTMS and the raw materials were proposed in Figure 5.2c. VTMS was firstly reacted with hydroxyl groups in wood flour by creating covalent bonds (Wood-O-Si), the hydrophobic part of the silane on the wood surface were thus chemically bonded and/or interacted through Van der Waals force with PE molecules.

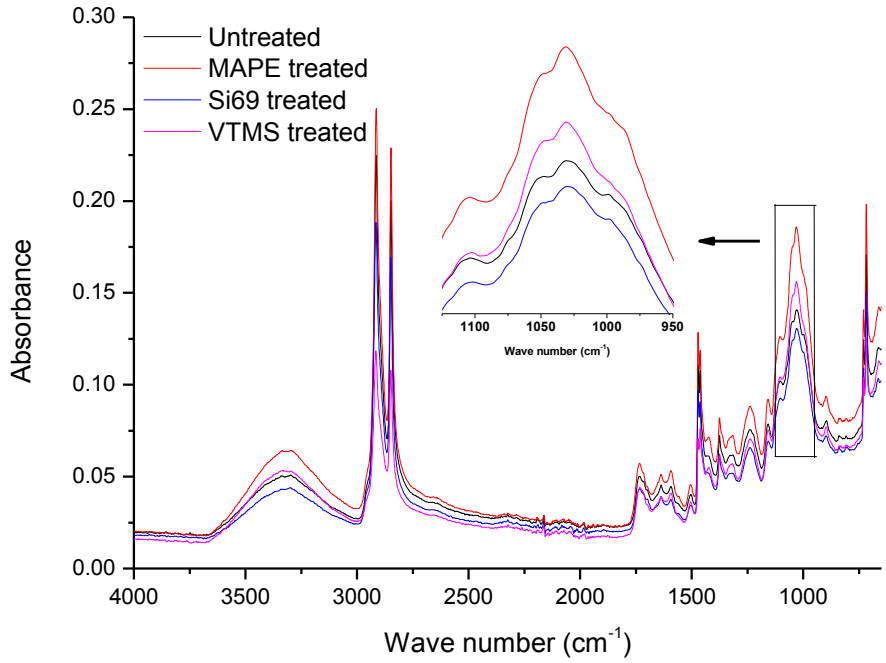

Figure 5.1 FTIR spectra of untreated, MAPE, Si69 and VTMS treated WPC

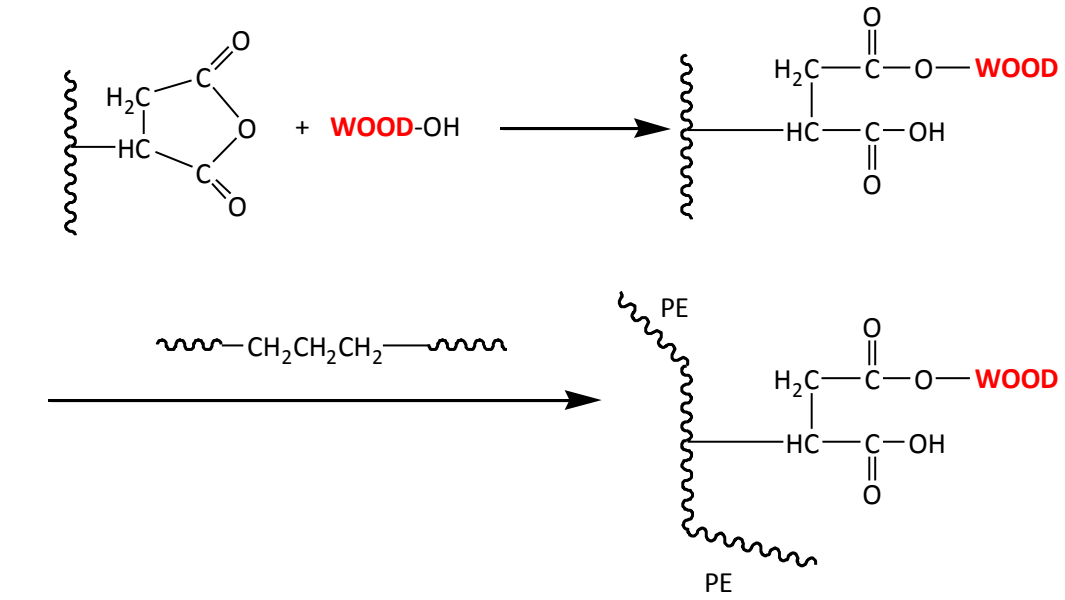

(a)

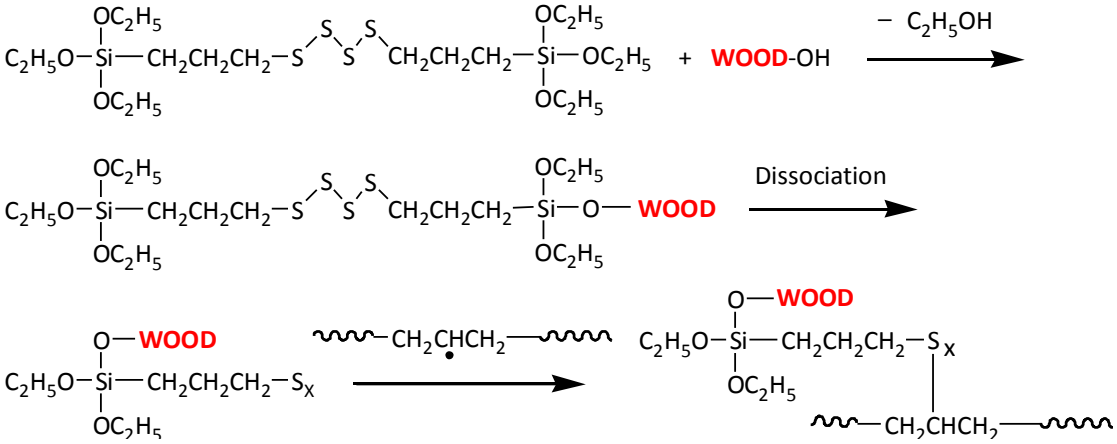

(b)

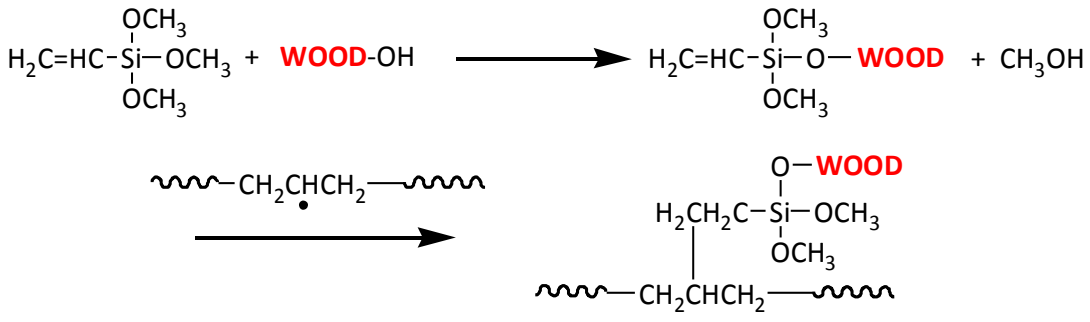

(c)

Figure 5.2 Proposed chemical reactions between the coupling agents (a: MAPE; b: Si69; c: VTMS) and the raw materials of the composites

5.2.1.2 NMR analysis

NMR was employed to further study the effect of the incorporation of the coupling agents on the variation of chemical structure of the composites. Figure 5.3 shows the comparison of the NMR spectra of untreated and treated WPC. The wood component in the composites was characterised by the spectral signals of cellulose (Figure 5.4) at 105.74 ppm for C1, 89.30 ppm and 84.15 ppm for C4 of crystalline and amorphous cellulose respectively, 74.76 ppm and 72.49 ppm for C2,3,5, 65.02 ppm and 63.04 ppm for C6 of crystalline and amorphous cellulose respectively (Santoni *et al.*, 2015; Grünewald *et al.*, 2013; Martins *et al.*, 2006; Renneckar, 2004; Stael *et al.*, 2000; Wikberg and Maunu, 2004). The diagnostic signals of hemicellulose (Figure 5.4) should be at around 105 ppm (C1), 84ppm (C4), 72-75 ppm (C2,3,5), and 65 ppm (C5), which had all overlapped with the more intense signals of cellulose due to their chemical similarities (Santoni *et al.*, 2015; Martins *et al.*, 2006). In terms of the characteristics of lignin in wood flour, the peak observed at 172.47 ppm was assigned to carboxyl groups in lignin, peaks at 150-154 ppm and 138-132 ppm were attributed to aryl groups, and the signal at 56.3 ppm was ascribed to methoxyl groups (Santoni *et al.*, 2015; Martins *et al.*, 2006; Stael *et al.*, 2000). The resonance peaks attributed to the PE component in the composites were distinguished at the chemical shifts of 43.80 ppm and 32.51 ppm assigning to methylene groups (-CH_2-), and the comparatively subtle peaks at 26.22 ppm and 21.53 ppm were referred to methine and methyl groups respectively (Wikberg and Maunu, 2004; Sombatsompop *et al.*, 2004a).

Regarding the resonance variations after the treatments, the first phenomenon observed was that all three treated samples demonstrated broader spectra than untreated WPC, which might be attributed to the less conformational exchange and rotational diffusion in the rigid phase (Stael *et al.*, 2000). As expected, compared to the untreated counterpart, the peak intensity at 32.51 ppm in the spectrum of MAPE treated sample dramatically increased, indicating that MAPE was covalently bonded to wood particles. Apart from that, the more prominent signal at 172.47 ppm was not only contributed by the more resolved lignin units, but should be also resulted from the introduced MA groups in MAPE and ester

linkages formed between the MA groups and hydroxyl groups of wood. These results were in a good agreement with the above FTIR analysis of MAPE treatment. The reaction mechanism of MAPE coupling agent with wood flour and PE could be explained as the activation of the copolymer by heating followed by the esterification of wood particles. This treatment increases the surface energy of wood flour to a level much closer to that of the matrix, and thus results in better wettability and enhances interfacial adhesion between the filler and matrix (Li *et al.*, 2007).

The incorporation of Si69 into the composites were discriminated by the appearance of resonance signals at 51.50 ppm, 49.18 ppm and 47.23 ppm, which were attributed to the C-S_x bonds, including C-S and C-S-S existed in Si69 molecules, and the C-S_x bonds formed between the dissociated coupling agent and the polymer chains of the matrix (Figure 5.2b) (Silverstein *et al.*, 2014; Andreis *et al.*, 1989; Zaper and Koenig, 1988). Compared to the spectrum of the untreated sample, the new shoulder at 60.50 ppm was probably contributed by Si-O-C bonds which existed in Si69 and covalently formed between Si69 and wood flour (Salon *et al.*, 2005; Fyfe and Niu, 1995). These spectral characteristics unveiled the reactions between Si69 and two constituents of the composite, which were unfortunately not discerned from FTIR analysis probably due to the overlapping of diagnostic signals and insufficient concentrations of these bonds to be detected. The proposed corresponding reactions were presented in Figure 5.2b. The ethoxy groups of Si69 first reacted with functional groups (mainly hydroxyl) of wood flour to form a siloxane bond, thus the sulfide group of Si69 bonded wood particle was dissociated and reacted with PE molecules to form a crosslinking between wood and matrix. Si69 has a sulfidic linkage of di- to octa-sulfides and the average number of S_x- is about 3.8. Polysulfides in Si69 could be dissociated at low temperature (near room temperature) to form radicals and thus reacted with polymer molecules with storage time elapses. Therefore, the polysulfides of retained silane in the composite should be able to be dissociated and further react with both PE molecules and unreacted functional groups on wood surface (Choi, 2002).

In the spectrum of VTMS treated WPC, the peak at 133.80 ppm was initially assigned to lignin units in wood particles. In addition to the more resolved signal after this treatment, the strengthened intensity of this peak was also resulted from the incorporated carbons of Si-C=C and O-Si-C=C within VTMS structure (Sitarz *et al.*, 2013; Fyfe and Niu, 1995). The reaction between VTMS and wood flour (Figure 5.2c) was confirmed by the occurrence of the peaks at 68 ppm and 58 ppm, since which were attributed to the carbons of Si-O-C (Salon *et al.*, 2005; Fyfe and Niu, 1995). The considerable enhancement of the intensity at 32.51 ppm ($-CH_2-$) suggested that the VTMS had successfully bonded to PE chains via its unsaturated C=C groups.

It should be pointed out that the relative resonance signals of crystalline carbohydrates (around 89 ppm and 65 ppm) to amorphous moieties (around 84 ppm and 63 ppm) decreased to some extent after the treatments, which might be an indication of the disordering of cellulose and the conversion to an amorphous state under these treatments. Transformation of crystalline cellulose to an amorphous state in hot and compressed water had been reported recently, which was determined as a consequence of synergetic effect between the thermal properties of crystalline cellulose and the unique properties of hot and compressed water (Deguchi *et al.*, 2008). It was reported that in the NMR spectra of g-methacryloxypropyl trimethoxy silane (MPS) grafted cellulose, the spectral signals of the grafted MPS and amorphous cellulose were emphasised after this silane treatment, while the crystalline cellulose form drastically decreased (Salon *et al.*, 2007). The possible explanation of this diminishing of relative resonance intensity of crystalline carbohydrates was that VTMS may penetrate into wood lumens and vessels, thus reacted with the functional groups of cellulose, which in the meantime underwent transformation into an amorphous form under high temperature and pressure.

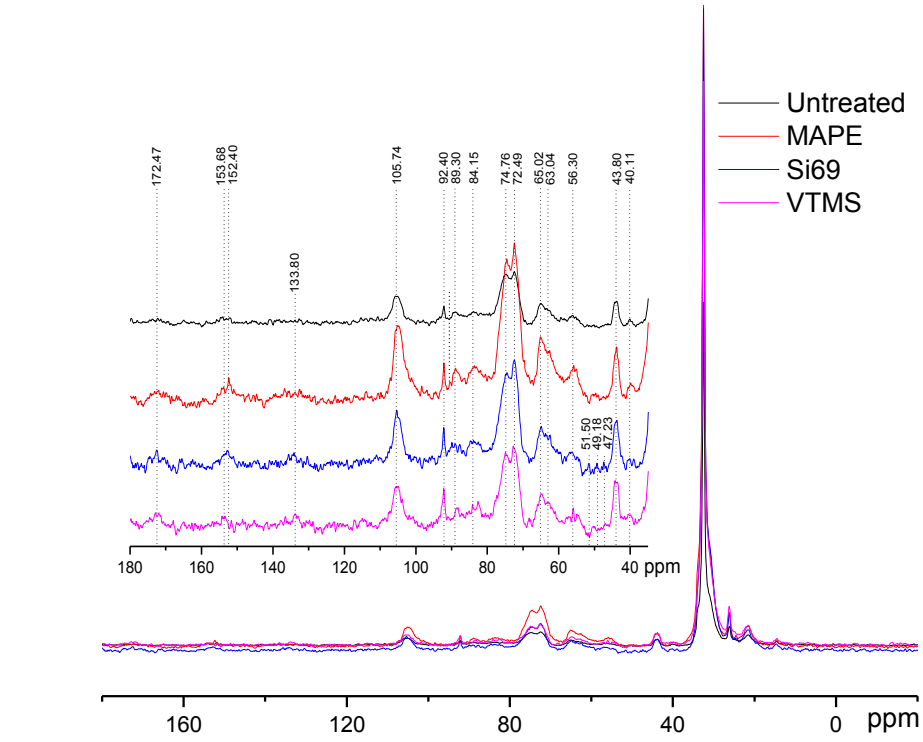

Figure 5.3 ^{13}C NMR spectra of untreated, MAPE, Si69 and VTMS treated WPC

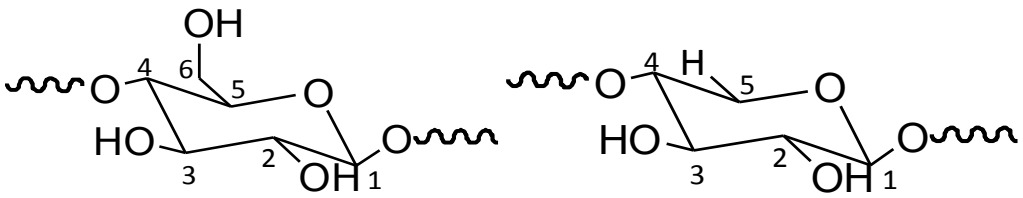

glucose **xylose**

Figure 5.4 Chemical structure of cellulose unit (glucose) and hemicellulose unit (xylose)

5.2.2 Interface bonding scenarios and mechanisms

The improvement of the chemical adhesion and compatibility between the constituents of WPC resulted from the chemical bonding and reactions between the incorporated coupling agents and constituents of WPC could be anticipated to contribute to the interface refinery. The effect of the coupling agent treatment on the interface bonding scenarios of the composites was scrutinised by the use of FM and SEM (Figure 5.5 and Figure 5.6). It can be seen a number of clear cracks or boundaries and voids between wood particles and the matrix occurred in the untreated WPC (Figure 5.5a and Figure 5.6a), which indicated a poor compatibility between the untreated raw materials. It was also observed that

there were agglomerated wood particles unevenly distributed in the matrix due to the readily formed hydrogen bonds within uncompatibilised wood particles (Osman *et al.*, 2010b). In addition, although there were a few cell lumens partially filled by the polymer resin, the majorly unfilled cell lumens along with the existence of micro cracks between wood and PE denoted the improper interfacial adhesion of the untreated WPC. Comparatively, in the treated WPC (Figure 5.5b-5.5d and Figure 5.6b-5.6d), wood flour was completely wetted by the matrix and firmly bonded to it, demonstrating superior interfacial adhesion with resin impregnation throughout the interface. More importantly, a large number of cell lumens of these samples were discerned to be partially or utterly filled by the resin, which again confirmed the enhanced interfacial adhesion and also the compatibility and wettability improvements.

It was interesting to notice that there existed deformed cell lumens in the treated WPC especially the VTMS treated sample (Figure 5.6d). Apart from the cell lumens, the vessels of the wood particles in VTMS treated sample (Figure 5.6d) were also completely or partially filled with PE resin. It was speculated that the coupling agent treatments would provide the resin with better fluidity, and the deformed lumens and vessels tended to facilitate the flow of resin in random directions. It has been reported that in the case of radial and tangential penetration of urea-formaldehyde adhesives into poplar wood, the resins preferably filled the wood vessels rather than the wood fibres when the wood fibres and vessels close to the bond line were deformed (Grmusa *et al.*, 2012a; Grmusa *et al.*, 2012b).

Hydrodynamic flow of molten PE resin in the composites was initiated by an external compression force through vessels, and then proceeded into the interconnected network of cell lumens and pits in interface region, with flow moving primarily in the paths of least resistance (Grmusa *et al.*, 2012a; Grmusa *et al.*, 2012b). The flow paths in any directions were in general a combination of open cut lumens and vessels as well as of large pits.

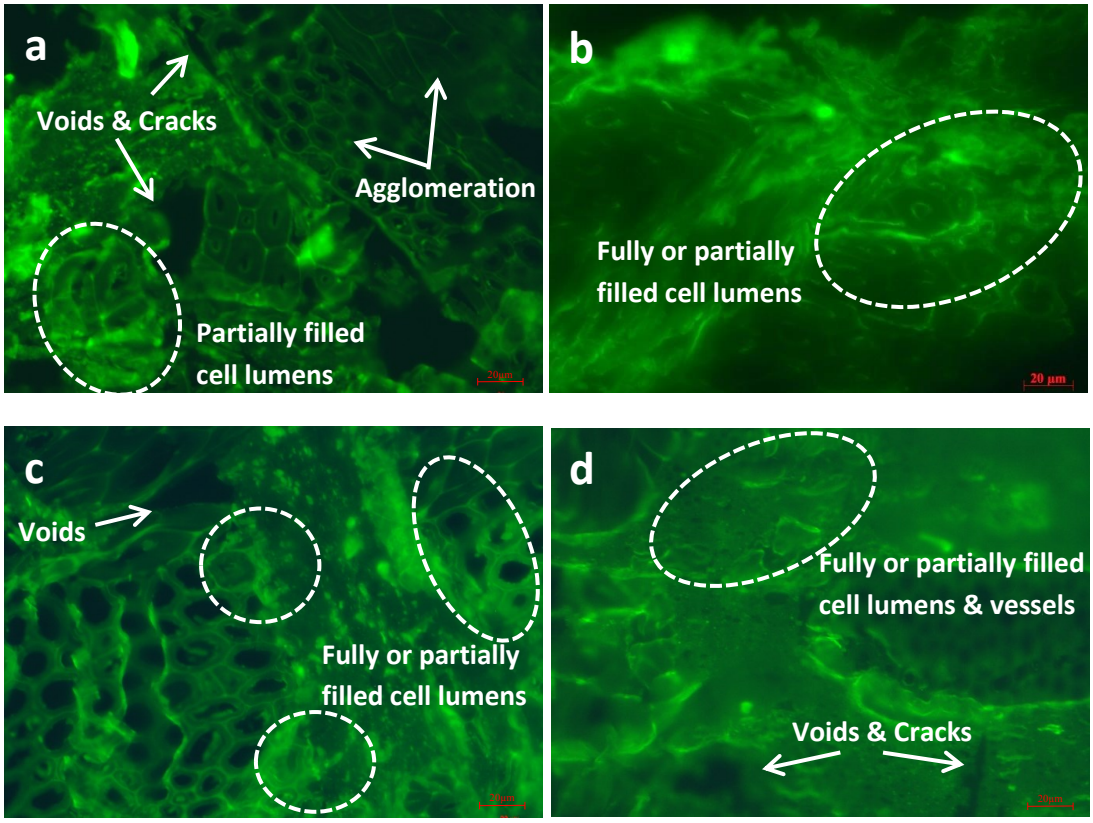

Figure 5.5 FM photographs of cross section of untreated (a), MAPE treated (b), Si69 treated (c) and VTMS treated (d) composites

The interface region formed between wood flour and matrix is in fact a zone of compositional, structural and property gradients, in which a set of processes occur on the atomic, microscopic and macroscopic levels. It has been recognised to play a predominant role in governing the global composite behaviour by controlling the stress transfer between wood and matrix, and is primarily dependent on the level of interfacial adhesion. The wood-matrix interfacial bonding mechanisms were assumed to include interdiffusion, electrostatic adhesion, chemical reactions and mechanical interlocking (Figure 5.7), which together were responsible for the interfacial adhesion.

Interdiffusion was developed on the basis of good wetting of wood particle (Figure 5.6) through intimate intermolecular interactions between the molecules of wood and polymer, e.g. hydrogen and covalent bonding, electrostatic and Van der Waals forces. Electrostatic adhesion was attributed to the creation of opposite charges (anionic and cationic) on the interacting surfaces of wood and polymer matrix; thus, an interface consisting of two layers of opposite charges

was formed, which accounted for the adhesion of two constituents of the composite. Chemisorption occurred when chemical bonds including atomic and ionic bonds, such as C-O-C, C-S and Si-O-C covalent bonds, were created between the substances of the composite as a result of chemical reactions. Mechanical interlocking took place through the resin penetration into the peaks, holes, valleys and crevices or other irregularities of the substrate, which can be seen in the FM and SEM images (Figure 5.5 and Figure 5.6), then anchored itself through solidification.

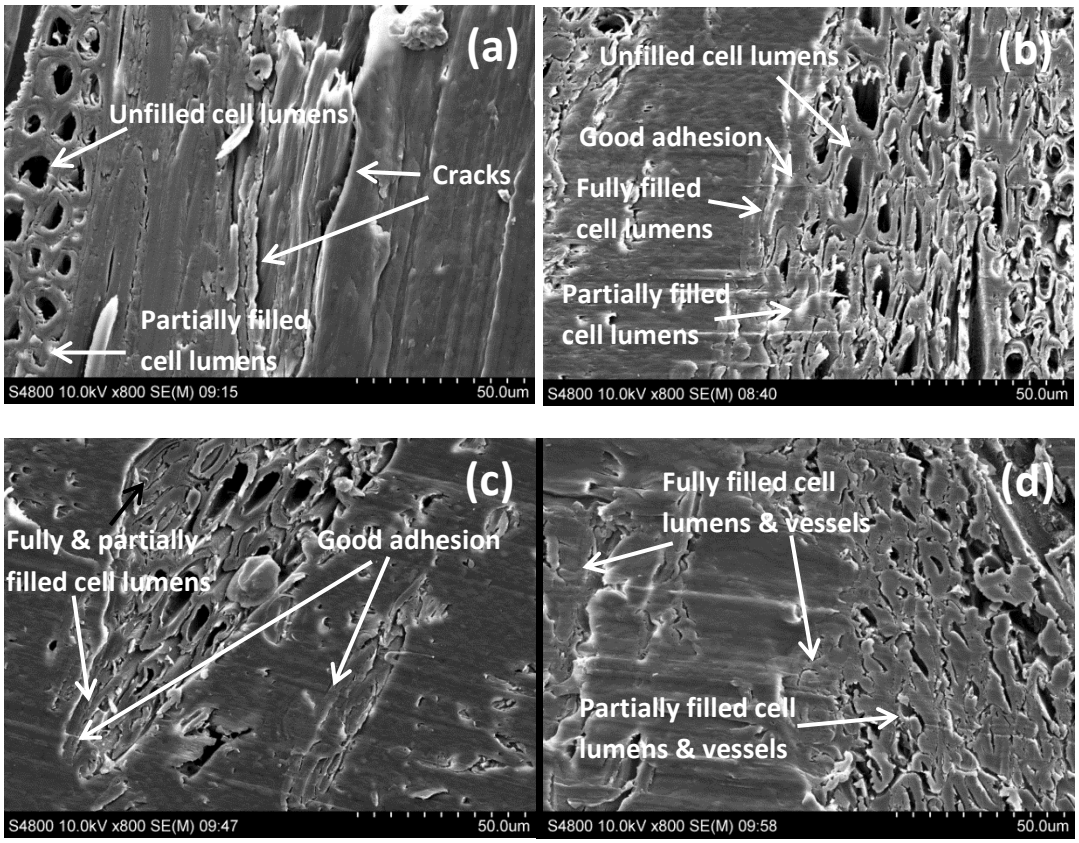

Figure 5.6 SEM photographs of cross section of untreated (a), MAPE treated (b), Si69 treated (c) and VTMS treated (d) composites

The distinguished enhancement of interfacial bonding of maleated and silane coupling agents treated WPC could be explained as follows: the hydrophilic moiety in the coupling agents reacted with the functional groups of wood flour to form covalent linkages, while the hydrocarbon chains crosslinked with the polymer matrix to create molecular entanglements. Specifically, as thoroughly discussed in the above section of chemical structure and bonding, the MA moiety in MAPE, the ethoxy groups of Si69 and the methoxyl groups of VTMS reacted

with the hydroxyl groups of wood flour, in the meantime, the grafted PE chains in MAPE, the dissociated sulfide groups in Si69, and the vinyl groups of VTMS chemically bonded and/or interacted with the PE macromolecules. Thus, the extent and degree of interdiffusion between wood and PE molecules were increased due to the better chemical compatibility resulted from these chemical reactions and the more flexibility of interchains explored in the NMR analysis (Section 5.2.1.2). The introduced hydrocarbon chains of coupling agents also led to the decrease of hydrophilicity and the increase of surface energy of wood flour, and improved the chemical affinity of the matrix, thereby resulted in enhanced wettability of wood flour by the resin and interfacial adhesion (Li *et al.*, 2007; Kalaprasad *et al.*, 2004; Mohanty *et al.*, 2004). In addition, more contact areas between wood and matrix were created for resin penetration and mechanical interlocking of the substrate (Figure 5.5 and Figure 5.6). In fact, an increase in any bonding mechanism (i.e. interdiffusion, chemical reactions, mechanical interlocking, etc.) would inevitably give rise to the enhancement of other bonding systems/mechanisms, which mutually accounted for the interfacial bonding refinery.

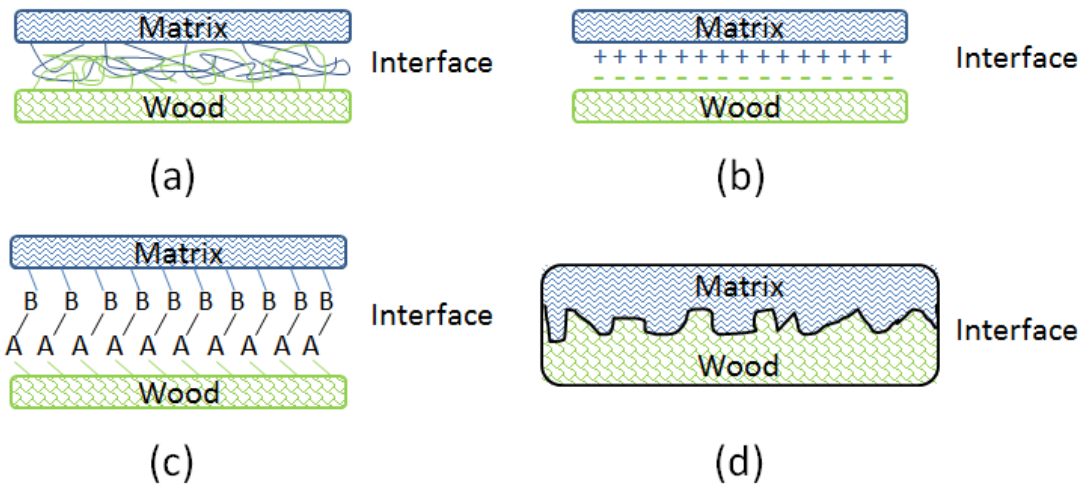

Figure 5.7 Wood-matrix interfacial bonding mechanisms: (a) molecular entanglement following interdiffusion, (b) electrostatic adhesion, (c) chemical bonding and (d) mechanical interlocking

5.3 Interim Conclusions

The interfaces of WPC were optimised by the incorporation of MAPE, Si69 and VTMS coupling agents. FTIR and NMR results confirmed the chemical reactions between the coupling agents and the constituents of the composites, i.e. the MA moiety in MAPE, the ethoxy groups of Si69 and the methoxyl groups of VTMS reacted with the hydroxyl groups of wood flour, in the meantime, the grafted PE chains in MAPE, the dissociated sulfide groups in Si69, and the vinyl groups of VTMS chemically bonded and/or interacted with the PE macromolecules. The introduced hydrocarbon chains of coupling agents also led to the decrease of hydrophilicity and the increase of surface energy of wood flour, and improved the chemical affinity of the matrix, thereby resulted in enhanced wettability of wood flour by the resin and interfacial adhesion. NMR results also indicated that there existed transformation of crystalline cellulose to an amorphous state during the coupling agent treatments, reflecting the inferior resonance of crystalline carbohydrates.

SEM observation revealed that the coupling agent treatments enhanced the interfacial compatibility and adhesion of WPC by promoting the dispersion of wood flour in the matrix, improving the wettability of wood flour by the resin, and facilitating the resin impregnation throughout the interface. The enhanced interface of the composites after the coupling agent treatments was resulted from the combination of increased macromolecular interdiffusion, chemical reactions and mechanical interlocking.

Chapter 6 Bulk and *In Situ* Mechanical Properties of WPC

6.1 Introduction

The performance and behaviour of wood plastic composites (WPC) are not only relying on the reinforcing wood and the polymer matrix, but also critically depending on the effectiveness of load/stress transfer across the interface (Kumar *et al.*, 2004; Downing *et al.*, 2000). The interface of WPC formed when the wood flour is embedded in the polymer matrix during fabrication of the composite is a heterogeneous transition zone with distinct chemical compositions, morphological features and mechanical properties from those of the reinforcing phase and the bulk polymer (Lee *et al.*, 2007a; Downing *et al.*, 2000; Kim and Mai, 1998). An appropriately engineered interface could considerably improve the strength and toughness of the composite as well as the environmental stability. Therefore, on the other hand, the determination of interfacial properties and characteristics would be of utmost importance in evaluating the overall property of the composite and enabling its optimal design (Graham *et al.*, 2000).

Nanoindentation technique has been proven to be an effective method in determining material surface properties at nanoscale, which is achieved by monitoring a probe penetrating into the specimen surface and synchronously recording the penetration load and depth (Oliveira *et al.*, 2014; Zhang *et al.*, 2012). It has recently found its application feasible to wood, natural fibres and plastics (Ghomsheh *et al.*, 2015; Lee and Deng, 2013; Zhang *et al.*, 2012; Wu *et al.*, 2010; Xing *et al.*, 2009; Lee *et al.*, 2007a; Tze *et al.*, 2007; Gindl *et al.*, 2006; Hobbs *et al.*, 2001; Oliver and Pharr, 1992), but it has been rarely employed in measuring the interface property and performance of WPC materials.

The incorporation of silane and maleated coupling agents exerted reinforcing impact on the bulk property of WPC materials, but its influence on the mechanical properties in the interface region has not yet been reported in the literatures. In this chapter, the influence of the coupling agent treatments on the *in situ* mechanical properties of WPC was first determined by carrying out nanoindentation analysis, which led to a thorough understanding of interfacial

characteristics and the correlation between *in situ* and bulk mechanical properties.

6.2 Results and Discussion

6.2.1 Bulk mechanical properties

6.2.1.1 Tensile properties

The effect of the incorporation of coupling agents on the tensile properties of WPC was summarised in Table 6.1. The application of MAPE, Si69 and VTMS led to a significant increase in the tensile strength of the composites by 135.40%, 15.63%, and 77.40% respectively. The treated WPC also demonstrated much greater tensile moduli than the untreated one (112.73%, 63.3%, and 114.15% respectively), indicating the notable enhancement of the stiffness of the composites. Similar results had been observed in the study of MAPP treated wood flour/recycled PE composites and VTMS treated wood flour/PE composites: the addition of 3% MAPP led to the increase of the tensile strength (48.78%) and Young's modulus (28.24%) of wood flour/recycled PE (50%/47%) composite (Adhikary *et al.*, 2008); the incorporation of VTMS (0.5%-2%) improved the tensile strength and tensile modulus of wood flour/PE composites by up to 62% and 14% respectively (Clemons *et al.*, 2011). These phenomena were evidently resulted from the enhanced physical, chemical and mechanical bonding of the interface between wood flour and matrix with the addition of the coupling agents, which was thoroughly discussed in Chapter 5.

In addition, according to the classic mechanics theory of particle-reinforced material (Ou *et al.*, 2014), the load applied to WPC was transferred from PE matrix to wood flour by shear stress along the interface. The presence of the coupling agents in WPC promoted the dispersion and distribution of wood flour in the matrix, resulting in better interfacial adhesion and more efficient stress transfer from the matrix to wood flour, thus the improvement of the mechanical properties. The tensile strain of the treated WPC was decreased by 24.58% (MAPE), 55.93% (Si69), and 59.32% (VTMS). This also reflected the more compact and stiffer structure of the treated WPC. Furthermore, it was worth mentioning that although the deviation of the tensile strain results (5%-10%)

was not as low as those of tensile stress and modulus (around or less than 5%), it did not appear to be affecting the investigation of the variation of the tensile properties of the composites.

Table 6.1 Tensile properties of recycled PE and WPC

Sample	Tensile stress (MPa)	Tensile strain (%)	Tensile modulus (MPa)
Recycled PE	23.05±0.17	10.35±0.32	2385.41±133.25
Untreated	5.31±0.23	2.36±0.19	1988.75±115.46
MAPE treated	12.50±0.30	1.78±0.16	4230.79±208.73
Si69 treated	6.14±0.25	1.04±0.11	3247.70±170.95
VTMS treated	9.42±0.31	0.96±0.10	4258.92±189.72

6.2.1.2 Dynamic mechanical analysis (DMA)

Storage modulus is closely related to the load bearing capacity of a material (Mohanty and Nayak, 2006; Mohanty *et al.*, 2006). The variation of the storage modulus of WPC as a function of temperature was graphically enumerated in Figure 6.1. It was observed that similar to the tensile modulus, the coupling agents MAPE and VTMS treated WPC had much higher storage moduli than the untreated one, primarily attributing to the improved interfacial adhesion between wood flour and the matrix. The storage moduli in all composites decreased with the increase of temperature, and the differentiation of the modulus between the treated and untreated WPC gradually diminished from the transition region (-100 – 75^{o}C) to plateau region (75 – 120^{o}C).

The loss modulus-temperature curves in Figure 6.1 were used to investigate the transition behaviour of the composites. There was one major transition (45 – 60^{o}C) existed in these curves corresponding to the α transition of PE matrix, which was associated with the chain segment mobility in the crystalline phase due to the reorientation of defect area in the crystals (Bengtsson *et al.*, 2005; Mohanty and Nayak, 2006; Mohanty *et al.*, 2006). In comparison to the relaxation peak of untreated WPC (Table 6.2), the counterparts of MAPE and VTMS treated WPC had shifted towards higher temperature regions, and the corresponding

moduli of the treated WPC were accordingly higher than that of the untreated one (181.4 MPa). These performance should be attributed to the generated constraints on the segmental mobility of polymeric molecules at the relaxation temperatures during the coupling agent treatments (Ou *et al.*, 2014; López-Manchado *et al.*, 2002).

It was worth noticing that compared to the untreated WPC, albeit the α transition appeared at higher temperature (52.9^{o}C) Si69 treated composite showed a reduced loss modulus (166.7 MPa), indicating that Si69 treatment did not lead to comparable segmental immobilisation of the matrix chains on the wood surface as MAPE and VTMS treatments. This might be related to the comparatively limited crosslinking between the polysulfides of Si69 and PE molecules compared to that between the grafted PE on MAPE or the unsaturated C=C groups of VTMS and the matrix molecules, which was in agreement with the less evident discrimination of the corresponding spectral characteristics in its chemical structure analysis, especially the FTIR analysis in Section 5.2.1. Similarly, the tensile strength and modulus of Si69 treated WPC were inferior to those of MAPE and VTMS treated composites. However, it had been reported that transition peak broadens and the peak position shifts if there is an interaction between the filler or reinforcement and matrix polymer (Lai *et al.*, 2003). Therefore, the broadening of the transition regions from around 10^{o}C to 85^{o}C discerned in all the treated composites (especially MAPE and VTMS treated composites) might be an indication of the existence of the interaction between the coupling agents and the constituents of the composites.

The ratio of the loss modulus to storage modulus defining as damping factor tanδ was also determined (Figure 6.1) for the benefits of better understanding the damping behaviour and interface property of the composites. As Figure 6.1 showed, the tanδ amplitude of the composites decreased with the addition of the coupling agents. This was expected since the enhanced interfacial adhesion provided the treated WPC with higher stiffness which in turn restrained the segmental mobility of polymer molecules leading to the decrease of tanδ magnitude (Ou *et al.*, 2014; López-Manchado *et al.*, 2002; Lai *et al.*, 2003). In addition, the composite with poorer interfacial bonding between wood flour and

matrix was inclined to dissipate more energy, showing greater tanδ amplitude than the composite with firmly bonded interface (Ou *et al.*, 2014; Felix and Gatenholm, 1991; Ashida *et al.*, 1984).

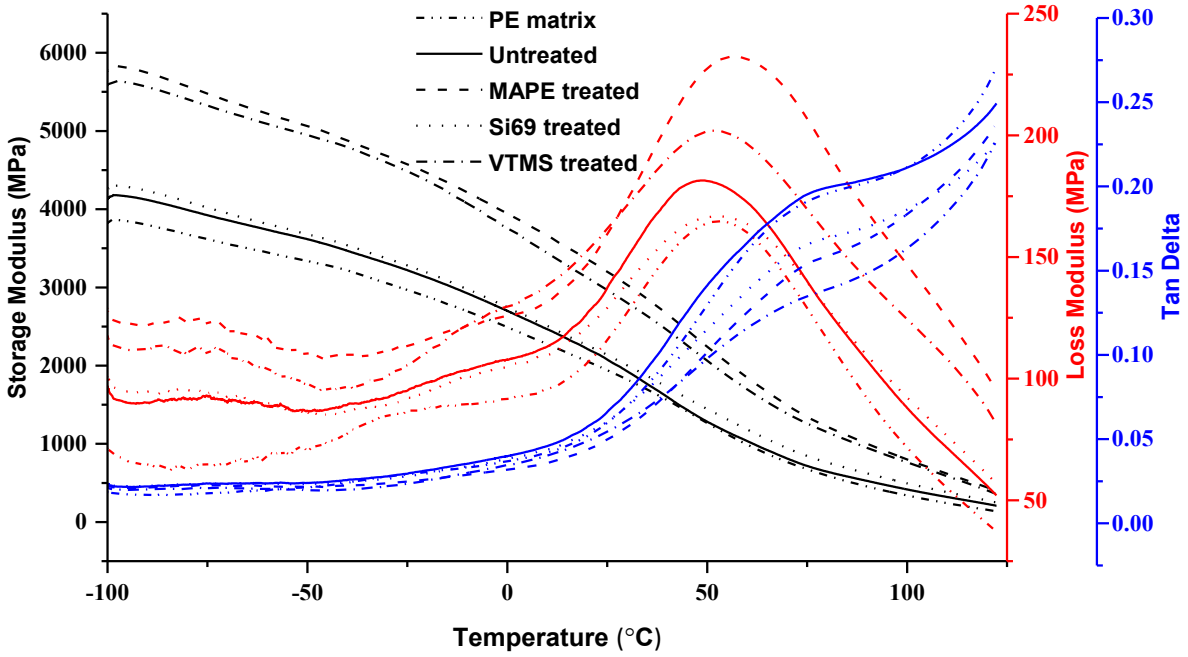

Figure 6.1 Storage modulus, loss modulus and tan δ of PE matrix, untreated WPC and treated WPC as a function of temperature

Table 6.2 Crucial parameters extracted from DMA curves of WPC

Sample	**Untreated**	**MAPE treated**	**Si69 treated**	**VTMS treated**
α transition temperature (T_α, °C)	47.9	57.4	52.9	51.8
Loss modulus at T_α (MPa)	181.4	232.4	166.7	201.9

Adhesion factor, A, was thus determined from the mechanical damping (tanδ) to further investigate the effect of the coupling agent treatments on the interfacial adhesion between the filler and matrix of the composites in accordance with the following equation reported by Correa (Correa *et al.*, 2007) and Kubat (Kubát *et al.*, 1990):

$$A = \frac{tan\delta_c}{(1-V_w)tan\delta_m} - 1 \qquad \text{Eq. 6.1}$$

Where, the subscripts *c*, *m* and *w* refer to composite, matrix, and wood flour respectively, and V_w is the volume fraction of wood flour in the composite. As Figure 6.2 showed, the untreated composite had higher adhesion factor than the coupling agent treated composites, which was consistent with the tanδ results. According to Correa (Correa *et al.*, 2007), the molecular mobility of the polymer surrounding the filler was reduced at high levels of interfacial adhesion, and consequently low values of the adhesion factor suggested improved interactions at the filler-matrix interface. The determined lower levels of adhesion factor in coupling agent treated WPC evidently confirmed the enhanced interfacial interactions after the treatments, which resulted in the decreased molecular mobility and mechanical damping (tanδ) (Poletto *et al.*, 2012; Ornaghi *et al.*, 2010). In addition, the adhesion factor of Si69 treated composite was higher than those of MAPE and VTMS treated composites. This result along with its relatively greater tanδ amplitude again substantiated the inferior interfacial adhesion improvement induced by Si69 treatment, resulting in the comparatively lower tensile strength, tensile modulus, storage modulus and loss modulus of the composite determined in the above sections.

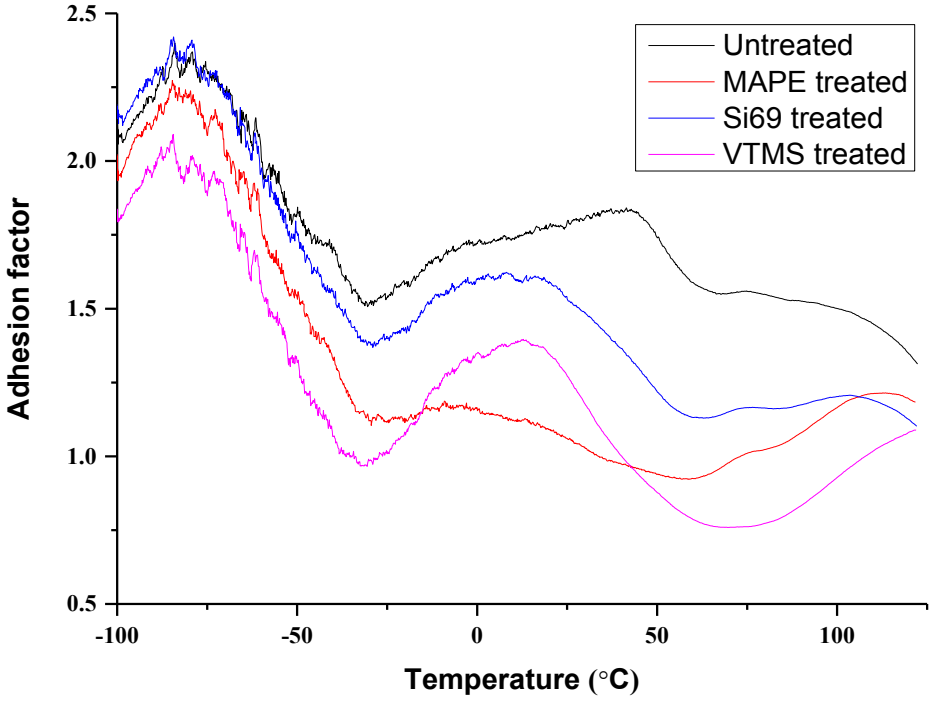

Figure 6.2 Adhesion factor of untreated and treated composites as a function of temperature

6.2.2 *In situ* mechanical properties

The examination of the mechanical properties at nanoscale would undeniably help reveal the interface characteristics and evaluate the overall property of the composites. Figure 6.3 demonstrated the nanomechanical properties of the wood cell walls of the composites determined by nanoindentation. It is most interesting that the untreated composite showed an elastic modulus of 16.42 GPa and a hardness of 0.53 GPa, while the counterparts of the MAPE and Si69 treated composites interestingly decreased to 11.46 GPa and 0.46 GPa (MAPE treated), and 15.60 GPa and 0.49 GPa (Si69 treated) respectively. This is in disagreement with that of the bulk properties tested. The drops of the modulus and hardness were assumed to be partially resulted from the fibre weakening or softening impact of the treatments, namely the chain scission (cleavage of β-1,4-glycosidic bonds between two anhydroglucose units) and weakening of interfibrillar interaction in cellulose occurred with the presence of maleic and silane coupling agents under high pressure and temperature during processing (Ganser *et al.*,

2013; Sawpan *et al.*, 2011). On the other hand, it might be associated with the degree of crystalline orientation in wood flour. NMR analysis results of the composites (Section 5.2.1.2) indicated that the crystalline carbohydrates in wood flour underwent transformation into an amorphous form during the treatments, which might facilitate the nanoindentation loading along the fibre direction, and thus, lower modulus and hardness were measured.

Although the VTMS treatment had the analogous effects on the composites, there was no noticeable difference between the untreated and VTMS treated composites, in terms of their elastic modulus and hardness. This suggested that there were other critical factors governing the *in situ* mechanical properties of the composites. Due to the relatively lower molecular weight (M_W) of Si69 (M_W=539) and VTMS (M_W=148) than MAPE (500 cps viscosity at 140^oC), silanes might be more capable of diffusing into cell walls and reacting with the structural components by forming hydrogen and covalent bonding, giving rise to more outstanding nanomechanical property. In addition, the maleic coupling agent was found to be able to create a thin, soft and ductile interfacial layer in the composite (Hristov and Vasileva, 2003), which might impart an adverse impact on the nanomechanical property of the composite. More importantly, the better nanomechanical property of VTMS treated composite over MAPE and Si69 treated composites should be ascribed to the severe deformation and damaging of its cell walls. The SEM analysis (Section 5.2.2) had shown that VTMS treated composite possessed much more deformed and damaged cell lumens and vessels than the untreated and MAPE and Si69 treated composites, which promoted the wetting of wood flour by the polymer and the polymer penetration into wood particles. The higher level of penetration was assumed to compensate the loss of the *in situ* mechanical properties due to the aforementioned fibre weakening or softening impact and crystalline structure transformation. Therefore, the nanomechanical property of the treated composites fell into the sequence: VTMS > Si69 > MAPE.

It should be pointed out that the employed coupling agent treatments enhanced the interfacial adhesion and bonding of the composites by strengthening the chemical, physical, and mechanical bonding, which had been substantiated by a

set of investigation including FTIR, NMR, FM, and SEM analyses in Chapter 5. The optimised interface contributed to the increase of the bulk mechanical properties of the composites. Although both the MAPE and VTMS treated composites demonstrated significant increase of bulk mechanical properties (i.e. tensile stress (Table 6.1), storage and loss modulus (Figure 6.1)) after the treatments, the corresponding *in situ* mechanical properties were different; MAPE treated composite possessed a softer interface by showing lower *in situ* elastic modulus and hardness than the VTMS treated. In comparison to that of VTMS treated composite, the comparatively softer and tougher interface of MAPE treated might provide it with greater resistance to fracture, which accounted for the higher tensile strain (85.42%, Table 6.1). In addition, owing to the inherently tough and ductile nature of PE matrix, the softer and tougher interface might benefit the continuity in load transfer from the matrix to wood flour, promoting the composite to function as a mechanical entity, thus leading to higher tensile strength.

It was evident that to what extent the bulk mechanical properties of the composite could be improved was predominantly relying on the level of the enhancement of compatibility, interfacial adhesion and bonding after different coupling agent treatments rather than individual local property within the interface. The distinct nature and characteristics of the interfaces might play another fundamental role in determining the global properties of the composites.

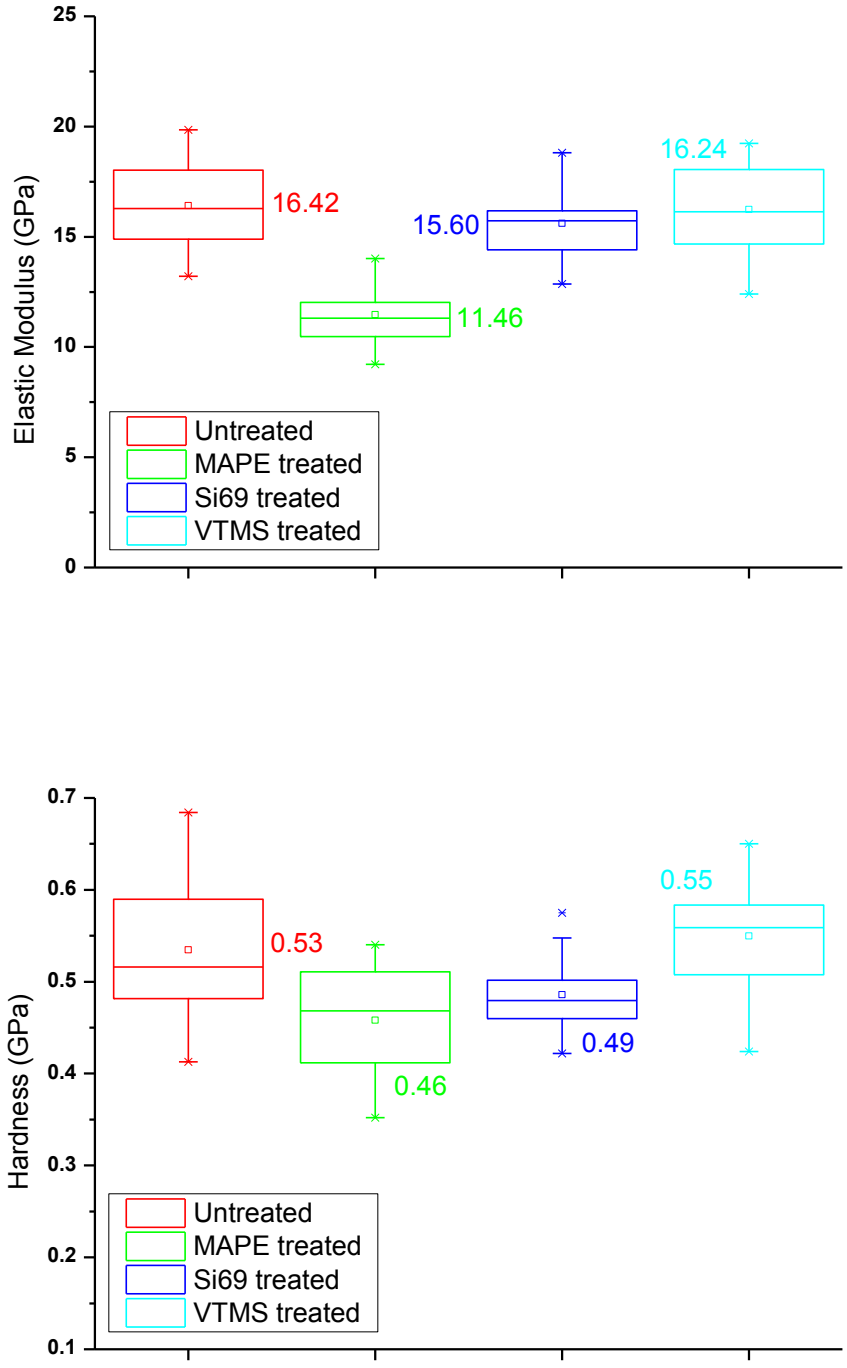

Figure 6.3 Nanomechanical property of the composites by nanoindentation

6.3 Interim Conclusions

The influence of the incorporation of MAPE, Si69 and VTMS coupling agents on the bulk and *in situ* mechanical properties of WPC has been examined. The better interfacial adhesion and more efficient stress transfer from the matrix to wood flour led to the improvement of the tensile strength (135.40%, 15.63%, and 77.40% respectively) and tensile modulus (112.73%, 63.3%, and 114.15% respectively) of MAPE, Si69 and VTMS treated WPC, while the tensile strain of the composites suffered from the stiffening impact of the treatments. The coupling agent treatments restrained the segmental mobility of polymer molecules of the matrix, resulted in the shift of relaxation peak and the diminutions of tanδ magnitude. The relatively lower level of adhesion factor confirmed the enhanced interfacial interactions in the treated composites.

The nanomechanical property of coupling agent treated composites fell into the sequence: VTMS > Si69 > MAPE. The decreased (MAPE and Si69 treated) and unaffected (VTMS treated) nanomechanical properties of the treated WPC determined by nanoindentation suggested that the *in situ* mechanical properties were not primarily governed by the interfacial adhesion, but more significantly affected by fibre weakening or softening impact (i.e. chain scission (cleavage of β-1,4-glycosidic bonds between two anhydroglucose units) and weakening of interfibrillar interaction in cellulose), crystalline structure transformation and cell wall deformation/damaging. To what extent the bulk mechanical properties of the composite could be improved was predominantly relying on the level of the enhancement of compatibility, interfacial adhesion and bonding after different coupling agent treatments rather than being governed by the individual local property of the material within the interface.

Chapter 7 Interface Structure and Bonding Mechanism of RubWPC

7.1 Introduction

The objective of this research was to develop a new generation of low carbon, reliably strong and eco-recycled materials (RubWPC) by turning ground tyre rubber (GTR) into sustainable resources for the existing wood plastic composites (WPC) production. Major benefits of the proposed solution include 1) to help resolve the disposal issue of the used tyre wastes, 2) to increase the resources and such eliminate resource pressure and hence reduce the production cost for classic WPC development, and 3) to add extra values to the reengineered composites (RubWPC) by enhancing the quality and sustainability. Prior to be equipped with these advantages, the formulated RubWPC should be of decent miscibility, compatibility and bonding among constituents.

The comprehensive study of interfacial optimisation of Rubber-PE composites and WPC by the use of coupling agents in Chapter 4 and Chapter 5 should serve as a fundamental basis for the reasonable formulation of RubWPC. However, the additional use of wood or rubber in Rubber-PE composites or WPC might alter the existing bonding scenarios in the systems with presence of coupling agents. The compatibility and bonding between wood and rubber is another crucial issue that should be taken into account during the development of RubWPC. Although there were numerous studies on wood flour or fibre filled rubber composites, virgin and unvulcanised natural rubber or synthetic rubber were extensively employed rather than vulcanised tyre rubber (Zhou *et al.*, 2015).

This chapter investigates the novel formulation of rubber-wood-plastic composites (RubWPC) based on recycled materials including GTR, wood flour and PE, with the focus on the optimisation of the constituent compatibility and interfacial bonding by employing MAPE, Si69 and VTMS coupling agents. Spectroscopic (ATR-FTIR and NMR) and microscopic (SEM) techniques were used to comprehensively scrutinise the surface chemical functionalities and structure, constituent compatibility, filler distribution, interfacial bonding

scenarios of the untreated and treated RubWPC, thus to unveil the bonding mechanisms of RubWPC.

7.2 Results and Discussion

7.2.1 Chemical structure and bonding

7.2.1.1 FTIR analysis

FTIR was used to investigate the surface chemical distribution of untreated and coupling agent treated RubWPC, the result was presented in Figure 7.1. In comparison to the untreated composite, the MAPE treated RubWPC showed sharper and more intense spectral bands at 1734 cm^{-1} and 1636 cm^{-1}, which were assigned to C=O and C=C stretching vibrations respectively (Osman *et al.*, 2010b; Ihemouchen *et al.*, 2013). On one hand this was because of the introduction of MA moiety in MAPE, but on the other hand it should be resulted from the esterification reaction occurred between the MA moiety and the hydroxyl groups of wood particles. It was reported that in the FTIR spectra of maleated polyolefins modified wood particles, the absorbance bands at near 2900 cm^{-1} (C-H stretching) and 1740 cm^{-1} (C=O stretching) were of special interest, since which suggested the formation of ester linkages (Carlborn and Matuana, 2006). A grafting index (*GI*) could be calculated based on the integrated areas under these peaks by using the following equation:

$$GI_x = \frac{A_{x(treated)}}{A_{x(untreated)}} \qquad \text{(Eq. 7.1)}$$

Where, x represents the absorbance band at either 2900 cm^{-1} or 1740 cm^{-1}, A_x represents the integrated peak area. *GI* was thus adopted to evaluate the grafting efficiency of RubWPC, the calculated results were shown as follows: GI_{2915} = 1.03, GI_{1734}= 1.03. In the previous FTIR study of MAPE treated WPC (Section 5.2.1.1), the corresponding indices were: GI_{2915} = 1.14, GI_{1734} = 1.09. The relatively lower values of RubWPC might indicate that the addition of rubber into the composite would restrict the esterification between MAPE and wood particles. In other words, although the rubber macromolecules crosslinked with the PE segment in MAPE, the MAPE crosslinked rubber might not further react with wood flour.

When Si69 was employed as the coupling agent for RubWPC, the chemical distribution and structure of the composite appeared to be barely affected by the treatment since the FTIR spectrum did not show considerable difference from that of the untreated composite in terms of the band appearances and intensities. The most distinguishing characteristic would be the presence of the slightly stronger and sharper band at 1032 cm^{-1}, which was an overlapped band originating from a number of vibrations including the C-S-C stretching of rubber and Si69, the Si-O-C stretching of Si69, and the C-O-C stretching, C-O deformation and aromatic C-H deformation vibrations of wood flour (Ihamouchen *et al.*, 2012; Abdelmouleh *et al.*, 2007; Gunasekaran *et al.*, 2007; Abdelmouleh *et al.*, 2004; Kotilainen *et al.*, 2000). It had been previously explored that in the FTIR spectra of Si69 treated WPC (Section 5.2.1.1), the area of interest namely 1020 cm^{-1} – 1100 cm^{-1} referring to C-O-Si and Si-O-Si bonds was not seen much variation after the treatment due to the limited crosslinking between the coupling agent and wood flour. Therefore, the slight intensity increase should be more predominantly contributed by the C-S linkages formed between Si69 and both rubber and PE molecules. In addition, the band at 967 cm^{-1} assigning to the C-H wagging motion vibration from the butadiene units in rubber (Gunasekaran *et al.*, 2007; Fernández-Berridi *et al.*, 2006) disappeared after its crosslinking reaction with the coupling agent. With respect to the RubWPC treated with the combination of MAPE and Si69, the spectral band at 1032 cm^{-1} turned to be much sharper with increased intensity. This was attributed to the formation of C-O-C bonds between MA groups and wood flour and the crosslinking reaction between the C-S-C linkages in rubber and the PE macromolecules in MAPE.

It was observed more prominent appearance of the band at 1031 cm^{-1} in the spectrum of VTMS treated composite. Chapter 4 suggested that VTMS was not an effective coupling agent in bridging the constituents of Rubber-PE composite. The intensity strengthening was primarily due to the Si-O-C linkages formed between the functional groups in wood flour (hydroxyl) and VTMS (methoxyl) along with the introduced Si-O-C groups within VTMS. Similar to MAPE&Si69 treated composite, MAPE&VTMS treated RubWPC demonstrated much more outstanding peaks at 1031 cm^{-1} and 1740 cm^{-1} than both the untreated and VTMS

treated composites, which was again due to the reactions between MAPE and wood flour and rubber particles.

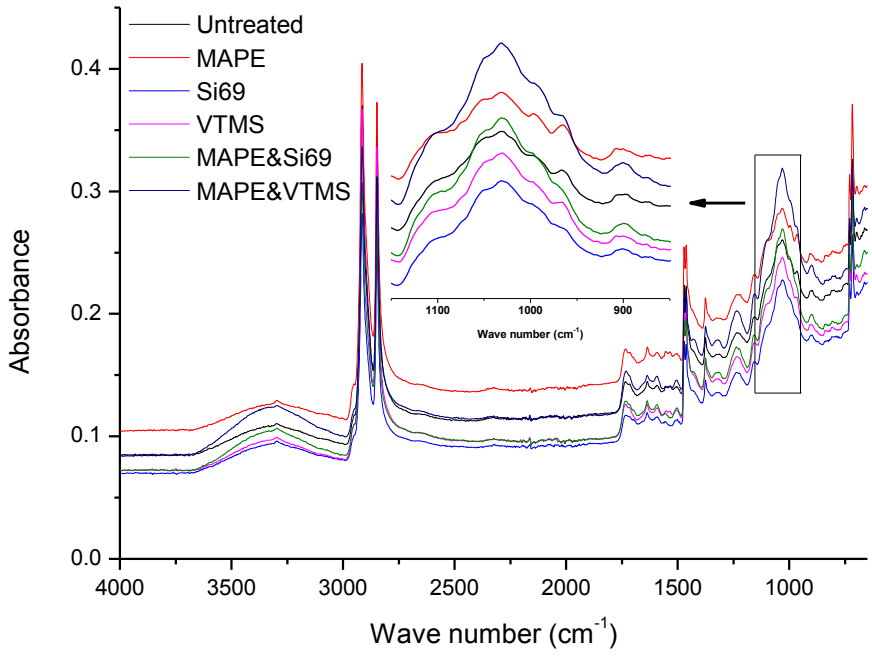

Figure 7.1. FTIR spectra of untreated and coupling agent treated RubWPC

7.2.1.2 NMR analysis

The comparison of NMR spectra of untreated and coupling agent treated RubWPC was presented in Figure 7.2 for further investigation of the variation of chemical structure after the treatments. Compared to the spectra of the untreated composite, the most noticeable difference in the spectra of MAPE treated composite was the occurrence of the resonance peak at 173.47 ppm, which was resulted from the MA groups in the incorporated MAPE and the ester bonds formed between the MA groups and the functional groups of raw materials. This result confirmed the aforementioned FTIR study of MAPE treatment of the composite. The reaction mechanism between MAPE and the raw materials was proposed in Figure 7.3a, namely the multifunctional MAPE first covalently bonded to the hydroxyl groups of wood flour to form ester linkages and thus crosslinked with PE and rubber macromolecules, acting as a bridge at composite interfaces.

Si69 treated composite showed a strong and wide peak at 55.52 ppm in its NMR spectrum, which was originally ascribed to the methoxyl groups of lignin unit in wood flour (Santoni *et al.*, 2015; Martins *et al.*, 2006; Stael *et al.*, 2000). The stronger appearance than that of the untreated was due to the existence of ethoxy groups within Si69. The above FTIR analysis revealed the crosslinking between Si69 and both rubber and PE macromolecules by forming C-S bonds, but there was unfortunately no resonance signal corresponding to these linkages in the NMR spectrum, which had also been detected in the previous study of Si69 treated Rubber-PE composites (Section 4.2.1.1). The lack of these bands in the NMR spectra might be explained by a number of reasons including: 1) insufficient concentrations of these bonds to be detected; 2) T_1 relaxation times of these units being much longer in comparison to the relaxation times of other molecular units in the polymers; and 3) T_2 relaxation times of these units being short enough to cause the signals to be broadened beyond detection (Sitarz *et al.*, 2013). The resonance peak at 65.08 ppm assigning to C6 of cellulose unit was widened and strengthened after the treatment, which indicated that the functional groups (ethoxy groups) of Si69 had successfully reacted with the hydroxyl groups linked to C6 of cellulose unit (Figure 7.4) in wood flour to form a siloxane bond, as the reaction shown in Figure 7.3b. The similar phenomenon was observed in the spectra of VTMS treated composite, and the chemical reaction between VTMS and the constituents of the composite was proposed in Figure 7.3c. In addition, the appearance of the peak at 153.33 ppm corresponding to aryl groups of lignin in the spectra of VTMS treated composite suggested that apart from the functional groups of carbohydrates (Figure 7.4) in wood, the lignin units might also be involved in the reaction with the coupling agent. Furthermore, it was interesting to notice that the composites treated with the combinations of different coupling agents did not demonstrate as intense resonance as the composite treated with solitary coupling agent.

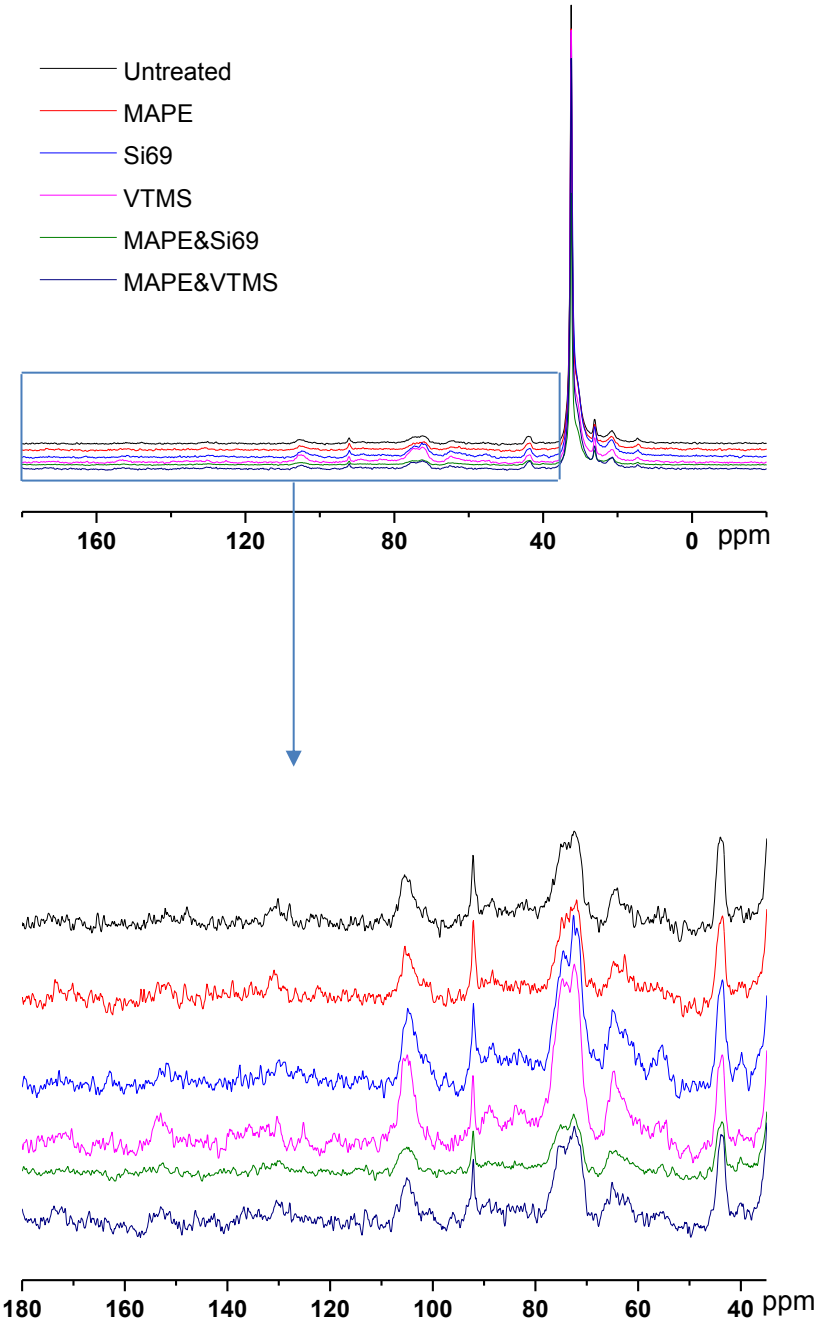

Figure 7.2 ^{13}C NMR spectra of untreated and coupling agent treated RubWPC

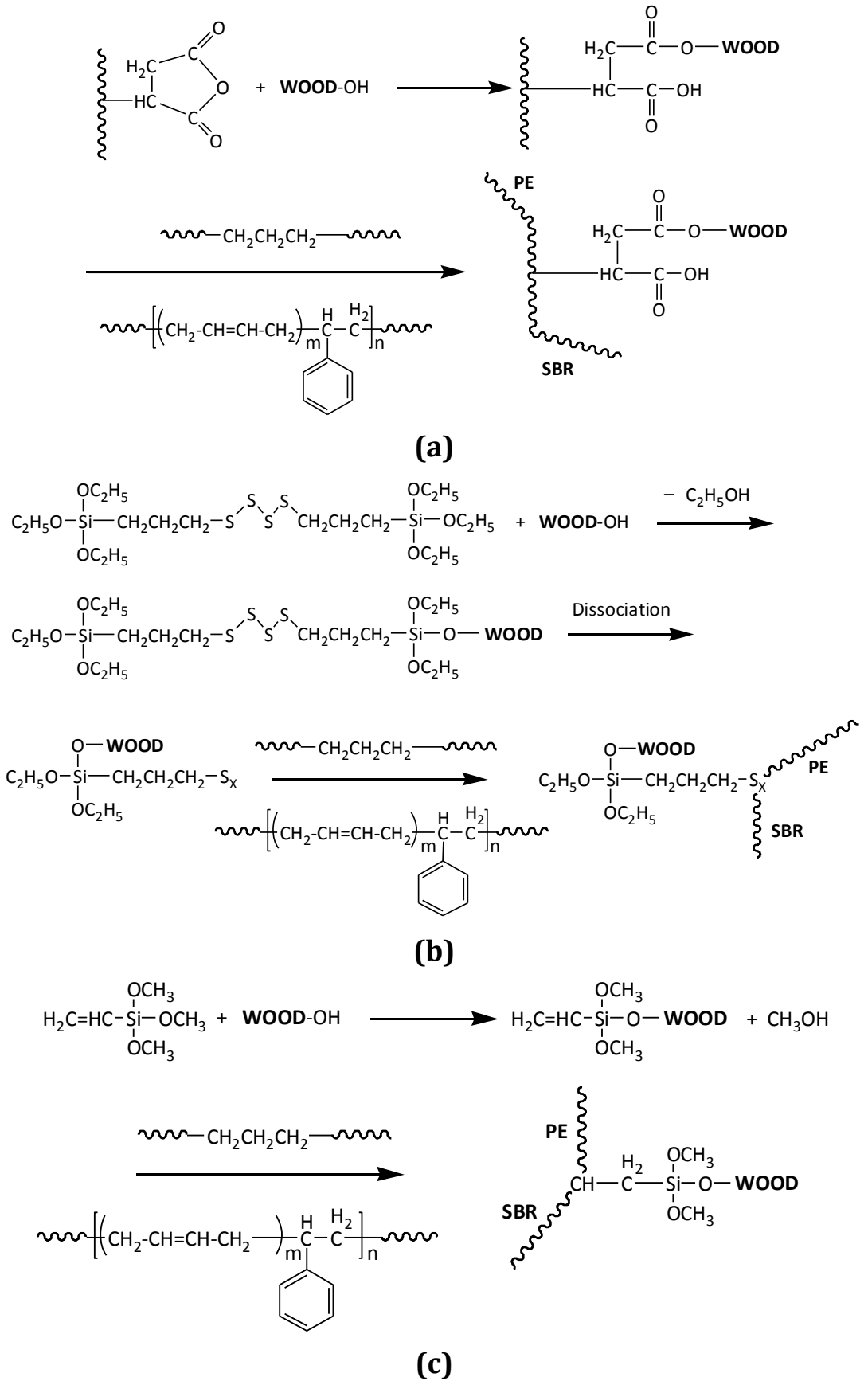

Figure 7.3 Proposed chemical reactions between the coupling agents (a: MAPE; b: Si69; c: VTMS) and the raw materials of RubWPC

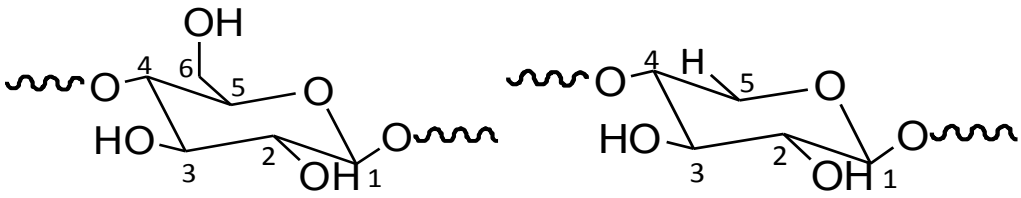

glucose **xylose**

Figure 7.4 Chemical structure of cellulose unit (glucose) and hemicellulose unit (xylose)

7.2.2 Interface structure and bonding mechanism

SEM was employed to investigate the interface microstructure and bonding scenarios of the untreated and treated RubWPC, the results were presented in Figure 7.5. The untreated composite (Figure 7.5a) displayed incompatible surface with the presence of microcracks and voids throughout the wood-matrix and rubber-matrix interfaces. There also existed noticeable agglomeration of rubber particles on the surface, which prevented the intimate contact and thus interaction with wood flour. These observations indicated the poor compatibility between the constituents in the untreated composites, leading to a discontinuous and inhomogeneous interfacial structure. With the incorporation of MAPE or Si69 coupling agents, rubber particle and wood flour were well distributed and embedded in the matrix and firmly bonded to it (Figure 7.5b and Figure 7.5c). It was also observed that more wood cell lumens were partially or utterly filled by the matrix polymer in the treated composites, substantiating the enhanced wood-PE compatibility and wettability of wood flour by matrix. Furthermore, although there still existed a few microcracks between wood flour and rubber particles, the observed close interfacial contact and compact structure confirmed the positive impact of the treatments on refining the inherent constituent immiscibility. These phenomena suggesting the improved interfacial adhesion and bonding after MAPE or Si69 treatments were discerned in the composite treated with the combination of these two coupling agents as well (Figure 7.5e).

The interface structure and bonding scenario in VTMS treated composite (Figure 7.5d) was found to be distinct from those in MAPE or Si69 treated composites. The absence of physical contact between rubber and wood phases in VTMS treated composite gave rise to the generation of voids and gaps, and the rubber

surface seemed to be clean, intact and free from adhering wood flour and matrix. This result was in accordance with the chemical structure analysis (section 7.2.1), namely that VTMS exerted superb compatibilisation impact on wood-matrix phase in the composite through intermolecular crosslinking and covalent bonding, but it was unfortunately not the suitable coupling agent for refining the rubber-PE or rubber-wood interfaces owing to its relatively limited physical and chemical interactions with rubber particles, which were evident in the chemical and interfacial structure analyses. However, as shown in Figure 7.5f, the addition of MAPE into the system provided the composite with decent interfacial bonding, which again confirmed that MAPE multifunctionally and effectively promoted the adhesion between rubber particles and either nonpolar matrix or polar wood flour.

The improvement of the interfacial bonding of the treated composites might be proposed in Figure 7.6. As unveiled in the above section of chemical structure and bonding, the coupling agents reacted with the substrates through the inherent multifunctional molecules, i.e. the hydrophilic moieties in coupling agents (MA of MAPE, ethoxy groups of Si69, and methoxyl groups of VTMS) reacted with the large amount of hydroxyl groups of wood flour to form strong covalent bonds, while the nonpolar molecules (PE chains in MAPE, dissociated sulfide groups of Si69, and vinyl groups of VTMS) chemically crosslinked with rubber and PE macromolecules. These chemical interactions clearly verified the enhanced chemical compatibility and adhesion after the treatments, which in turn provided the basis for intimate contact between constituents and thus good wetting of fillers. Hence, the chemical reactions along with other molecular attractions, such as electrostatic adhesion and Van der Waals forces, triggered a greater extent and degree of interdiffusion among the filler and matrix molecules as graphically demonstrated in Figure 7.6. Furthermore, mechanical interlocking might be another mechanism concerning the outstanding bonding, which took place through the penetration of polymer resin into the holes, valleys, crevices and other irregularities of the substrates, and then anchored itself through solidification. Figure 7.5 showed that the MAPE and Si69 treated composites possessed much more noticeable resin penetration into the fillers and resin impregnation at rubber-PE and wood-PE interfaces, denoting the existence of

more contact areas for mechanical interlocking of the substrates. It was undoubted that the interface development was a mutual result of the above bonding mechanisms (i.e. interdiffusion, chemical reaction, mechanical interlocking, etc.), which should be dependent, namely an increase in any bonding mechanism would benefit the enhancement of other bonding systems. In addition, since it was observed reduced agglomeration of rubber particles in the treated composites (Figure 7.5), the coupling agents, especially MAPE and Si69, might also act as a dispersing agent between rubber and PE matrix to form hydrogen bonds, promoting the dispersion of rubber particles in the resin (Osman *et al.*, 2010b).

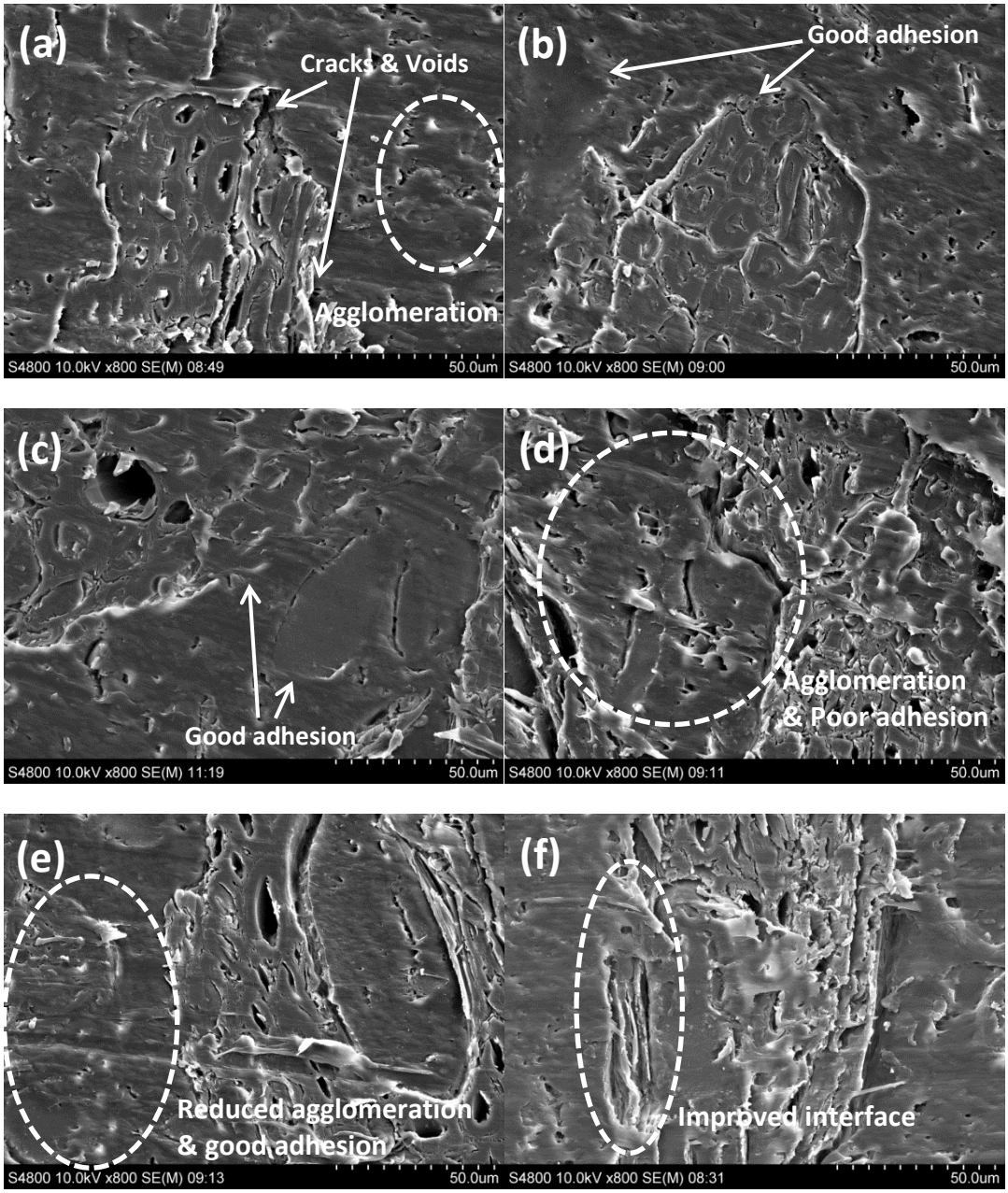

Figure 7.5 Microstructures of cross section of untreated (a), MAPE treated (b), Si69 treated (c), VTMS treated (d), MAPE&Si69 treated (e), and MAPE&VTMS treated (f) composites

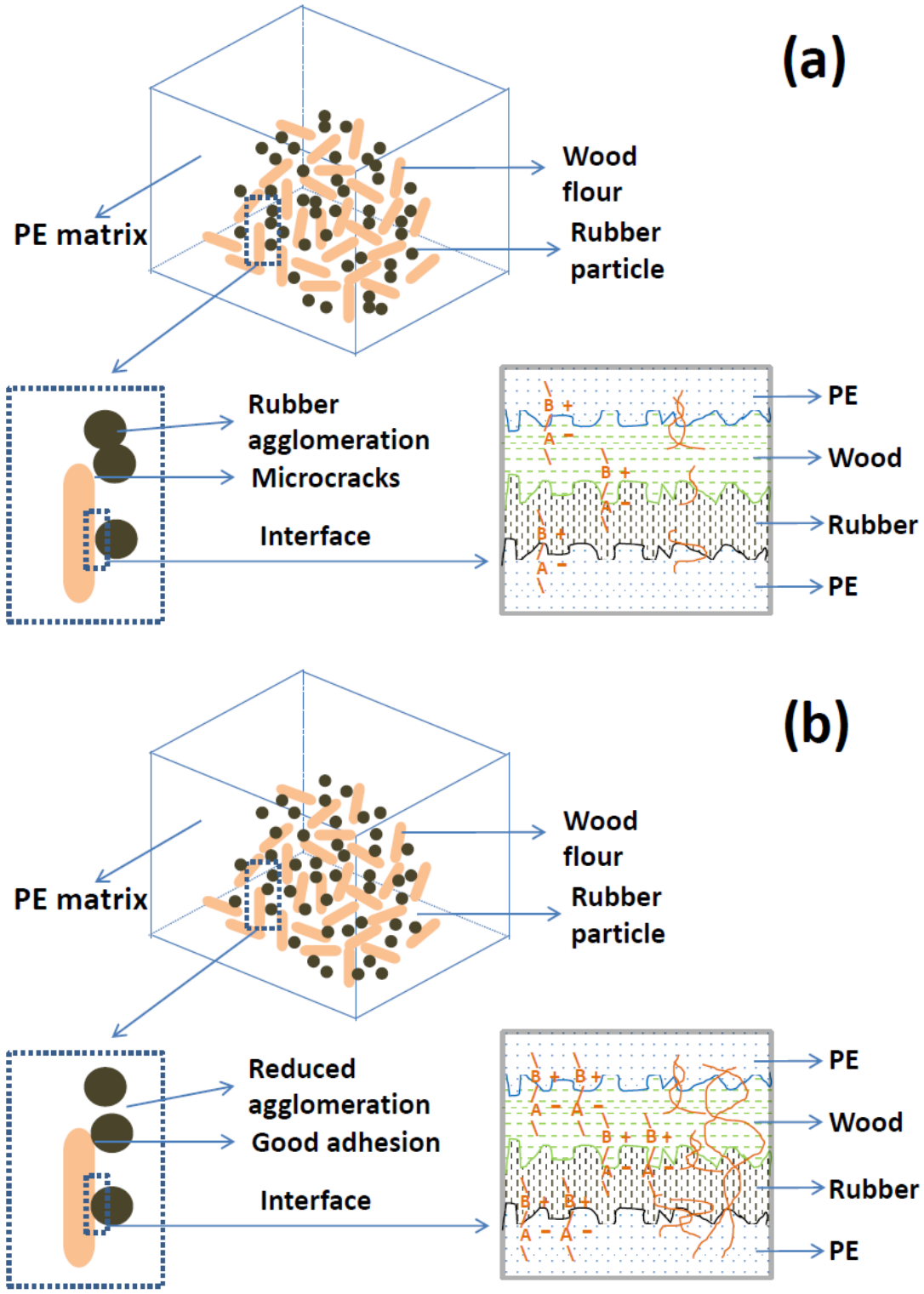

Figure 7.6 Proposed interfacial bonding mechanisms of untreated (a) and coupling agent treated (b) RubWPC

7.3 Interim Conclusions

The effect of the incorporation of MAPE, Si69 and VTMS coupling agents on the surface chemistry, interfacial structure and bonding of RubWPC material has

been determined. FTIR and NMR analyses unveiled the chemical reactions of the coupling agents with the substrates through their intrinsic multifunctional molecules, i.e. the hydrophilic moieties in coupling agents (MA of MAPE, ethoxy groups of Si69, and methoxyl groups of VTMS) reacted with the hydroxyl groups of wood flour to form strong covalent bonds, while the nonpolar molecules (PE chains in MAPE, dissociated sulfide groups of Si69, and vinyl groups of VTMS) chemically crosslinked with rubber and PE macromolecules. These chemical reactions substantiated the improvement of chemical compatibility and adhesion of the composites after coupling agent treatments, which benefitted the macromolecular interdiffusion and the wetting of the fillers by the matrix.

The incorporation of MAPE and Si69 coupling agents promoted the intimate contact between the constituents of the composites and the distribution and embedment of rubber particle and wood flour in the matrix with reduced filler agglomerations, which were evident in their microstructures. MAPE and Si69 treated composites possessed more resin penetration into the fillers and resin impregnation at rubber-PE and wood-PE interfaces, providing a rigorous basis for the mechanical interlocking of the substrates, and thus improving the interfacial bonding. VTMS treatment effectively improved the wood-PE interface within the composite, but it was not the appropriate coupling agent for refining rubber-PE or rubber-wood interfaces due to its poor interactions with rubber particles. Interdiffusion, molecular attractions, chemical reactions, and mechanical interlocking were mutually responsible for the enhancement of the interfacial adhesion and bonding of the RubWPC treated with MAPE and Si69 coupling agents.

Chapter 8 Bulk and *In Situ* Mechanical Properties of RubWPC

8.1 Introduction

The major factors affecting the mechanical performance of cellulosic polymer composites include: 1) the strength and modulus of reinforcing fibre, 2) the strength and chemical stability of polymer matrix, and 3) the effectiveness of load transfer across interface (Kumar *et al.*, 2004). Investigation of interface is of special significance in understanding the macro-behaviour of the composites (Zhang *et al.*, 2012). Interface is the region separating the bulk polymer from the fibrous reinforcement. It is not a distinct phase with clear boundaries, it is more accurately viewed as a transition zone with three-dimensional and heterogeneous nature. Interface region is hypothesised to possess mechanical properties distinct from those of the reinforcing phase and bulk polymer (Downing *et al.*, 2000). Recently, the direct determination of the property and size of interface of cellulosic polymer composites have been achieved with the advent of depth sensing indentation technique, which is generally referred to nanoindentation. This technique allows the penetration of an indenter into the material surface with controlled force and synchronous recording of the force applied as a function of indentation depth, thus provides considerable local mechanical property information (Yedla *et al.*, 2008).

In this chapter, the bulk mechanical properties of RubWPC were determined by tensile test analysis and dynamic mechanical analysis (DMA) aiming at understanding the reinforcing impact resulted from the coupling agent treatments and the influence of compositional variation on the properties. Furthermore, the *in situ* mechanical properties of both untreated and treated RubWPC were determined by carrying out nanoindentation analysis, which helped in unveiling the contribution of the coupling agent treatments to the *in situ* mechanical properties and also the correlation between bulk and *in situ* mechanical properties, thus enabled the optimal design of RubWPC materials.

8.2 Results and Discussion

8.2.1 Bulk mechanical properties

8.2.1.1 Tensile property analysis

Table 8.1 gives the tensile properties of the composites after coupling agent treatments. The incorporation of MAPE and VTMS coupling agents led to a subtle increment (i.e. 6.40%) of the tensile strength, while that of Si69 resulted in an increase of 31.07%. It was apparent that the strengthening effect was a result of the aforementioned enhanced interfacial adhesion and bonding between the fillers and matrix after the treatments, which in the meantime provided the composites with better stress distribution and more efficient stress transfer throughout the interfaces (Raju *et al.*, 2008). Moreover, as observed in the SEM analysis (Section 7.2.2), the uncompatibilised composite had more agglomeration of filler particles (i.e. wood and rubber) than the treated composites, which led to relatively poor dispersal of the particles in the homogeneous matrix. The more homogeneous distribution of filler particles after the treatments promoted the particle-matrix interaction and reduced the particle-particle interaction, thus facilitated the better energy transfer within the system (Ahmed *et al.*, 2014).

It can be seen from Table 8.1 that the tensile strain of the treated composites were decreased by 6.34% (MAPE), 17.61% (Si69), and 4.58% (VTMS) respectively, indicating that the coupling agent might impart a stiffening impact on the composites. This behaviour has also been found in WPC materials (Section 6.2.1), which contributed to the decreased deformability of the composites by restricting the mobility of the polymer chains (Osman *et al.*, 2010b; Osman *et al.*, 2012). However, the previous study of Rubber-PE composites suggested that the coupling agent treatments made the composite more ductile with enhanced resistance to crack propagation by showing much higher tensile strain (Section 4.2.3). In order to further investigate the variation of the rigidity and ductility of the composites, the tensile moduli were also determined and listed in Table 8.1. MAPE and VTMS treated composites showed marginally lower tensile moduli (4.39% and 0.07%) than untreated composite. These results along with their subtle decrease of tensile strain denoted that the treatments did not alter the

overall rigidity or ductility of the composites. In other words, the nature of the treated composites was not dominated by either stiffness increase from wood-matrix moiety or the ductility increase from rubber-matrix moiety within the composites. Instead, it was a result of mutual impacts. Contrary to the comparatively unremarkable differentiations, the tensile modulus of Si69 treated composite was increased by 18.00%, which seemed to indicate that the stiffening impact was more pronounced in its system.

The composites treated with the combination of distinct coupling agents, especially the combination of MAPE and Si69, showed superior tensile properties (i.e. higher tensile strength and tensile modulus) than the composites treated with single coupling agent. This result indicated that the combination of coupling agents was capable of equipping the resulted composite with better interfacial bonding and stress transfer by taking the advantage and avoiding the disadvantage of individual coupling agent. For instance, MAPE was exceptionally effective in refining wood-PE interface, but not rubber related interfaces. By contrast, Si69 was not as efficient as MAPE in terms of the wood-PE interface refinery, but it seemed to be the optimal candidate for addressing the interfacial bonding between rubber and other constituents (i.e. wood and PE) in the composite. Therefore, the combination of the coupling agents generated a complementary influence, maximising the capability of interface refining and bonding strengthening of each coupling agent. The macroscopic behaviour of heterogeneous materials mainly depends on the following four parameters: i) the behaviour of each phase; ii) the volume fraction of each phase; iii) the spatial arrangement of the phase or morphology; and iv) the interface properties (Abdelmouleh *et al.*, 2007). The latter was dependent on the degree of interaction between phases. The treatments with multiple coupling agents benefitted the chemical reaction and interdiffusion (FTIR analysis) along with filler wettability and embedment (SEM analysis), providing the composites with better interface properties.

With respect to the influence of the compositional variation on the tensile properties of the composites (Table 8.1), the continuous addition of rubber led to the decrease of the stiffness of the composites by showing higher tensile strain

and lower tensile modulus. This result was in agreement with the widely reported statement, namely the more incorporation of wood flour into polymer matrix resulted in higher rigidity of the composite (Santiagoo *et al.*, 2011; Raju *et al.*, 2008). It was found that the composite with 20% rubber had slightly higher tensile strength (1.96%) than that with 10% rubber. However, the more addition of rubber (30%) by reducing the matrix composition had a deleterious effect on the tensile strength of the composite. This was because the filler particles were no longer equally distributed and wetted by the polymer matrix, and the agglomeration of fillers tended to form a foreign domain undermining the homogeneity of the resulted composite.

Table 8.1 Tensile properties of untreated and coupling agent treated RubWPC

Sample	**Tensile stress (MPa)**	**Tensile strain (%)**	**Tensile modulus (MPa)**
Untreated	5.31±0.17	2.84±0.12	1405.64±63.74
MAPE treated	5.65±0.21	2.66±0.14	1343.90±85.51
Si69 treated	6.96±0.26	2.34±0.08	1658.62±101.68
VTMS treated	5.64±0.20	2.71±0.16	1402.12±60.25
MAPE&Si69	8.34±0.23	2.74±0.09	1696.63±102.10
MAPE&VTMS	6.15±0.24	2.56±0.12	1554.92±78.27
MAPE&Si69-10	8.18±0.31	1.66±0.14	2624.23±135.85
MAPE&Si69-30	5.40±0.19	2.64±0.11	1079.12±102.36

8.2.1.2 Dynamic mechanical analysis (DMA)

The transition of a polymeric material from glassy state to rubbery state, commonly investigated by the use of DMA, has been considered as a significant material property. Figure 8.1 illustrated the temperature dependence of the storage moduli of untreated and treated RubWPC. The storage moduli of all the composites gradually decreased with the increase of temperature. Compared to the untreated counterpart, the single coupling agent treated composites showed inferior storage moduli in the temperature range from -100^{o}C to -50^{o}C. At the temperature above -50^{o}C, the storage moduli of MAPE and Si69 treated

composites were higher than that of the untreated, while that of VTMS treated remained slightly lower but appeared to be much closer. It was worth noticing that the composites treated with combined coupling agents, especially MAPE&VTMS, exhibited greater modulus values than both untreated and single coupling agent treated composites. This result was in accordance with the tensile properties owing to the superior interfacial adhesion and bonding quality which had been revealed in the previous structure analyses (Section 7.2.1 and 7.2.2).

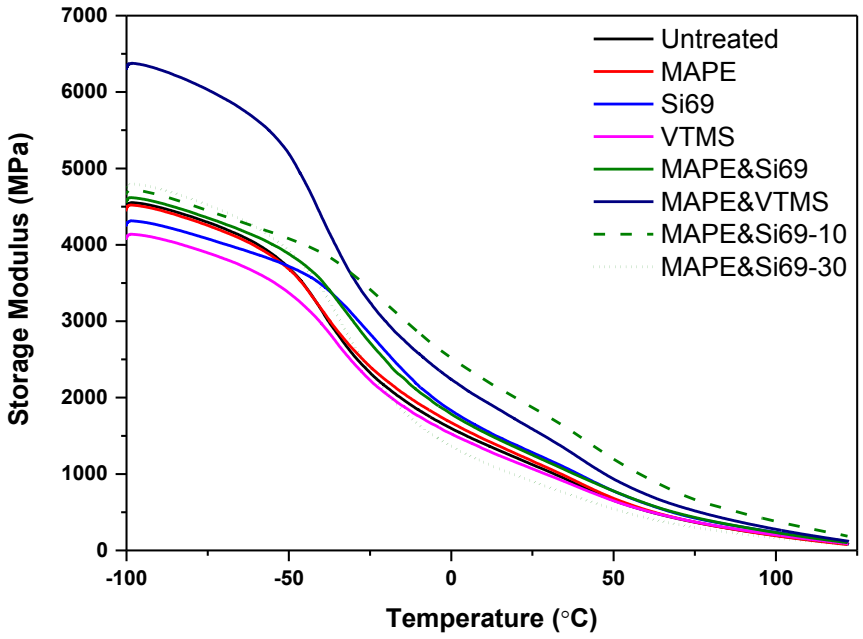

Figure 8.1 Storage modulus of untreated and treated composites as a function of temperature

The loss modulus is a measure of the energy dissipated as heat, representing the viscous portion of the material which flows under certain condition of stress. Figure 8.2 presented the variation of the loss modulus as a function of temperature of the composites. The relaxation peaks at -38°C to -20°C in the curves were associated with the molecular motion of rubber phase corresponding to its glass transition (Table 8.2). It was observed that the coupling agent treatments led to a flattening of the relaxation peaks with lowered loss modulus values, and the shift of relaxation peaks from -38.0°C (untreated) towards higher temperatures, indicating the enhanced interfacial interaction and adhesion between rubber particles and other constituents of the composites. In

addition, the relaxation peaks observed at around 50°C were attributed to the α transition of PE matrix, corresponding to its chain segment mobility (Bengtsson *et al.*, 2005; Mohanty and Nayak, 2006; Mohanty *et al.*, 2006). The relevant loss modulus at this temperature was seen a marginal increase after the coupling agent treatments, which was probably due to the reduced flexibility by introducing constraints on the segmental mobility of macromolecules at the relaxation temperatures (Ou *et al.*, 2014; López-Manchado *et al.*, 2002).

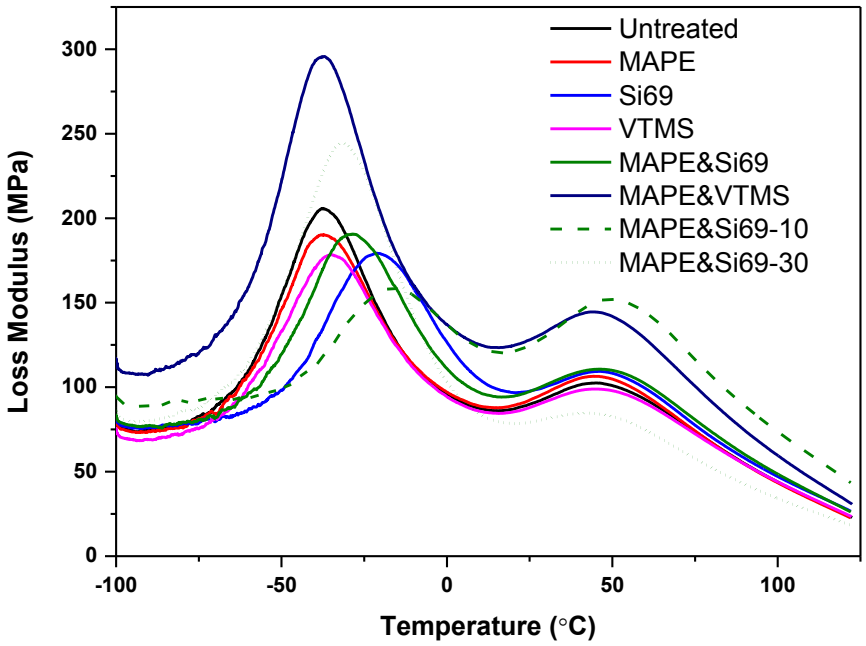

Figure 8.2 Loss modulus of untreated and treated composites as a function of temperature

The damping property of material gives a balance between the elastic phase and viscous phase in a polymeric structure. The mechanical loss factor or damping factor tanδ of the composites as a function of temperature was represented in Figure 8.3. The glass transition temperatures (T_g) of the treated composites shifted to higher temperatures, namely from -33.2°C (untreated) to -32.3°C (MAPE treated), -13.0°C (Si69 treated), -29.3°C (VTMS treated), -21.7°C (MAPE&Si69 treated), and -32.8°C (MAPE&VTMS treated) respectively (Table 8.2). This observation should be associated with the intermolecular crosslinking

induced by the coupling agent treatments (Ratnam *et al.*, 2001b), which had been thoroughly discussed in the previous section of chemical structure analysis (Section 7.2.1). The presence of the crosslinking was assumed to restrict the mobility of the polymeric chains so that more energy was required for the transition to occur (Mehdi *et al.*, 2004). On the other hand, the decline in the tanδ intensity or amplitude of the treated composites (Table 8.2) suggested the number of molecular portions responsible for the transitions had decreased after the treatments (Mehdi *et al.*, 2004). This result along with their better interfacial bonding, reduced interchain chemical heterogeneity, and relatively restricted segmental mobility of polymer molecules gave rise to less energy dissipation in the treated composites, leading to the reduction in the tanδ amplitude.

It could be seen that there was a gradual decrease in the storage modulus with the continuous addition of rubber particles into MAPE&Si69 treated composites, which affirmed the decrease of stiffness of the composites. It should be mentioned that regarding the difference between the composites with 20% and 30% rubber, the lower storage modulus in the composite with 30% rubber was ascribed to the poorer filler distribution and wetting due to the lower concentration of polymer matrix in the system. The relaxation peaks of the composites with less rubber addition were observed at higher temperature regions which were consistent with their higher T_g, suggesting that the stronger rubber-wood and rubber-PE interactions occurred in the composites contributed to the segmental immobilisation of the polymer chain along the interfaces and hence caused a lowering of the corresponding tanδ amplitude (Ahmad *et al.*, 2006).

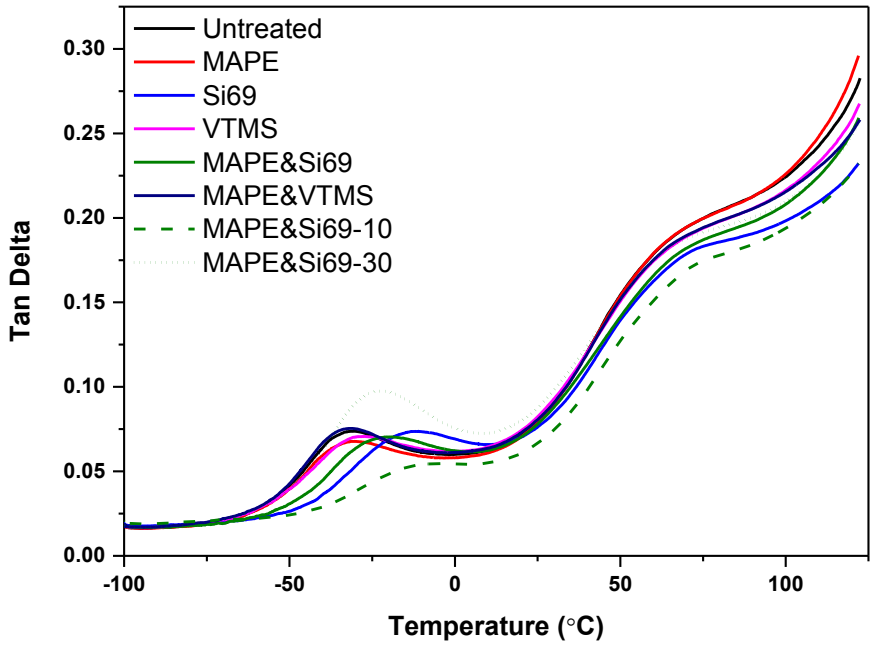

Figure 8.3 Tanδ of untreated and treated composites as a function of temperature

Table 8.2 Crucial parameters extracted from DMA curves of RubWPC

Sample	Temperature of rubber relaxation peak (T_r, °C)	Loss modulus at T_r (MPa)	Glass transition temperature (T_g, °C)	Tanδ at T_g
Untreated	-38.0	205.7	-33.2	0.073
MAPE treated	-37.5	190.1	-32.3	0.067
Si69 treated	-20.5	179.1	-13.0	0.073
VTMS treated	-34.8	178.6	-29.3	0.071
MAPE&Si69	-28.9	190.5	-21.7	0.070
MAPE&VTMS	-37.5	295.6	-32.8	0.075
MAPE&Si69-10	-16.4	158.5	-9.1	0.054
MAPE&Si69-30	-31.7	244.5	-22.5	0.098

8.2.2 Nanomechanical property analysis

Figure 8.4 shows the nanoindentation test regions of untreated and MAPE&Si69 treated RubWPC, the results from these measurements are presented in Figure 8.5. The hardness of the cell walls in the treated composite was nearly equal to

that of untreated composite. In contrast, the reduced elastic modulus of the treated cell walls was significantly increased by 20.84% compared to that of untreated cell walls, which was well in line with its bulk properties such as tensile modulus (Table 8.1) and storage modulus (Figure 8.1). This result might be associated with the considerable penetration of polymer resin into the more deformed and accessible cell lumens and vessels after the treatment, which were detected in its microstructure analysis (Section 7.2.2). Although it was widely accepted that the indentation modulus in damaged cell walls were lower than that in intact cell walls, the resin filling in cell lumens was a mechanical interlock that provided additional strength, recovering the loss of elastic behaviour due to mechanical processing (Konnerth and Gindl, 2006; Frihart, 2005; Gindl *et al.*, 2004). It was worth mentioning that in the previous nanoindentation study of WPC (Section 6.2.2), the coupling agent treatment might exert a weakening or softening impact on the cell walls through chain scission (i.e. cleavage of β-1,4-glycosidic bonds between two anhydroglucose units) or weakening of interfibrillar interaction, resulting in lower mechanical properties compared to untreated cell walls. The contrary behaviour explored in RubWPC indicated that with respect to the influence on nanomechanical properties of treated cell walls, the resin penetration was more pronounced over the weakening or softening impact with the inclusion of rubber particles into the composite, probably due to the physical, mechanical and chemical interactions between wood flour and rubber particles with the aid of coupling agents, which had been thoroughly discussed in Chapter 7. Therefore, the nanomechanical properties of the cell walls in untreated RubWPC remained unaffected by the rubber particles due to the lack of intimate physical contact between wood flour and rubber particle in untreated RubWPC (Figure 7.5), leading to subtle distinction from the nanomechanical properties of WPC (Fugure 5.4). In addition, MAPE and Si69 coupling agents might be able to diffuse into wood cell wall and form hydrogen bonding and covalent bonding with the structural components of the cell wall especially hemicellulose owing to its greater accessibility (Frihart, 2005), thus increase the nanomechanical property of the treated RubWPC.

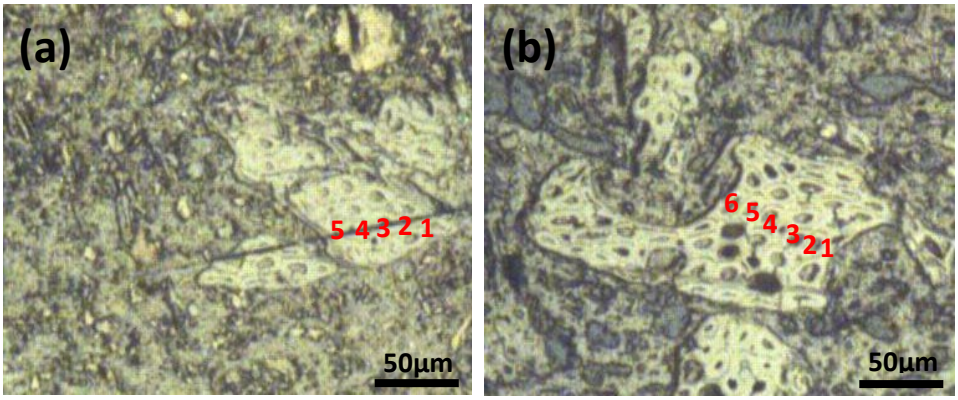

Figure 8.4 Microscope images of nanoindentation test regions of untreated and MAPE&Si69 treated RubWPC

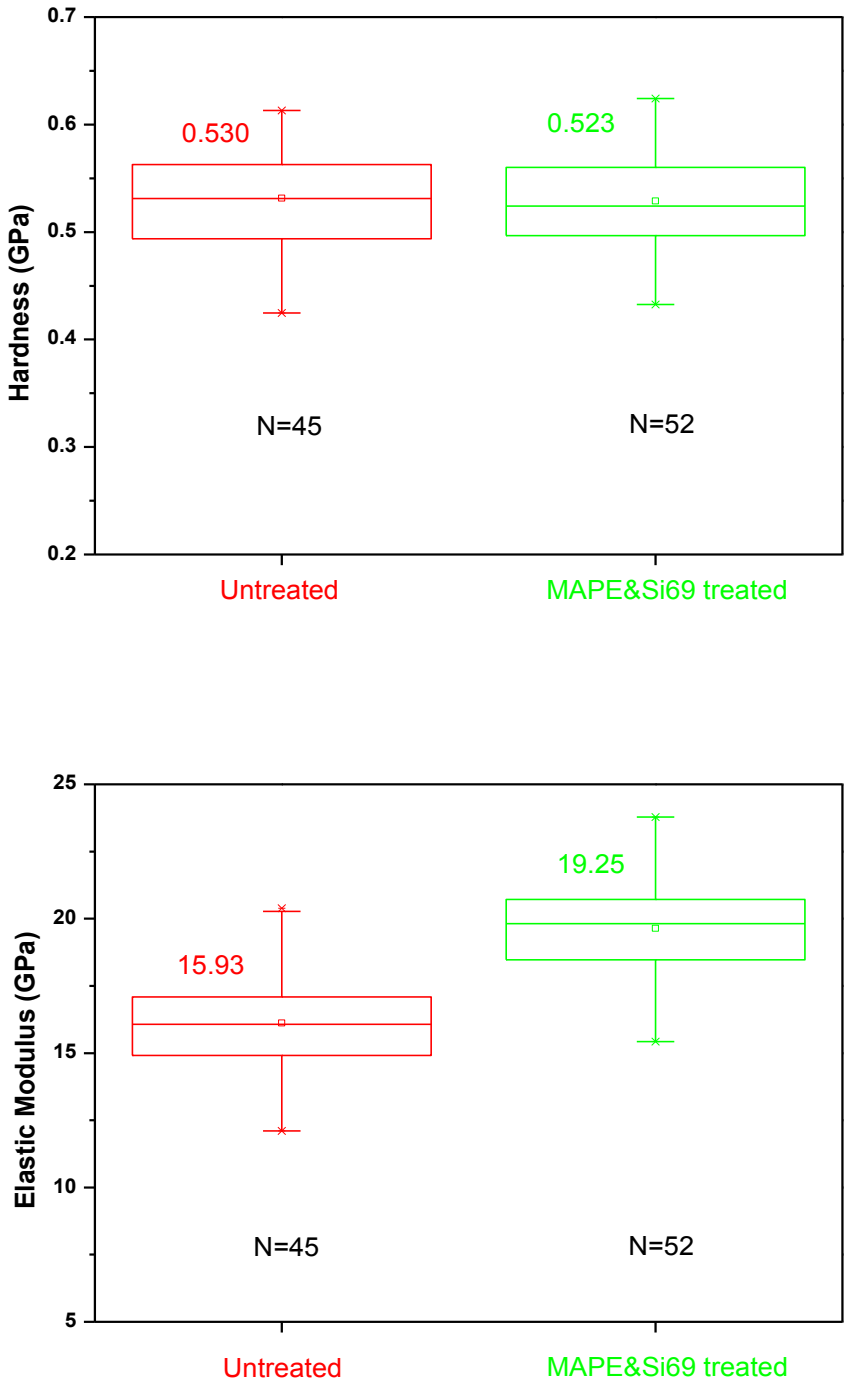

Figure 8.5 Nanomechanical properties of untreated and MAPE&Si69 treated RubWPC by nanoindentation

The individual nanomechanical property of every marked region in Figure 8.4 were presented in Figure 8.6 and Figure 8.7 for the purpose of figuring out the variation of the nanomechanical behaviour of the cell walls. The hardness and

indentation modulus of the cell wall in both untreated and treated composites increased with the increase of its distance to the zone being of immediate contact with rubber particle and PE matrix. For instance, the elastic moduli in region 1 (15.64 GPa) and region 5 (14.45 GPa) were lower than those in region 3 (16.67 GPa) and region 4 (17.50 GPa) of the untreated composite, the hardness in region 1 or region 6 of the treated composite was not comparable to the counterpart in other regions. This was because of the cell wall intimately contacting with other components was more deformed than the cell wall being further away from the bonding region, leading to inferior local mechanical property (Gindl *et al.*, 2004), albeit it might have more resin penetration into the adjacent cell lumen and coupling agent diffusion. Furthermore, the hardness or modulus distinction among different regions of the untreated composite (up to 0.05 GPa and 3.05 GPa respectively) was not as apparent as that of the treated composite (up to 0.06 GPa and 4.64 GPa respectively) due to the less deformed and accessible cell walls in the untreated composite, which was in accordance with the microstructure investigation in Section 7.2.2.

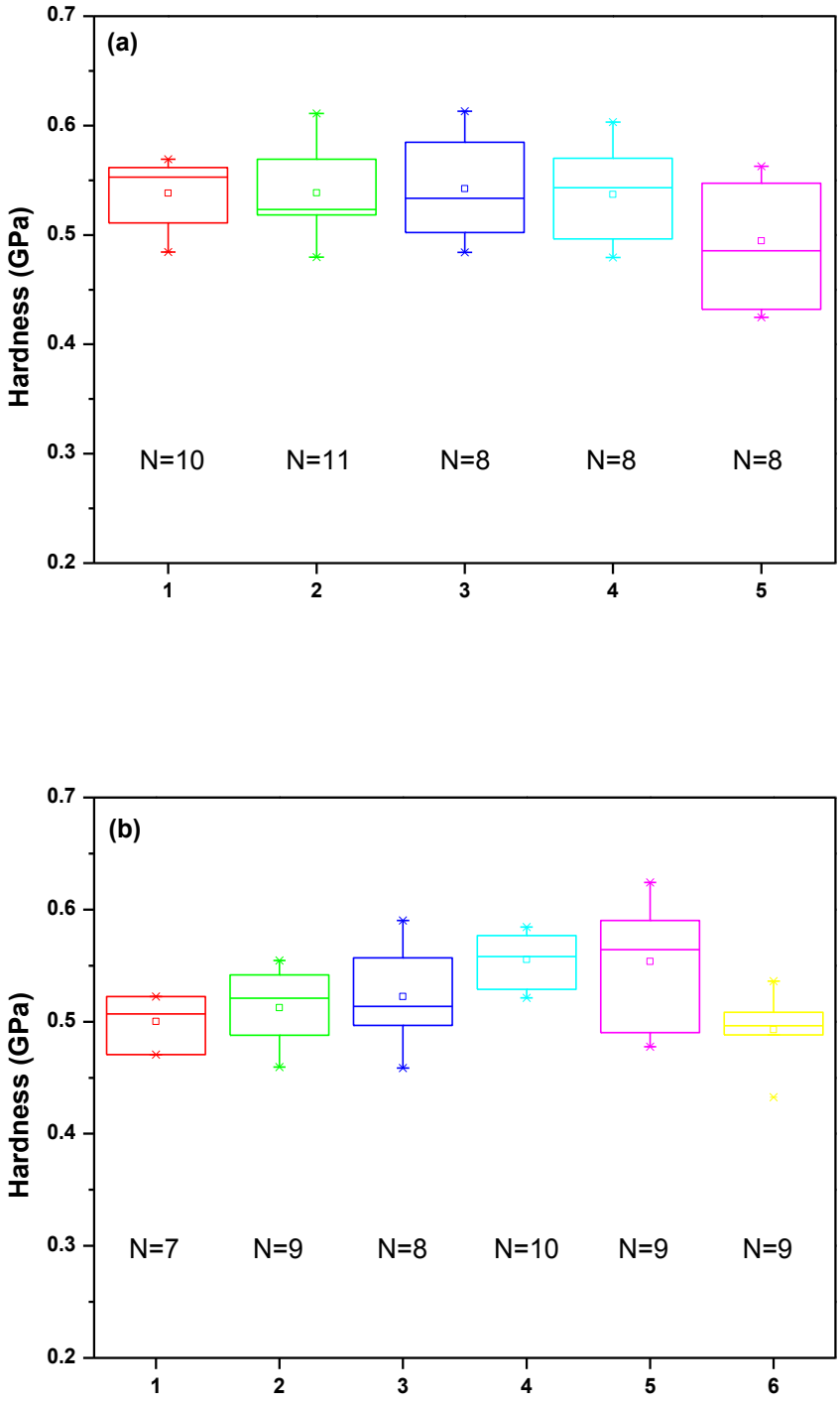

Figure 8.6 Comparison of the hardness in different test regions of untreated (a) and MAPE&Si69 treated (b) RubWPC

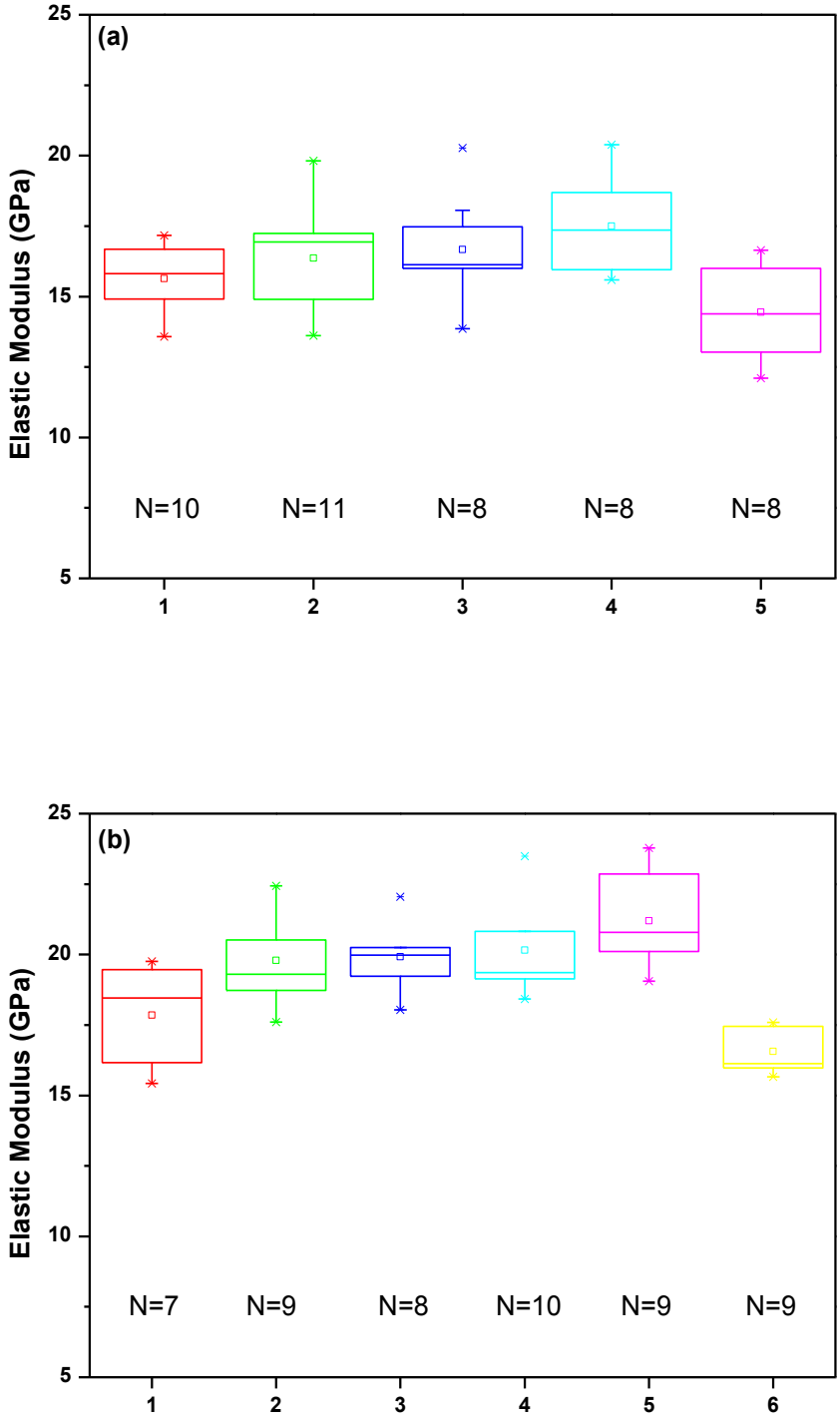

Figure 8.7 Comparison of the reduced elastic modulus in different test regions of untreated (a) and MAPE&Si69 treated (b) RubWPC

8.3 Interim Conclusions

The assessment of bulk and *in situ* mechanical properties of untreated and coupling agent treated RubWPC was accomplished by systematically carrying out tensile property analysis, DMA and nanoindentation measurements. The coupling agent treatments led to an increment in the tensile strength of RubWPC due to the enhanced interfacial bonding. Tensile strain and tensile modulus results denoted that the mechanical behaviour of the treated RubWPC was a mutual result of the stiffening impact of wood-PE moiety and the more ductile structure of rubber-PE phase within the composites rather than being dominated by either impact. The continuous addition of rubber into the composites impaired the tensile strength, while the ductility was increased with higher tensile strain and lower tensile modulus.

The enhanced interfacial bonding of the treated RubWPC was confirmed by the shift of relaxation peak and T_g towards higher temperatures along with the reduction in tanδ amplitude, which were associated with the restricted segmental polymer motion and less energy dissipation. The composites with less rubber addition demonstrated the corresponding relaxation peaks at higher temperatures with higher T_g and lower tanδ amplitude, primarily due to their stronger interfacial interactions. MAPE&Si69 treated RubWPC possessed more outstanding nanomechanical property than the untreated counterpart, which was ascribed to the considerable resin penetration into the more deformed and accessible cell lumens and vessels as well as the bonding formed between the diffused coupling agents and the structural components of cell walls. In addition, the nanomechanical properties (harness and elastic modulus) of the cell wall in both untreated and treated composites increased with the increase of its distance to the zone being of intimate contact with rubber particle and PE matrix.

Chapter 9 Conclusions and Recommendations for Future Work

9.1 Summary of the research

This research is devoted to 1) the formulation of Rubber-PE composites with optimised interface (Chapter 4), 2) thorough understanding of the chemical, physical and mechanical bonding mechanisms of WPC (Chapter 5), 3) the determination of bulk and *in situ* mechanical performance of WPC and their correlation with composite structures (Chapter 6), 4) novel formulation of RubWPC and comprehensive unveiling of the structure and bonding mechanism (Chapter 7), and 5) the investigation of the influence of interfacial bonding and compositional variation on the mechanical performance of RubWPC (Chapter 8). The major outcomes are summarised as follows:

1) The application of MAPE, Si69 and VTMS coupling agents improved the compatibility, homogeneity and interfacial bonding of Rubber-PE composites. FTIR results revealed that the crosslinking reactions occurred between the functional groups of MAPE (MA groups) and Si69 (sulfide groups) and the constituents of the composites, which gave rise to the enhancement of chemical compatibility and interdiffusion, rubber wettability by the matrix, and thus the interfacial adhesion of the composites. The spectral characteristics unveiling the chemical interactions between the coupling agents and raw materials were unfortunately not detected in NMR analysis probably due to insufficient concentration or inappropriate relaxation time of the corresponding bonds (e.g. C-O and C-O-Si).

SEM observations substantiated the improvement of the constituent compatibility, rubber wettability and embedment, and interfacial bonding after MAPE and Si69 treatments. VTMS treatment was not as effective as MAPE and Si69 treatments by showing comparatively limited crosslinking with the constituents and poorer interface within the composite. NMR analysis suggested the constraints on the segmental mobility of the polymers resulting from the treatments, which contributed to the shift of glass transition peaks and inferior tanδ amplitude as explored in DMA study. The mechanical properties including storage modulus, tensile strength and tensile strain of the composites were

increased due to the better interfacial compatibility and adhesion as well as more efficient stress transfer from the matrix to rubber particles after the treatments.

2) The physical, chemical and mechanical bonding mechanisms of WPC were systematically revealed by carrying out a set of assessments including ATR-FTIR, NMR, SEM and FM analyses. FTIR and NMR results confirmed the chemical reactions between the coupling agents and the constituents of the composites, i.e. the MA moiety in MAPE, the ethoxy groups of Si69 and the methoxyl groups of VTMS reacted with the hydroxyl groups of wood flour, in the meantime, the grafted PE chains in MAPE, the dissociated sulfide groups in Si69, and the vinyl groups of VTMS chemically bonded and/or interacted with the PE macromolecules. The introduced hydrocarbon chains of coupling agents also led to the decrease of hydrophilicity and the increase of surface energy of wood flour, and improved the chemical affinity of the matrix, thereby resulted in enhanced wettability of wood flour by the resin and interfacial adhesion. NMR results also indicated that there existed transformation of crystalline cellulose to an amorphous state during the coupling agent treatments, reflecting the inferior resonance of crystalline carbohydrates.

SEM observation revealed that the coupling agent treatments enhanced the interfacial compatibility and adhesion of WPC by promoting the dispersion of wood flour in the matrix, improving the wettability of wood flour by the resin, and facilitating the resin impregnation throughout the interface. The enhanced interface of the composites after the coupling agent treatments was resulted from the combination of increased macromolecular interdiffusion, chemical reactions and mechanical interlocking.

3) The better interfacial adhesion and more efficient stress transfer from the matrix to wood flour led to the improvement of the tensile strength (135.40%, 15.63%, and 77.40% respectively) and tensile modulus (112.73%, 63.3%, and 114.15% respectively) of MAPE, Si69 and VTMS treated WPC, while the tensile strain of the composites suffered from the stiffening impact of the treatments. The coupling agent treatments restrained the segmental mobility of polymer molecules of the matrix, resulted in the shift of relaxation peak and the diminution of tanδ magnitude. The broadening of the transition regions from

around 10°C to 85°C discerned in all the treated composites (especially MAPE and VTMS treated composites) might confirm the existence of the interactions between the coupling agents and the constituents of the composites.

The influence of the coupling agent treatments on the *in situ* mechanical properties of WPC has been first examined by nanoindentation analysis, and their correlation with bulk mechanical properties and composite structures have been established. The nanomechanical property of coupling agent treated composites fell into the sequence: VTMS > Si69 > MAPE. The decreased (MAPE and Si69 treated) and unaffected (VTMS treated) nanomechanical properties of the treated WPC determined by nanoindentation suggested that the *in situ* mechanical properties were not primarily governed by the interfacial adhesion, but more significantly affected by fibre weakening or softening impact (i.e. chain scission (cleavage of β-1,4-glycosidic bonds between two anhydroglucose units) and weakening of interfibrillar interaction in cellulose), crystalline structure transformation and cell wall deformation/damaging. To what extent the bulk mechanical properties of the composite could be improved was predominantly relying on the level of the enhancement of compatibility, interfacial adhesion and bonding after different coupling agent treatments rather than being governed by the individual local property of the material within the interface.

4) RubWPC materials have been innovatively developed with the additional use of GTR as raw material in WPC. The variation of the chemical functionalities and structure, interface microstructure, and bonding scenarios during coupling agent treatments of RubWPC has been comprehensively scrutinised. FTIR and NMR analyses unveiled the chemical reactions of the coupling agents with the substrates through their intrinsic multifunctional molecules, i.e. the hydrophilic moieties in coupling agents (MA of MAPE, ethoxy groups of Si69, and methoxyl groups of VTMS) reacted with the hydroxyl groups of wood flour to form strong covalent bonds, while the nonpolar molecules (PE chains in MAPE, dissociated sulfide groups of Si69, and vinyl groups of VTMS) chemically crosslinked with rubber and PE macromolecules. These chemical reactions substantiated the improvement of chemical compatibility and adhesion of the composites after

coupling agent treatments, which benefitted the macromolecular interdiffusion and the wetting of the fillers by the matrix.

The incorporation of MAPE and Si69 coupling agents promoted the intimate contact between the constituents of the composites and the distribution and embedment of rubber particle and wood flour in the matrix with reduced filler agglomerations, which were evident in their microstructures. MAPE and Si69 treated composites possessed more resin penetration into the fillers and resin impregnation at rubber-PE and wood-PE interfaces, providing a rigorous basis for the mechanical interlocking of the substrates, and thus improving the interfacial bonding. VTMS treatment effectively improved the wood-PE interface within the composite, but it was not the appropriate coupling agent for refining rubber-PE or rubber-wood interfaces due to its poor interactions with rubber particles. Interdiffusion, molecular attractions, chemical reactions, and mechanical interlocking were mutually responsible for the enhancement of the interfacial adhesion and bonding of the RubWPC treated with MAPE and Si69 coupling agents.

5) The assessment of bulk and *in situ* mechanical properties of untreated and coupling agent treated RubWPC was accomplished by systematically carrying out tensile property analysis, DMA and nanoindentation measurements. The coupling agent treatments led to an increment in the tensile strength of RubWPC due to the enhanced interfacial bonding. Tensile strain and tensile modulus results denoted that the mechanical behaviour of the treated RubWPC was a mutual result of the stiffening impact of wood-PE moiety and the more ductile structure of rubber-PE phase within the composites rather than being dominated by either impact. The continuous addition of rubber into the composites impaired the tensile strength, while the ductility was increased with higher tensile strain and lower tensile modulus.

The enhanced interfacial bonding of the treated RubWPC was confirmed by the shift of relaxation peak and T_g towards higher temperatures along with the reduction in tanδ amplitude, which were associated with the restricted segmental polymer motion and less energy dissipation. The composites with less rubber addition demonstrated the corresponding relaxation peaks at higher

temperatures with higher T_g and lower tanδ amplitude, primarily due to their stronger interfacial interactions. MAPE&Si69 treated RubWPC possessed more outstanding nanomechanical property than the untreated counterpart, which was ascribed to the considerable resin penetration into the more deformed and accessible cell lumens and vessels as well as the bonding formed between the diffused coupling agents and the structural components of cell walls. In addition, the nanomechanical properties (harness and elastic modulus) of the cell wall in both untreated and treated composites increased with the increase of its distance to the zone being of intimate contact with rubber particle and PE matrix.

9.2 Recommendations for future work

This research provides a scientifically and industrially promising approach for realising valorisation of waste tyre rubber through the development of RubWPC materials. Beyond the knowledge established in this work, the following suggestions should be considered and carried out in the future development of RubWPC materials:

1) The development and/or selection of efficient and cost effective surface modification method for both the fillers and matrix are the first critical area to be considered for future development of RubWPC. The tendency is in favour of treatment that not only provides superb tailoring but also has minimal impact on economics.

2) It is well known that rubber can be used as an acoustic absorbing material for noise and vibration control. Since the undesirable and potentially hazardous noise is considered as serious environmental pollution, the acoustic properties of RubWPC should be determined for the benefits of broadening its potential applications in different industrial sectors.

3) The particle size of GTR is postulated to affect the structure and performance of the formulated RubWPC. Hence, the effect of varying particle size of GTR on the filler distribution, interfacial bonding, physical and mechanical properties should be taken into account in the future study of RubWPC.

4) Although the application of nanoscience in lignocellulosic polymer composites is currently at the infant state, nano-enhanced polymer composites will become

inevitable in the near future. Nanofillers, such as nanorubber, nanocellulose and graphene, should be considered in the further formulation of RubWPC, which might equip the resulted material with more attractive properties.

REFERENCES

Abdelmouleh, M., Boufi, S., Belgacem, M.N., Duarte, A.P., Salah, A.B. and Gandini, A. (2004) 'Modification of cellulosic fibres with functionalised silanes: development of surface properties', *International Journal of Adhesion and Adhesives,* 24(1), pp. 43-54.

Abdelmouleh, M., Boufi, S., Belgacem, M.N. and Dufresne, A. (2007) 'Short natural-fibre reinforced polyethylene and natural rubber composites: Effect of silane coupling agents and fibres loading', *Composites Science and Technology,* 67(7–8), pp. 1627-1639.

Adhikary, K.B., Pang, S. and Staiger, M.P. (2008) 'Dimensional stability and mechanical behaviour of wood–plastic composites based on recycled and virgin high-density polyethylene (HDPE)', *Composites Part B: Engineering,* 39(5), pp. 807-815.

Aganov, A.V. and Antonovskii, V.L. (1982) '^{13}C NMR Spectra of organic peroxides', *Bulletin of the Academy of Sciences of the USSR,* 31(2), pp. 247-250.

Ahmad, I., Wong, P.Y. and Abdullah, I. (2006) 'Effects of fiber composition and graft-copoly(ethylene/maleic anhydride) on thermoplastic natural rubber composites reinforced by aramid fiber', *Polymer Composites,* 27(4), pp. 395-401.

Ahmed, K., Nizami, S.S. and Riza, N.Z. (2014) 'Reinforcement of natural rubber hybrid composites based on marble sludge/Silica and marble sludge/rice husk derived silica', *Journal of Advanced Research,* 5(2), pp. 165-173.

Akiba, M. and Hashim, A.S. (1997) 'Vulcanization and crosslinking in elastomers', *Progress in Polymer Science,* 22(3), pp. 475-521.

Alvarez, V. and Vazquez, A. (2004) 'Thermal degradation of cellulose derivatives/starch blends and sisal fibre biocomposites', *Polymer Degradation and Stability,* 84(1), pp. 13-21.

Andreis, M., Liu, J. and Koenig, J.L. (1989) 'Solid-state carbon-13 NMR Studies of vulcanized elastomers. V. Observation of new structures in sulfur-vulcanized natural rubber', *Journal of Polymer Science Part B: Polymer Physics,* 27(7), pp. 1389-1404.

Anuar, H., Ahmad, S.H., Rasid, R. and Daud, N.S.N. (2006) 'Tensile and Impact Properties of Thermoplastic Natural Rubber Reinforced Short Glass Fiber and Empty Fruit Bunch Hybrid Composites', *Polymer-Plastics Technology and Engineering,* 45(9), pp. 1059-1063.

Anuar, H., Ahmad, S.H., Rasid, R., Surip, S.N., Czigany, T. and Romhany, G. (2007) 'Essential Work of Fracture and Acoustic Emission Study on TPNR Composites Reinforced by Kenaf Fiber', *Journal of Composite Materials,* 41(25), pp. 3035-3049.

Anuar, H. and Zuraida, A. (2011) 'Improvement in mechanical properties of reinforced thermoplastic elastomer composite with kenaf bast fibre', *Composites Part B: Engineering,* 42(3), pp. 462-465.

Arantes, T.M., Leão, K.V., Tavares, M.I.B., Ferreira, A.G., Longo, E. and Camargo, E.R. (2009) 'NMR study of styrene-butadiene rubber (SBR) and TiO2 nanocomposites', *Polymer Testing,* 28(5), pp. 490-494.

Araújo, J.R., Waldman, W.R. and De Paoli, M.A. (2008) 'Thermal properties of high density polyethylene composites with natural fibres: Coupling agent effect', *Polymer Degradation and Stability,* 93(10), pp. 1770-1775.

Ashida, M., Noguchi, T. and Mashimo, S. (1984) 'Dynamic moduli for short fiber-CR composites', *Journal of Applied Polymer Science,* 29(2), pp. 661-670.

Azlinaa, H.N., Sahrima, H.A. and Rozaidia, R. (2011) 'Enhanced Tensile and Dynamic Mechanical Properties of Thermoplastic Natural Rubber Nanocomposites', *Polymer-Plastics Technology and Engineering,* 50(3), pp. 1383-1387.

Azwa, Z.N., Yousif, B.F., Manalo, A.C. and Karunasena, W. (2013) 'A review on the degradability of polymeric composites based on natural fibres', *Materials and Design,* 47, pp. 424-442.

Bajpai, P.K., Singh, I. and Madaan, J. (2013) 'Tribological behavior of natural fiber reinforced PLA composites', *Wear,* 297(1–2), pp. 829-840.

Belgacem, M.N. and Gandini, A. (2005) 'The surface modification of cellulose fibres for use as reinforcing elements in composite materials', *Composite Interfaces,* 12(1-2), pp. 41-75.

Bengtsson, M., Gatenholm, P. and Oksman, K. (2005) 'The effect of crosslinking on the properties of polyethylene/wood flour composites', *Composites Science and Technology,* 65(10), pp. 1468-1479.

Bengtsson, M. and Oksman, K. (2006) 'The use of silane technology in crosslinking polyethylene/wood flour composites', *Composites Part A: Applied Science and Manufacturing,* 37(5), pp. 752-765.

Bengtsson, M., Stark, N.M. and Oksman, K. (2007) 'Durability and mechanical properties of silane cross-linked wood thermoplastic composites', *Composites Science and Technology,* 67(13), pp. 2728-2738.

Bhardwaj, R., Mohanty, A.K., Drzal, L.T., Pourboghrat, F. and Misra, M. (2006) 'Renewable resource-based green composites from recycled cellulose fiber and poly(3-hydroxybutyrate-co-3-hydroxyvalerate) bioplastic', *Biomacromolecules,* 7(6), pp. 2044-2051.

Bledzki, A.K., Gassan, J. and Theis, S. (1998) 'Wood-filled thermoplastic composites', *Mechanics of Composite Materials,* 34(6), pp. 563-568.

Bledzki, A.K. and Gassan, J. (1999) 'Composites reinforced with cellulose based fibres', *Progress in Polymer Science,* 24(2), pp. 221-274.

Bledzki, A.K., Mamun, A.A., Lucka-Gabor, M. and Gutowski, V.S. (2008) 'The effects of acetylation on properties of flax fibre and its polypropylene composites', *Express Polymer Letters,* 2(6), pp. 413-422.

Bocz, K., Szolnoki, B., Marosi, A., Tábi, T., Wladyka-Przybylak, M. and Marosi, G. (2014) 'Flax fibre reinforced PLA/TPS biocomposites flame retarded with multifunctional additive system', *Polymer Degradation and Stability,* 106, pp. 63-73.

Buzaré, J.Y., Silly, G., Emery, J., Boccaccio, G. and Rouault, E. (2001) 'Aging effects on vulcanized natural rubber studied by high resolution solid state 13C-NMR', *European Polymer Journal,* 37(1), pp. 85-91.

Cantero, G., Arbelaiz, A., Llano-Ponte, R. and Mondragon, I. (2003) 'Effects of fibre treatment on wettability and mechanical behaviour of flax/polypropylene composites', *Composites Science and Technology,* 63(9), pp. 1247-1254.

Carlborn, K. and Matuana, L.M. (2006) 'Functionalization of wood particles through a reactive extrusion process', *Journal of Applied Polymer Science,* 101(5), pp. 3131-3142.

Choi, S. (2002) 'Influence of storage time and temperature and silane coupling agent on bound rubber formation in filled styrene–butadiene rubber compounds', *Polymer Testing,* 21(2), pp. 201-208.

Clemons, C.M., Sabo, R.C. and Hirth, K.C. (2011) 'The effects of different silane crosslinking approaches on composites of polyethylene blends and wood flour', *Journal of Applied Polymer Science,* 120(4), pp. 2292-2303.

Coats, E.R., Loge, F.J., Wolcott, M.P., Englund, K. and McDonald, A.G. (2008) 'Production of natural fiber reinforced thermoplastic composites through the use of polyhydroxybutyrate-rich biomass', *Bioresource technology,* 99(7), pp. 2680-2686.

Colom, X., Cañavate, J., Carrillo, F., Velasco, J.I., Pagès, P., Mujal, R. and Nogués, F. (2006) 'Structural and mechanical studies on modified reused tyres composites', *European Polymer Journal,* 42(10), pp. 2369-2378.

Correa, C.A., Razzino, C.A. and Hage, E. (2007) 'Role of Maleated Coupling Agents on the Interface Adhesion of Polypropylene—Wood Composites', *Journal of Thermoplastic Composite Materials,* 20(3), pp. 323-339.

Cunha, M., Berthet, M., Pereira, R., Covas, J.A., Vicente, A.A. and Hilliou, L. (2015) 'Development of polyhydroxyalkanoate/beer spent grain fibers composites for film blowing applications', *Polymer Composites,* 36(10), pp. 1859-1865.

Curvelo, A.A.S., de Carvalho, A.J.F. and Agnelli, J.A.M. (2001) 'Thermoplastic starch–cellulosic fibers composites: preliminary results', *Carbohydrate Polymers,* 45(2), pp. 183-188.

De, D., Das, A., De, D., Dey, B., Debnath, S.C. and Roy, B.C. (2006) 'Reclaiming of ground rubber tire (GRT) by a novel reclaiming agent', *European Polymer Journal,* 42(4), pp. 917-927.

Deguchi, S., Tsujii, K. and Horikoshi, K. (2008) 'Crystalline-to-amorphous transformation of cellulose in hot and compressed water and its implications for hydrothermal conversion', *Green Chemistry,* 10(2), pp. 191-196.

Deshmukh, A.P., Simpson, A.J. and Hatcher, P.G. (2003) 'Evidence for cross-linking in tomato cutin using HR-MAS NMR spectroscopy', *Phytochemistry,* 64(6), pp. 1163-1170.

Dhakal, H.N., Zhang, Z.Y., Richardson, M.O.W. and Errajhi, O.A.Z. (2007) 'The low velocity impact response of non-woven hemp fibre reinforced unsaturated polyester composites', *Composite Structures,* 81(4), pp. 559-567.

Dhakal, H., Zhang, Z., Bennett, N., Lopez-Arraiza, A. and Vallejo, F. (2014) 'Effects of water immersion ageing on the mechanical properties of flax and jute fibre biocomposites evaluated by nanoindentation and flexural testing', *Journal of Composite Materials,* 48(11), pp. 1399-1406.

Diao, B., Isayev, A.I. and Levin, V.Y. (1999) 'Basic Study of Continuous Ultrasonic Devulcanization of Unfilled Silicone Rubber', *Rubber Chemistry and Technology,* 72(1), pp. 152-164.

Ding, W., Jahani, D., Chang, E., Alemdar, A., Park, C.B. and Sain, M. (2016) 'Development of PLA/cellulosic fiber composite foams using injection molding: Crystallization and foaming behaviors', *Composites Part A: Applied Science and Manufacturing,* 83, pp. 130-139.

Dittenber, D.B. and Gangarao, H.V.S. (2012) 'Critical review of recent publications on use of natural composites in infrastructure', *Composites Part A: Applied Science and Manufacturing,* 43(8), pp. 1419-1429.

Doan, T., Brodowsky, H. and Mäder, E. (2012) 'Jute fibre/epoxy composites: Surface properties and interfacial adhesion', *Composites Science and Technology,* 72(10), pp. 1160-1166.

Downing, T.D., Kumar, R., Cross, W.M., Kjerengtroen, L. and Kellar, J.J. (2000) 'Determining the interphase thickness and properties in polymer matrix composites using phase imaging atomic force microscopy and nanoindentation', *Journal of Adhesion Science and Technology,* 14(14), pp. 1801-1812.

Drzal, L.T. and Madhukar, M. (1993) 'Fibre-matrix adhesion and its relationship to composite mechanical properties', *Journal of Materials Science,* 28(3), pp. 569-610.

El-Abbassi, F., Assarar, M., Ayad, R. and Lamdouar, N. (2015) 'Effect of alkali treatment on Alfa fibre as reinforcement for polypropylene based eco-composites: Mechanical behaviour and water ageing', *Composite Structures,* 133, pp. 451-457.

Faludi, G., Dora, G., Imre, B., Renner, K., Móczó, J. and Pukánszky, B. (2014) 'PLA/lignocellulosic fiber composites: Particle characteristics, interfacial adhesion, and failure mechanism', *Journal of Applied Polymer Science,* 131(4), pp. 39902(1-10).

Feih, S., Wonsyld, K., Minzari, D., Westermann, P. and Lilholt, H. (2004) *Testing Procedure for the Single Fiber Fragmentation Test.* Denmark: Technical University of Denmark.

Felix, J.M. and Gatenholm, P. (1991) 'The nature of adhesion in composites of modified cellulose fibers and polypropylene', *Journal of Applied Polymer Science,* 42(3), pp. 609-620.

Fernandes, E.M., Mano, J.F. and Reis, R.L. (2013) 'Hybrid cork-polymer composites containing sisal fibre: Morphology, effect of the fibre treatment on the mechanical properties and tensile failure prediction', *Composite Structures,* 105, pp. 153-162.

Fernández-Berridi, M.J., González, N., Mugica, A. and Bernicot, C. (2006) 'Pyrolysis-FTIR and TGA techniques as tools in the characterization of blends of natural rubber and SBR', *Thermochimica Acta,* 444(1), pp. 65-70.

Frihart, C.R. (2005) 'Adhesive Bonding and Performance Testing of Bonded Wood Products', *Journal of ASTM International,* 2(7), pp. 1-10.

Fuhrmann, I. and Karger-Kocsis, J. (1999) 'Promising approach to functionalisation of ground tyre rubber -photochemically induced grafting: Short Communication', *Plastics, Rubber and Composites,* 28(10), pp. 500-504.

Fyfe, C.A. and Niu, J. (1995) 'Direct Solid-state 13C NMR Evidence for Covalent Bond Formation between an Immobilized Vinylsilane Linking Agent and Polymer Matrices ', *Macromolecules,* 28, pp. 3894-3897.

Ganser, C., Hirn, U., Rohm, S., Schennach, R. and Teichert, C. (2013) 'AFM nanoindentation of pulp fibers and thin cellulose films at varying relative humidity', *Holzforschung,* 68(1), pp. 53-60.

Gao, H., Xie, Y., Ou, R. and Wang, Q. (2012) 'Grafting effects of polypropylene/polyethylene blends with maleic anhydride on the properties of the resulting wood–plastic composites', *Composites Part A: Applied Science and Manufacturing,* 43(1), pp. 150-157.

Gáspár, M., Benkő, Z., Dogossy, G., Réczey, K. and Czigány, T. (2005) 'Reducing water absorption in compostable starch-based plastics', *Polymer Degradation and Stability,* 90(3), pp. 563-569.

Gassan, J. and Gutowski, V.S. (2000) 'Effects of corona discharge and UV treatment on the properties of jute-fibre expoxy composites', *Composites Science and Technology,* 60(15), pp. 2857-2863.

George, J., Sreekala, M.S. and Thomas, S. (2001) 'A review on interface modification and characterization of natural fiber reinforced plastic composites', *Polymer Engineering & Science,* 41(9), pp. 1471-1485.

Ghomsheh, M.Z., Spieckermann, F., Polt, G., Wilhelm, H. and Zehetbauer, M. (2015) 'Analysis of strain bursts during nanoindentation creep of high-density polyethylene', *Polymer International,* 64(11), pp. 1537-1543.

Gindl, W., Konnerth, J. and Schöberl, T. (2006) 'Nanoindentation of regenerated cellulose fibres', *Cellulose,* 13(1), pp. 1-7.

Gindl, W., Schöberl, T. and Jeronimidis, G. (2004) 'The interphase in phenol–formaldehyde and polymeric methylene di-phenyl-di-isocyanate glue lines in wood', *International Journal of Adhesion and Adhesives,* 24(4), pp. 279-286.

Gironès, J., Méndez, J.A., Boufi, S., Vilaseca, F. and Mutjé, P. (2007) 'Effect of silane coupling agents on the properties of pine fibers/polypropylene composites', *Journal of Applied Polymer Science,* 103(6), pp. 3706-3717.

Glasser, W.G., Taib, R., Jain, R.K. and Kander, R. (1999) 'Fiber-reinforced cellulosic thermoplastic composites', *Journal of Applied Polymer Science,* 73(7), pp. 1329-1340.

Graham, J.F., McCague, C., Warren, O.L. and Norton, P.R. (2000) 'Spatially resolved nanomechanical properties of Kevlar® fibers', *Polymer,* 41(12), pp. 4761-4764.

Grmusa, I.G., Dunky, M., Miljkovic, J. and Momcilovic, M.D. (2012a) 'Influence of the degree of condensation of urea-formaldehyde adhesives on the tangential penetration into beech and fir and on the shear strength of the adhesive joints', *European Journal of Wood and Wood Products,* 70(5), pp. 655-665.

Grmusa, I.G., Dunky, M., Miljkovic, J. and Momcilovic, M.D. (2012b) 'Influence of the viscosity of UF resins on the radial and tangential penetration into poplar

wood and on the shear strength of adhesive joints', *Holzforschung,* 66(7), pp. 849-856.

Grünewald, T., Grigsby, W., Tondi, G., Ostrowski, S., Petutschnigg, A., Wieland,S. (2013) 'Chemical Characterization of Wood-Leather Panels by Means of 13C NMR Spectroscopy', *BioResources,* 8(2) , pp. 2442-2452.

Guimarães, J.L., Wypych, F., Saul, C.K., Ramos, L.P. and Satyanarayana, K.G. (2010) 'Studies of the processing and characterization of corn starch and its composites with banana and sugarcane fibers from Brazil', *Carbohydrate Polymers,* 80(1), pp. 130-138.

Gunasekaran, S., Natarajan, R.K. and Kala, A. (2007) 'FTIR spectra and mechanical strength analysis of some selected rubber derivatives', *Spectrochimica Acta Part A: Molecular and Biomolecular Spectroscopy,* 68(2), pp. 323-330.

Gunning, M.A., Geever, L.M., Killion, J.A., Lyons, J.G. and Higginbotham, C.L. (2013) 'Mechanical and biodegradation performance of short natural fibre polyhydroxybutyrate composites', *Polymer Testing,* 32(8), pp. 1603-1611.

Haseena, A.P., Unnikrishnan, G. and Kalaprasad, G. (2007) 'Dielectric properties of short sisal/coir hybrid fibre reinforced natural rubber composites', *Composite Interfaces,* 14(7), pp. 763-786.

Haydaruzzaman, Khan, M.A., Khan, R.A., Khan, A.H. and Hossain, M.A. (2009) 'Effect of gamma radiation on the performance of jute fabrics-reinforced polypropylene composites', *Radiation Physics and Chemistry,* 78(11), pp. 986-993.

Heredia, A. (2003) 'Biophysical and biochemical characteristics of cutin, a plant barrier biopolymer', *Biochimica et biophysica acta,* 1620(1-3), pp. 1-7.

Hobbs, J.K., Winkel, A.K., McMaster, T.J., Humphris, A.D.L., Baker, A.A., Blakely, S., Aissaoui, M. and Miles, M.J. (2001) 'Nanoindentation of polymers: An overview', *Macromolecular Symposia,* 167(1), pp. 15-43.

Hong, C.K. and Isayev, A.I. (2001) 'Plastic/Rubber Blends of Ultrasonically Devulcanized GRT with HDPE', *Journal of Elastomers and Plastics,* 33(1), pp. 47-71.

Hristov, V. and Vasileva, S. (2003) 'Dynamic Mechanical and Thermal Properties of Modified Poly(propylene) Wood Fiber Composites', *Macromolecular Materials and Engineering,* 288(10), pp. 798-806.

Huda, M.S., Drzal, L.T., Misra, M. and Mohanty, A.K. (2006) 'Wood-fiber-reinforced poly(lactic acid) composites: Evaluation of the physicomechanical and morphological properties', *Journal of Applied Polymer Science,* 102(5), pp. 4856-4869.

Ihamouchen, C., Djidjelli, H., Boukerrou, A., Krim, S., Kaci, M. and Martinez, J.J. (2012) 'Effect of surface treatment on the physicomechanical and thermal properties of high-density polyethylene/olive husk flour composites', *Journal of Applied Polymer Science,* 123(3), pp. 1310-1319.

Ihemouchen, C., Djidjelli, H., Boukerrou, A., Fenouillot, F. and Barres, C. (2013) 'Effect of compatibilizing agents on the mechanical properties of high-density polyethylene/olive husk flour composites', *Journal of Applied Polymer Science,* 128(3), pp. 2224-2229.

Ismail, H. and Nasir, S., M. (2001) 'Dynamic vulcanization of rubberwood-filled polypropylene/natural rubber blends', *Polymer Testing,* 20(7), pp. 819-823.

Ismail, H., Salmah and Nasir, M. (2003) 'The effect of dynamic vulcanization on mechanical properties and water absorption of silica and rubberwood filled polypropylene/natural rubber hybrid composites', *International Journal of Polymeric Materials and Polymeric Biomaterials,* 52(3), pp. 229-238.

Ismail, H., Nasaruddin, M.N. and Ishiaku, U.S. (1999) 'White rice husk ash filled natural rubber compounds: the effect of multifunctional additive and silane coupling agents', *Polymer Testing,* 18(4), pp. 287-298.

Ismail, H., Shuhelmy, S. and Edyham, M.R. (2002) 'The effects of a silane coupling agent on curing characteristics and mechanical properties of bamboo fibre filled natural rubber composites', *European Polymer Journal,* 38(1), pp. 39-47.

Ja, M.H., Majid, M.A., Afendi, M., Marzuki, H., Fahmi, I. and Gibson, A. (2016) 'Mechanical properties of Napier grass fibre/polyester composites', *Composite Structures,* 136, pp. 1-10.

Jana, G.K., Mahaling, R.N. and Das, C.K. (2006) 'A novel devulcanization technology for vulcanized natural rubber', *Journal of Applied Polymer Science,* 99(5), pp. 2831-2840.

Jandas, P.J., Mohanty, S., Nayak, S.K. and Srivastava, H. (2011) 'Effect of surface treatments of banana fiber on mechanical, thermal, and biodegradability

properties of PLA/banana fiber biocomposites', *Polymer Composites,* 32(11), pp. 1689-1700.

Jiang, L., Morelius, E., Zhang, J., Wolcott, M. and Holbery, J. (2008) 'Study of the Poly(3-hydroxybutyrate-co-3-hydroxyvalerate)/Cellulose Nanowhisker Composites Prepared by Solution Casting and Melt Processing', *Journal of Composite Materials,* 42(24), pp. 2629-2645.

John, M.J. and Anandjiwala, R.D. (2008) 'Recent developments in chemical modification and characterization of natural fiber-reinforced composites', *Polymer Composites,* 29(2), pp. 187-207.

John, M.J. and Thomas, S. (2008) 'Biofibres and biocomposites', *Carbohydrate Polymers,* 71(3), pp. 343-364.

Joseph, K., Joseph, P.V., Thomas, S., Pillai, C.K.S., Prasad, V.S., Groeninckx, G. and Sarkissova, M. (2003) 'The thermal and crystallisation studies of short sisal fibre reinforced polypropylene composites', *Composites Part A: Applied Science and Manufacturing,* 34(3), pp. 253-266.

Joseph, K., Thomas, S. and Pavithran, C. (1996) 'Effect of chemical treatment on the tensile properties of short sisal fibre-reinforced polyethylene composites', *Polymer,* 37(23), pp. 5139-5149.

Joseph, S., Koshy, P. and Thomas, S. (2005) 'The role of interfacial interactions on the mechanical properties of banana fibre reinforced phenol formaldehyde composites', *Composite Interfaces,* 12(6), pp. 581-600.

Kabir, M.M., Wang, H., Lau, K.T. and Cardona, F. (2012) 'Chemical treatments on plant-based natural fibre reinforced polymer composites: An overview', *Composites Part B: Engineering,* 43(7), pp. 2883-2892.

Kaewtatip, K. and Thongmee, J. (2012) 'Studies on the structure and properties of thermoplastic starch/luffa fiber composites', *Materials and Design,* 40, pp. 314-318.

Kakroodi, A.R. and Rodrigue, D. (2013) 'Degradation behavior of maleated polyethylene/ground tire rubber thermoplastic elastomers with and without stabilizers', *Polymer Degradation and Stability,* 98(11), pp. 2184-2192.

Kakroodi, A.R., Leduc, S., González-Núñez, R. and Rodrigue, D. (2012) 'Mechanical properties of recycled polypropylene/SBR rubber crumbs blends reinforced by birch wood flour', *Polymers and Polymer Composites,* 20(5), pp. 439-444.

Kalaprasad, G., Francis, B., Thomas, S., Kumar, C.R., Pavithran, C., Groeninckx, G. and Thomas, S. (2004) 'Effect of fibre length and chemical modifications on the tensile properties of intimately mixed short sisal/glass hybrid fibre reinforced low density polyethylene composites', *Polymer International,* 53(11), pp. 1624-1638.

Kalia, S., Kaith, B.S. and Kaur, I. (2009) 'Pretreatments of natural fibers and their application as reinforcing material in polymer composites-a review', *Polymer Engineering and Science,* 49(7), pp. 1253-1272.

Karger-Kocsis, J., Meszaros, L. and Barany, T. (2013) 'Ground tyre rubber (GTR) in thermoplastics, thermosets, and rubbers', *Journal of Materials Science,* 48(1), pp. 1-36.

Kaushik, A., Singh, M. and Verma, G. (2010) 'Green nanocomposites based on thermoplastic starch and steam exploded cellulose nanofibrils from wheat straw', *Carbohydrate Polymers,* 82(2), pp. 337-345.

Kaynak, C., Sipahi-Saglam, E. and Akovali, G. (2001) 'A fractographic study on toughening of epoxy resin using ground tyre rubber', *Polymer,* 42(9), pp. 4393-4399.

Kaynak, C., Celikbilek, C. and Akovali, G. (2003) 'Use of silane coupling agents to improve epoxy–rubber interface', *European Polymer Journal,* 39(6), pp. 1125-1132.

Kazayawoko, M., Balatinecz, J.J. and Matuana, L.M. (1999) 'Surface modification and adhesion mechanisms in woodfiber-polypropylene composites', *Journal of Materials Science,* 34(24), pp. 6189-6199.

Kehlet, C., Catalano, A. and Dittmer, J. (2014) 'Degradation of natural rubber in works of art studied by unilateral NMR and high field NMR spectroscopy', *Polymer Degradation and Stability,* 107, pp. 270-276.

Kelly, A. and Tyson, W.R. (1965) 'Tensile properties of fibre-reinforced metals: Copper/tungsten and copper/molybdenum', *Journal of the Mechanics and Physics of Solids,* 13(6), pp. 329-350.

Khalil, H. and Ismail, H. (2001) 'Effect of acetylation and coupling agent treatments upon biological degradation of plant fibre reinforced polyester composites', *Polymer Testing,* 20(1), pp. 65-75.

Khan, M.A., Khan, R.A., Haydaruzzaman, Hossain, A. and Khan, A.H. (2009) 'Effect of Gamma Radiation on the Physico-Mechanical and Electrical Properties of Jute Fiber-Reinforced Polypropylene Composites', *Journal of Reinforced Plastics and Composites,* 28(13), pp. 1651-1660.

Kim, J.K. and Pal, K. (2011) *Recent Advances in the Processing of Wood-Plastic Composites.* Springer-Verlag Berlin Heidelberg.

Kim, J. and Mai, Y.W. (1998) *Engineered interfaces in fiber reinforced composites.* Oxford; New York: Elsevier Sciences.

Kodal, M., Topuk, Z.D. and Ozkoc, G. (2015) 'Dual effect of chemical modification and polymer precoating of flax fibers on the properties of short flax fiber/poly(lactic acid) composites', *Journal of Applied Polymer Science,* 132(48), pp. 42564(1-13).

Konnerth, J. and Gindl, W. (2006) 'Mechanical characterisation of wood-adhesive interphase cell walls by nanoindentation', *Holzforschung,* 60(4), pp. 429-433.

Kotilainen, R.A., Toivanen, T. and Alén, R.J. (2000) 'FTIR Monitoring of Chemical Changes in Softwood During Heating', *Journal of Wood Chemistry and Technology,* 20(3), pp. 307-320.

Krishnaprasad, R., Veena, N.R., Maria, H.J., Rajan, R., Skrifvars, M., Joseph, K. (2009) 'Mechanical and Thermal Properties of Bamboo Microfibril Reinforced Polyhydroxybutyrate Biocomposites', *Journal of Polymers and the Environment,* 17(2), pp. 109-114.

Kubát, J., Rigdahl, M. and Welander, M. (1990) 'Characterization of interfacial interactions in high density polyethylene filled with glass spheres using dynamic-mechanical analysis', *Journal of Applied Polymer Science,* 39(7), pp. 1527-1539.

Kumar, C.R., Fuhrmann, I. and Karger-Kocsis, J. (2002) 'LDPE-based thermoplastic elastomers containing ground tire rubber with and without dynamic curing', *Polymer Degradation and Stability,* 76(1), pp. 137-144.

Kumar, R., Cross, W.M., Kjerengtroen, L. and Kellar, J.J. (2004) 'Fiber bias in nanoindentation of polymer matrix composites', *Composite Interfaces,* 11(5-6), pp. 431-440.

Kuo, P., Wang, S., Chen, J., Hsueh, H. and Tsai, M. (2009) 'Effects of material compositions on the mechanical properties of wood–plastic composites manufactured by injection molding', *Materials & Design,* 30(9), pp. 3489-3496.

Kurita, K. (2001) 'Controlled functionalization of the polysaccharide chitin', *Progress in Polymer Science,* 26(9), pp. 1921-1971.

Lai, S., Yeh, F., Wang, Y., Chan, H. and Shen, H. (2003a) 'Comparative study of maleated polyolefins as compatibilizers for polyethylene/wood flour composites', *Journal of Applied Polymer Science,* 87(3), pp. 487-496.

Lee, J. and Deng, Y. (2013) 'Nanoindentation study of individual cellulose nanowhisker-reinforced PVA electrospun fiber', *Polymer Bulletin,* 70(4), pp. 1205-1219.

Lee, S., Wang, S., Pharr, G.M. and Xu, H. (2007a) 'Evaluation of interphase properties in a cellulose fiber-reinforced polypropylene composite by nanoindentation and finite element analysis', *Composites Part A: Applied Science and Manufacturing,* 38(6), pp. 1517-1524.

Lee, S.H., Balasubramanian, M. and Kim, J.K. (2007b) 'Dynamic reaction inside co-rotating twin screw extruder. II. Waste ground rubber tire powder/polypropylene blends', *Journal of Applied Polymer Science,* 106(5), pp. 3209-3219.

Lee, S.H., Zhang, Z.X., Xu, D., Chung, D., Oh, G.J. and Kim, J.K. (2009) 'Dynamic reaction involving surface modified waste ground rubber tire powder/polypropylene', *Polymer Engineering & Science,* 49(1), pp. 168-176.

Li, R., Gu, Y., Yang, Z., Li, M., Wang, S. and Zhang, Z. (2015) 'Effect of γ irradiation on the properties of basalt fiber reinforced epoxy resin matrix composite', *Journal of Nuclear Materials,* 466, pp. 100-107.

Li, X., Tabil, L.G. and Panigrahi, S. (2007) 'Chemical Treatments of Natural Fiber for Use in Natural Fiber-Reinforced Composites: A Review', *Journal of Polymers and the Environment,* 15(1), pp. 25-33.

Liu, D., Song, J., Anderson, D.P., Chang, P.R. and Hua, Y. (2012) 'Bamboo fiber and its reinforced composites: structure and properties', *Cellulose,* 19(5), pp. 1449-1480.

Liu, J., Scott, C., Winroth, S., Maia, J. and Ishida, H. (2015) 'Copolymers based on telechelic benzoxazine with a reactive main-chain and anhydride: monomer and polymer synthesis, and thermal and mechanical properties of carbon fiber composites', *RSC Advances*, 5, pp.16785-16791.

López-Manchado, M.A., Biagitti, J. and Kenny, J.M. (2002) 'Comparative study of the effects of different fibers on the processing and properties of ternary composites based on PP-EPDM blends', *Polymer Composites,* 23(5), pp. 779-789.

Loureiro, N.C., Esteves, J.L., Viana, J.C. and Ghosh, S. (2014) 'Development of polyhydroxyalkanoates/poly(lactic acid) composites reinforced with cellulosic fibers', *Composites Part B: Engineering,* 60, pp. 603-611.

Lu, J.Z., Negulescu, I.I. and Wu, Q. (2005) 'Maleated wood-fiber/high-density-polyethylene composites: Coupling mechanisms and interfacial characterization', *Composite Interfaces,* 12(1-2), pp. 125-140.

Lu, J.Z., Wu, Q. and McNabb Jr, H.S. (2000) 'Chemical coupling in wood fiber and polymer composites: A review of coupling agents and treatments', *Wood and Fiber Science,* 32(1), pp. 88-104.

Lu, T., Liu, S., Jiang, M., Xu, X., Wang, Y., Wang, Z., Gou, J., Hui, D. and Zhou, Z. (2014) 'Effects of modifications of bamboo cellulose fibers on the improved mechanical properties of cellulose reinforced poly(lactic acid) composites', *Composites Part B: Engineering,* 62, pp. 191-197.

Malkapuram, R., Kumar, V. and Negi, Y.S. (2009) 'Recent Development in Natural Fiber Reinforced Polypropylene Composites', *Journal of Reinforced Plastics and Composites,* 28(10), pp. 1169-1189.

Mansour, S.H., El-Nashar, D.E. and Abd-El-Messieh, S.L. (2006) 'Effect of chemical treatment of wood flour on the properties of styrene butadiene rubber/polystyrene composites', *Journal of Applied Polymer Science,* 102(6), pp. 5861-5870.

Maridass, B. and Gupta, B.R. (2008) 'Process optimization of devulcanization of waste rubber powder from syringe stoppers by twin screw extruder using response surface methodology', *Polymer Composites,* 29(12), pp. 1350-1357.

Martínez-Barrera, G., López, H., Castaño, V.M. and Rodríguez, R. (2004) 'Studies on the rubber phase stability in gamma irradiated polystyrene-SBR blends by using FT-IR and Raman spectroscopy', *Radiation Physics and Chemistry,* 69(2), pp. 155-162.

Martins, M.A., Forato, L.A., Mattoso, L.H.C. and Colnago, L.A. (2006) 'A solid state 13C high resolution NMR study of raw and chemically treated sisal fibers', *Carbohydrate Polymers,* 64(1), pp. 127-133.

Matas, A.J., Cuartero, J. and Heredia, A. (2004) 'Phase transitions in the biopolyester cutin isolated from tomato fruit cuticles', *Thermochimica Acta,* 409(2), pp. 165-168.

Mehdi, B., Mehdi, T., Ghanbar, E. and Robert, H.,Falk (2004) ' Dynamic mechanical analysis of compatibilizer effect on the mechanical properties of wood flour/high-density polyethylene composites', *IJE Transactions B: Applications,* 17(1), pp. 95-104.

Mészáros, L., Bárány, T. and Czvikovszky, T. (2012a) 'EB-promoted recycling of waste tire rubber with polyolefins', *Radiation Physics and Chemistry,* 81(9), pp. 1357-1360.

Mészáros, L., Fejos, M. and Bárány, T. (2012b) 'Mechanical properties of recycled LDPE/EVA/ground tyre rubber blends: Effects of EVA content and postirradiation', *Journal of Applied Polymer Science,* 125(1), pp. 512-519.

Migneault, S., Koubaa, A., Perre, P. and Riedl, B. (2015) 'Effects of wood fiber surface chemistry on strength of wood-plastic composites', *Applied Surface Science,* 343, pp. 11-18.

Mohanty, A.K., Khan, M.A. and Hinrichsen, G. (2000) 'Surface modification of jute and its influence on performance of biodegradable jute-fabric/Biopol composites', *Composites Science and Technology,* 60(7), pp. 1115-1124.

Mohanty, S., Nayak, S.K., Verma, S.K. and Tripathy, S.S. (2004) 'Effect of MAPP as Coupling Agent on the Performance of Sisal-PP Composites', *Journal of Reinforced Plastics and Composites,* 23(18), pp. 2047-2063.

Mohanty, S. and Nayak, S.K. (2006) 'Interfacial, dynamic mechanical, and thermal fiber reinforced behavior of MAPE treated sisal fiber reinforced HDPE composites', *Journal of Applied Polymer Science,* 102(4), pp. 3306-3315.

Mohanty, S., Verma, S.K. and Nayak, S.K. (2006) 'Dynamic mechanical and thermal properties of MAPE treated jute/HDPE composites', *Composites Science and Technology,* 66(3–4), pp. 538-547.

Morales, J., Olayo, M.G., Cruz, G.J., Herrera-Franco, P. and Olayo, R. (2006) 'Plasma modification of cellulose fibers for composite materials', *Journal of Applied Polymer Science,* 101(6), pp. 3821-3828.

Mukhopadhyay, S., Deopura, B.L. and Alagiruswamy, R. (2003) 'Interface Behavior in Polypropylene Composites', *Journal of Thermoplastic Composite Materials,* 16(6), pp. 479-495.

Mwaikambo, L.Y. and Ansell, M.P. (2002) 'Chemical modification of hemp, sisal, jute, and kapok fibers by alkalization', *Journal of Applied Polymer Science,* 84(12), pp. 2222-2234.

Ngah, S.A. (2013) *Static and fatigue behaviour of fibre composites infused with rubber- and silica nanoparticle-modified epoxy* PhD. Imperial College London.

Noriman, N.Z. and Ismail, H. (2012) 'Properties of styrene butadiene rubber (SBR)/recycled acrylonitrile butadiene rubber (NBRr) blends: The effects of carbon black/silica (CB/Sil) hybrid filler and silane coupling agent, Si69', *Journal of Applied Polymer Science,* 124(1), pp. 19-27.

Nuthong, W., Uawongsuwan, P., Pivsa-Art, W. and Hamada, H. (2013) 'Impact Property of Flexible Epoxy Treated Natural Fiber Reinforced PLA Composites', *Energy Procedia,* 34, pp. 839-847.

Ochi, S. (2008) 'Mechanical properties of kenaf fibers and kenaf/PLA composites', *Mechanics of Materials,* 40(4–5), pp. 446-452.

Okubo, K., Fujii, T. and Thostenson, E.T. (2009) 'Multi-scale hybrid biocomposite: Processing and mechanical characterization of bamboo fiber reinforced PLA with microfibrillated cellulose', *Composites Part A: Applied Science and Manufacturing,* 40(4), pp. 469-475.

Oliveira, G.L., Costa, C.A., Teixeira, S.C.S. and Costa, M.F. (2014) 'The use of nano- and micro-instrumented indentation tests to evaluate viscoelastic behavior of poly(vinylidene fluoride) (PVDF)', *Polymer Testing,* 34, pp. 10-16.

Oliver, W.C. and Pharr, G.M. (1992) 'An improved technique for determining hardness and elastic modulus using load and displacement sensing indentation experiments', *Journal of Materials Research,* 7(6), pp. 1564-1583.

Oporto, G.S., Gardner, D.J., Bernhardt, G. and Neivandt, D.J. (2009) 'Forced Air Plasma Treatment (FAPT) of Hybrid Wood Plastic Composite (WPC)-Fiber Reinforced Plastic (FRP) Surfaces', *Composite Interfaces,* 16(7), pp. 847-867.

Ornaghi, H.L., Bolner, A.S., Fiorio, R., Zattera, A.J. and Amico, S.C. (2010) 'Mechanical and dynamic mechanical analysis of hybrid composites molded by resin transfer molding', *Journal of Applied Polymer Science,* 118(2), pp. 887-896.

Osman, H., Ismail, H. and Mariatti, M. (2012) 'Polypropylene/natural rubber composites filled with recycled newspaper: Effect of chemical treatment using maleic anhydride-grafted polypropylene and 3-aminopropyltriethoxysilane', *Polymer Composites,* 33(4), pp. 609-618.

Osman, H., Ismail, H. and Mariatti, M. (2010a) 'Comparison of Reinforcing Efficiency between Recycled Newspaper (RNP)/Carbon Black (CB) and Recycled Newspaper (RNP)/Silica Hybrid Filled Polypropylene (PP)/Natural Rubber (NR) Composites', *Journal of Reinforced Plastics and Composites,* 29(1), pp. 60-75.

Osman, H., Ismail, H. and Mustapha, M. (2010b) 'Effects of Maleic Anhydride Polypropylene on Tensile, Water Absorption, and Morphological Properties of Recycled Newspaper Filled Polypropylene/ Natural Rubber Composites', *Journal of Composite Materials,* 44(12), pp. 1477-1491.

Ou, R., Xie, Y., Wolcott, M.P., Sui, S. and Wang, Q. (2014) 'Morphology, mechanical properties, and dimensional stability of wood particle/high density polyethylene composites: Effect of removal of wood cell wall composition', *Materials & Design,* 58, pp. 339-345.

Ouajai, S. and Shanks, R.A. (2005) 'Composition, structure and thermal degradation of hemp cellulose after chemical treatments', *Polymer Degradation and Stability,* 89(2), pp. 327-335.

Pickering, K. (2008) *Properties and Performance of Natural-Fibre Composites.* 1st edn. Cambridge: Woodhead Publishing.

Pinto, M., Chalivendra, V., Kim, Y. and Lewis, A. (2013) 'Effect of surface treatment and Z-axis reinforcement on the interlaminar fracture of jute/epoxy laminated composites', *Engineering Fracture Mechanics,* 114, pp. 104-114.

Poletto, M., Zeni, M. and Zattera, A.J. (2012) 'Dynamic mechanical analysis of recycled polystyrene composites reinforced with wood flour', *Journal of Applied Polymer Science,* 125(2), pp. 935-942.

Prachayawarakorn, J., Sangnitidej, P. and Boonpasith, P. (2010) 'Properties of thermoplastic rice starch composites reinforced by cotton fiber or low-density polyethylene', *Carbohydrate Polymers,* 81(2), pp. 425-433.

Prachayawarakorn, J., Chaiwatyothin, S., Mueangta, S. and Hanchana, A. (2013) 'Effect of jute and kapok fibers on properties of thermoplastic cassava starch composites', *Materials & Design,* 47, pp. 309-315.

Ragoubi, M., George, B., Molina, S., Bienaimé, D., Merlin, A., Hiver, J.M. and Dahoun, A. (2012) 'Effect of corona discharge treatment on mechanical and thermal properties of composites based on miscanthus fibres and polylactic acid or polypropylene matrix', *Composites Part A: Applied Science and Manufacturing,* 43(4), pp. 675-685.

Ragoubi, M., Bienaimé, D., Molina, S., George, B. and Merlin, A. (2010) 'Impact of corona treated hemp fibres onto mechanical properties of polypropylene composites made thereof', *Industrial Crops & Products,* 31(2), pp. 344-349.

Rai, A.K., Singh, R., Singh, K.N. and Singh, V.B. (2006) 'FTIR, Raman spectra and ab initio calculations of 2-mercaptobenzothiazole', *Spectrochimica Acta Part A: Molecular and Biomolecular Spectroscopy,* 63(2), pp. 483-490.

Raj, R.G., Kokta, B.V., Dembele, F. and Sanschagrain, B. (1989) 'Compounding of cellulose fibers with polypropylene. Effect of fiber treatment on dispersion in the polymer matrix', *Journal of Applied Polymer Science,* 38(11), pp. 1987-1996.

Rajesh, G. and Prasad, A.V.R. (2014) 'Tensile Properties of Successive Alkali Treated Short Jute Fiber Reinforced PLA Composites', *Procedia Materials Science,* 5, pp. 2188-2196.

Raju, G., Ratnam, C.T., Ibrahim, N.A., Rahman, M.Z.A. and Yunus, W.M.Z.W. (2008) 'Enhancement of PVC/ENR blend properties by poly(methyl acrylate)

grafted oil palm empty fruit bunch fiber', *Journal of Applied Polymer Science,* 110(1), pp. 368-375.

Ratnam, C.T., Nasir, M., Baharin, A. and Zaman, K. (2001a) 'Electron-beam irradiation of poly(vinyl chloride)/epoxidized natural rubber blend in the presence of Irganox 1010', *Polymer Degradation and Stability,* 72(1), pp. 147-155.

Ratnam, C.T., Nasir, M., Baharin, A. and Zaman, K. (2001b) 'Effect of electron-beam irradiation on poly(vinyl chloride)/epoxidized natural rubber blend: dynamic mechanical analysis', *Polymer International,* 50(5), pp. 503-508.

Ratnam, C.T., Raju, G., Ibrahim, N.A., Rahman, M.Z.A, and WanYunus, W.M.Z. (2008) 'Characterization of Oil Palm Empty Fruit Bunch (OPEFB) Fiber Reinforced PVC/ENR Blend', *Journal of Composite Materials,* 42(20), pp. 2195-2204.

Ray, D., Sarkar, B.K., Rana, A.K. and Bose, N.R. (2001) 'Effect of alkali treated jute fibres on composite properties', *Bulletin of Materials Science,* 24(2), pp. 129-135.

Renneckar, S.H. (2004) *Modification of Wood Fiber with Thermoplastics by Reactive Steam-Explosion* PhD. Virginia Polytechnic Institute and State University.

Renneckar, S., Johnson, R.K., Zink-Sharp, A., Sun, N. and Glasser, W.G. (2005) 'Fiber modification by steam-explosion: 13C NMR and dynamic mechanical analysis studies of co-refined wood and polypropylene', *Composite Interfaces,* 12(6), pp. 559-580.

Ricardo, N.M., Lahtinen, M., Price, C. and Heatley, F. (2002) 'Blends of natural rubber and polyurethane latices studied by 1H wideline and 13C MAS solid-state NMR', *Polymer International,* 51(7), pp. 627-634.

Saheb, D.N. and Jog, J.P. (1999) 'Natural fiber polymer composites: A review', *Advances in Polymer Technology,* 18(4), pp. 351-363.

Sakdapipanich, J.T., Kowitteerawut, T., Tuampoemsab, S. and Kawahara, S. (2006) 'Structural characterization of sulfur vulcanized deproteinized natural rubber by solid-state 13C NMR spectroscopy', *Journal of Applied Polymer Science,* 100(3), pp. 1875-1880.

Salimi, D., Khorasani, S.N., Abadchi, M.R. and Veshare, S.J. (2009) 'Optimization of physico-mechanical properties of silica-filled NR/SBR compounds', *Advances in Polymer Technology,* 28(4), pp. 224-232.

Salmah, H. and Ismail, H. (2008) 'The Effect of Filler Loading and Maleated Polypropylene on Properties of Rubberwood Filled Polypropylene/Natural Rubber Composites', *Journal of Reinforced Plastics and Composites,* 27(16-17), pp. 1867-1876.

Salon, M.B., Abdelmouleh, M., Boufi, S., Belgacem, M.N. and Gandini, A. (2005) 'Silane adsorption onto cellulose fibers: Hydrolysis and condensation reactions', *Journal of Colloid and Interface Science,* 289(1), pp. 249-261.

Salon, M.B., Gerbaud, G., Abdelmouleh, M., Bruzzese, C., Boufi, S. and Belgacem, M.N. (2007) 'Studies of interactions between silane coupling agents and cellulose fibers with liquid and solid-state NMR', *Magnetic Resonance in Chemistry,* 45(6), pp. 473-483.

Sameni, J.K., Ahmad, S.H. and Zakaria, S. (2004) 'Effect of mape on the mechanical properties of rubber wood fiber/thermoplastic natural rubber composites', *Advances in Polymer Technology,* 23(1), pp. 18-23.

Santiagoo, R., Ismail, H., Hussin,K. (2011) 'Mechanical properties, water absorption, and swelling behaviour of rice husk powder filled polypropylene/recycled acrylonitrile butadiene rubber (pp/NBRr/RHP) biocomposites using silane as a coupling agent', *BioResources,* 6(4), pp. 3714-3726.

Santoni, I., Callone, E., Sandak, A., Sandak, J. and Dirè, S. (2015) 'Solid state NMR and IR characterization of wood polymer structure in relation to tree provenance', *Carbohydrate Polymers,* 117, pp. 710-721.

Sarikanat, M., Seki, Y., Sever, K., Bozaci, E., Demir, A. and Ozdogan, E. (2016) 'The effect of argon and air plasma treatment of flax fiber on mechanical properties of reinforced polyester composite', *Journal of Industrial Textiles,* 45(6), pp. 1252-1267.

Satyanarayana, K.G., Arizaga, G.G.C. and Wypych, F. (2009) 'Biodegradable composites based on lignocellulosic fibers—An overview', *Progress in Polymer Science,* 34(9), pp. 982-1021.

Sawpan, M.A., Pickering, K.L. and Fernyhough, A. (2011) 'Effect of various chemical treatments on the fibre structure and tensile properties of industrial hemp fibres', *Composites Part A: Applied Science and Manufacturing,* 42(8), pp. 888-895.

Seki, Y. (2009) 'Innovative multifunctional siloxane treatment of jute fiber surface and its effect on the mechanical properties of jute/thermoset composites', *Materials Science and Engineering: A,* 508(1–2), pp. 247-252.

Seldén, R., Nyström, B. and Långström, R. (2004) 'UV aging of poly(propylene)/wood-fiber composites', *Polymer Composites,* 25(5), pp. 543-553.

Sienkiewicz, M., Kucinska-Lipka, J., Janik, H. and Balas, A. (2012) 'Progress in used tyres management in the European Union: A review', *Waste Management,* 32(10), pp. 1742-1751.

Silverstein, R.M., Webster, F.X., Kiemle, D.J. and Bryce, D.L. (2014) *Spectrometric Identification of Organic Compounds.* 8th Edition edn. USA: Petra Recter.

Sitarz, M., Czosnek, C., Jeleń, P., Odziomek, M., Olejniczak, Z., Kozanecki, M. and Janik, J.F. (2013) 'SiOC glasses produced from silsesquioxanes by the aerosol-assisted vapor synthesis method', *Spectrochimica Acta Part A: Molecular and Biomolecular Spectroscopy,* 112, pp. 440-445.

Sombatsompop, N., Sungsanit, K. and Thongpin, C. (2004a) 'Analysis of low-density polyethylene-g-poly(vinyl chloride) copolymers formed in poly(vinyl chloride)/low-density polyethylene melt blends with gel permeation chromatography and solid-state 13C-NMR', *Journal of Applied Polymer Science,* 92(5), pp. 3167-3172.

Somers, A.E., Bastow, T.J., Burgar, M.I., Forsyth, M. and Hill, A.J. (2000) 'Quantifying rubber degradation using NMR', *Polymer Degradation and Stability,* 70(1), pp. 31-37.

Song, Z., Xiao, H. and Zhao, Y. (2014) 'Hydrophobic-modified nano-cellulose fiber/PLA biodegradable composites for lowering water vapor transmission rate (WVTR) of paper', *Carbohydrate Polymers,* 111, pp. 442-448.

Sonnier, R., Leroy, E., Clerc, L., Bergeret, A. and Lopez-Cuesta, J.M. (2006) 'Compatibilisation of polyethylene/ground tyre rubber blends by γ irradiation', *Polymer Degradation and Stability,* 91(10), pp. 2375-2379.

Sousa, F.D.B., Scuracchio, C.H., Hu, G. and Hoppe, S. (2016) 'Effects of processing parameters on the properties of microwave-devulcanized ground tire rubber/polyethylene dynamically revulcanized blends', *Journal of Applied Polymer Science,* 133(23), pp. 43503(1-11).

Spear, M.J., Eder, A. and Carus, M. (2015) '10 - Wood polymer composites', in Ansell, M.P. (ed.) *Wood Composites.* Woodhead Publishing, pp. 195-249.

Sreekala, M.S., Kumaran, M.G., Joseph, S., Jacob, M. and Thomas, S. (2000) 'Oil Palm Fibre Reinforced Phenol Formaldehyde Composites: Influence of Fibre Surface Modifications on the Mechanical Performance', *Applied Composite Materials,* 7(5), pp. 295-329.

Sreekala, M.S., Kumaran, M.G. and Thomas, S. (2002) 'Water sorption in oil palm fiber reinforced phenol formaldehyde composites', *Composites Part A: Applied Science and Manufacturing,* 33(6), pp. 763-777.

Stael, G.C., D'Almeida, J.R.M. and Tavares, M.I.B. (2000) 'A solid state NMR carbon-13 high resolution study of natural fiber from sugar cane and their composites with EVA', *Polymer Testing,* 19(3), pp. 251-259.

Summerscales, J., Dissanayake, N.P.J., Virk, A.S. and Hall, W. (2010) 'A review of bast fibres and their composites. Part 1 – Fibres as reinforcements', *Composites Part A: Applied Science and Manufacturing,* 41(10), pp. 1329-1335.

Tavares, M.I.B., Mothé, C.G. and Araújo, C.R. (2002) 'Solid-state nuclear magnetic resonance study of polyurethane/natural fibers composites', *Journal of Applied Polymer Science,* 85(7), pp. 1465-1468.

Teixeira, E.d.M., Pasquini, D., Curvelo, A.A.S., Corradini, E., Belgacem, M.N. and Dufresne, A. (2009) 'Cassava bagasse cellulose nanofibrils reinforced thermoplastic cassava starch', *Carbohydrate Polymers,* 78(3), pp. 422-431.

Thakur, V.K. and Thakur, M.K. (2015) *Eco-friendly polymer nanocomposites: chemistry and applications.* New Delhi: Springer.

Thongsang, S. and Sombatsompop, N. (2006) 'Effect of NaOH and Si69 treatments on the properties of fly ash/natural rubber composites', *Polymer Composites,* 27(1), pp. 30-40.

Torretta, V., Rada, E.C., Ragazzi, M., Trulli, E., Istrate, I.A. and Cioca, L.I. (2015) 'Treatment and disposal of tyres: Two EU approaches. A review', *Waste Management,* 45, pp. 152-160.

Tran, L.Q.N., Fuentes, C.A., Dupont-Gillain, C., Van Vuure, A.W. and Verpoest, I. (2013) 'Understanding the interfacial compatibility and adhesion of natural coir fibre thermoplastic composites', *Composites Science and Technology,* 80, pp. 23-30.

Tze, W.T.Y., Wang, S., Rials, T.G., Pharr, G.M. and Kelley, S.S. (2007) 'Nanoindentation of wood cell walls: Continuous stiffness and hardness measurements', *Composites Part A: Applied Science and Manufacturing,* 38(3), pp. 945-953.

Vladkova, T., Vassileva, S. and Natov, M. (2003) 'Wood flour: A new filler for the rubber processing industry. I. Cure characteristics and mechanical properties of wood flour-filled NBR and NBR/PVC compounds', *Journal of Applied Polymer Science,* 90(10), pp. 2734-2739.

Vladkova, T.G., Dineff, P.D. and Gospodinova, D.N. (2004a) 'Wood flour: A new filler for the rubber processing industry. II. Cure characteristics and mechanical properties of NBR compounds filled with corona-treated wood flour', *Journal of Applied Polymer Science,* 91(2), pp. 883-889.

Vladkova, T.G., Dineff, P.D. and Gospodinova, D.N. (2004b) 'Wood flour: A new filler for the rubber processing industry. III. Cure characteristics and mechanical properties of nitrile butadiene rubber compounds filled by wood flour in the presence of phenol-formaldehyde resin', *Journal of Applied Polymer Science,* 92(1), pp. 95-101.

Vladkova, T.G., Dineff, P.D., Gospodinova, D.N. and Avramova, I. (2006) 'Wood flour: New filler for the rubber processing industry. IV. Cure characteristics and mechanical properties of natural rubber compounds filled by non-modified or corona treated wood flour', *Journal of Applied Polymer Science,* 101(1), pp. 651-658.

Wahab, M.K.A., Ismail, H. and Othman, N. (2012a) 'Effects of dynamic vulcanization on the physical, mechanical, and morphological properties of high-density polyethylene/(natural rubber)/(thermoplastic tapioca starch) blends', *Journal of Vinyl and Additive Technology,* 18(3), pp. 192-197.

Wahab, M.K.A., Ismaila, H. and Othman, N. (2012b) 'Compatibilization Effects of PE-g-MA on Mechanical, Thermal and Swelling Properties of High Density Polyethylene/Natural Rubber/Thermoplastic Tapioca Starch Blends', *Polymer-Plastics Technology and Engineering,* 51(3), pp. 298-303.

Wang, B., Panigrahi, S., Tabil, L. and Crerar, W. (2007) 'Pre-treatment of Flax Fibers for use in Rotationally Molded Biocomposites', *Journal of Reinforced Plastics and Composites,* 26(5), pp. 447-463.

Wang, Y., Weng, Y. and Wang, L. (2014) 'Characterization of interfacial compatibility of polylactic acid and bamboo flour (PLA/BF) in biocomposites', *Polymer Testing,* 36, pp. 119-125.

Wikberg, H. and Maunu, S.L. (2004) 'Characterisation of thermally modified hard- and softwoods by 13C CPMAS NMR', *Carbohydrate Polymers,* 58(4), pp. 461-466.

Wollerdorfer, M. and Bader, H. (1998) 'Influence of natural fibres on the mechanical properties of biodegradable polymers', *Industrial Crops & Products,* 8(2), pp. 105-112.

Wong, K.J., Yousif, B.F. and Low, K.O. (2010) 'The effects of alkali treatment on the interfacial adhesion of bamboo fibres', *Proceedings of the Institution of Mechanical Engineers, Part L: Journal of Materials: Design and Applications,* 224(3), pp. 139-148.

Wu, C. (2013) 'Preparation, characterization and biodegradability of crosslinked tea plant-fibre-reinforced polyhydroxyalkanoate composites', *Polymer Degradation and Stability,* 98(8), pp. 1473-1480.

Wu, Y., Wang, S., Zhou, D., Xing, C., Zhang, Y. and Cai, Z. (2010) 'Evaluation of elastic modulus and hardness of crop stalks cell walls by nano-indentation', *Bioresource technology,* 101(8), pp. 2867-2871.

Xie, Y., Hill, C.A.S., Xiao, Z., Militz, H. and Mai, C. (2010) 'Silane coupling agents used for natural fiber/polymer composites: A review', *Composites Part A: Applied Science and Manufacturing,* 41(7), pp. 806-819.

Xing, C., Wang, S. and Pharr, G.M. (2009) 'Nanoindentation of juvenile and mature loblolly pine (Pinus taeda L.) wood fibers as affected by thermomechanical refining pressure', *Wood Science and Technology,* 43(7-8), pp. 615-625.

Xu, C., Kim, S., Hwang, H., Choi, J. and Yun, J. (2003) 'Optimization of submerged culture conditions for mycelial growth and exo-biopolymer production by Paecilomyces tenuipes C240', *Process Biochemistry,* 38(7), pp. 1025-1030.

Yan, L., Chouw, N. and Jayaraman, K. (2014) 'Flax fibre and its composites - A review', *Composites Part B: Engineering,* 56, pp. 296-317.

Yedla, S.B., Kalukanimuttam, M., Winter, R.M. and Khanna, S.K. (2008) 'Effect of Shape of the Tip in Determining Interphase Properties in Fiber Reinforced Plastic Composites Using Nanoindentation', *Journal of Engineering Materials and Technology,* 130(4), pp. 041010(1-15).

Zadorecki, P. and Michell, A.J. (1989) 'Future prospects for wood cellulose as reinforcement in organic polymer composites', *Polymer Composites,* 10(2), pp. 69-77.

Zaman, H.U., Khan, M.A. and Khan, R.A. (2009) 'Improvement of Mechanical Properties of Jute Fibers-Polyethylene/Polypropylene Composites: Effect of Green Dye and UV Radiation', *Polymer-Plastics Technology and Engineering,* 48(11), pp. 1130-1138.

Zaman, H.U., Khan, M.A., Khan, R.A., Mollah, M.Z.I., Pervin, S. and Al-Mamun, M. (2010) 'A Comparative Study between Gamma and UV Radiation of Jute fabrics/Polypropylene Composites: Effect of Starch', *Journal of Reinforced Plastics and Composites,* 29(13), pp. 1930-1939.

Zanetti, M.C., Fiore, S., Ruffino, B., Santagata, E., Dalmazzo, D. and Lanotte, M. (2015) 'Characterization of crumb rubber from end-of-life tyres for paving applications', *Waste Management,* 45, pp. 161-170.

Zaper, A.M. and Koenig, J.L. (1988) 'Solid-state 13C NMR studies of vulcanized elastomers, 4. Sulfur-vulcanized polybutadiene', *Die Makromolekulare Chemie,* 189(6), pp. 1239-1251.

Zhang, H. (2014) 'Effect of a novel coupling agent, alkyl ketene dimer, on the mechanical properties of wood–plastic composites', *Materials & Design,* 59, pp. 130-134.

Zhang, T., Bai, S.L., Zhang, Y.F. and Thibaut, B. (2012) 'Viscoelastic properties of wood materials characterized by nanoindentation experiments', *Wood Science and Technology,* 46(5), pp. 1003-1016.

Zhou, Y., Fan, M. and Chen, L. (2016) 'Interface and bonding mechanisms of plant fibre composites: An overview', *Composites Part B: Engineering,* 101, pp. 31-45.

Zhou, Y., Fan, M., Chen, L. and Zhuang, J. (2015) 'Lignocellulosic fibre mediated rubber composites: An overview', *Composites Part B: Engineering,* 76, pp. 180-191.

Zurina, M., Ismail, H. and Bakar, A.A. (2004) 'Rice husk powder–filled polystyrene/styrene butadiene rubber blends', *Journal of Applied Polymer Science,* 92(5), pp. 3320-3332.

APPENDIX Publications and Conferences

Journal Articles

- **Zhou, Y.**, Fan, M., Luo, X., Huang, L. and Chen, L. (2014) 'Acidic ionic liquid catalyzed crosslinking of oxycellulose with chitosan for advanced biocomposites', *Carbohydrate Polymers,* 113, pp. 108-114.
- **Zhou, Y.**, Fan, M., Chen, L. and Zhuang, J. (2015) 'Lignocellulosic fibre mediated rubber composites: An overview', *Composites Part B: Engineering,* 76, pp. 180-191.
- **Zhou, Y.**, Luo, X., Huang, L., Lin, S. and Chen, L. (2015) 'Development of Ionic Liquid-Mediated Antibacterial Cellulose-Chitosan Films', *Journal of Biobased Materials and Bioenergy,* 9(4), pp. 389-395.
- **Zhou, Y.**, Fan, M. and Chen, L. (2016) 'Interface and bonding mechanisms of plant fibre composites: An overview', *Composites Part B: Engineering,* 101, pp. 31-45.
- **Zhou, Y.**, Fan, M. and Lin, L. (2017) 'Investigation of bulk and in situ mechanical properties of coupling agents treated wood plastic composites', *Polymer Testing,* 58, pp. 292-299.
- **Zhou, Y.** and Fan, M. (2017) 'Recycled tyre rubber-thermoplastic composites through interface optimisation', *RSC Advances,* 7(47), pp. 29263-29270.
- Rao, J., **Zhou, Y**.* and Fan, M. (2018) 'Revealing the Interface Structure and Bonding Mechanism of Coupling Agent Treated WPC', *Polymers,* 10(3), pp. 266(1-13).

Papers under review

- 'Rubber fusion of wood plastic composites to develop novel multifunctional composites: Interface and bonding mechanisms'.
- 'Influence of coupling agent treatment and compositional variation on bulk and in situ mechanical properties of rubber-wood-plastic composites'.

Oral and/or paper presentations at Conferences

- European Workshop on Bioconversion of Waste Materials to Bio-products, 20 June 2015, Grow2Build European Centre of Excellence, London, UK.
- International Conference of Biocomposites and Sustainable Development in Construction, 09-10 September 2015, Grow2Build European Centre of Excellence, London, UK.
- The 25th Annual International Conference on Composites/Nano Engineering (ICCE25), 16-21 July 2017, Rome, Italy.

Poster presentations at Conferences

- Brunel Graduate School Conference, 11-12 March 2014, Brunel University London, UK.
- Royal Society of Chemistry Symposium – Renewable Chemicals from Lignin, 18 November 2014, Royal Society of Chemistry, London, UK.